Regional Variations in the Molecular Structure and Mechanics of the Lumbar Intervertebral Disc Annulus

by

Tyler Herod

Submitted in partial fulfilment of the requirements
for the degree of Master of Applied Science

at

Dalhousie University
Halifax, Nova Scotia
March 2019

Table of Contents

List of Tables

List of Figures

Abstract

Despite the prevalence of lumbar intervertebral disc related pathologies, fundamental aspects of the structure and mechanics of healthy discs remain unexplored. Little is known about whether the collagen structure of the annulus varies between different circumferential locations at the sub-microscopic level. Moreover, while studies have explored regional variations in the tensile mechanics of the annulus, none have done this for the entire disc wall, with annulus/endplate/vertebrae integrations preserved. The objectives of this study were to investigate (i) whether molecular-level regional variations exist between the anterior and posterior regions of the lumbar intervertebral disc annulus, and (ii) whether potential differences in molecular structure are accompanied by differences in the tensile mechanics of the disc wall.

Mature ovine lumbar spines were used as a model for the human lumbar spine. To assess collagen nanostructure of the anterior vs. posterior annulus, hydrothermal isometric tension analysis and differential scanning calorimetry were used. The mechanics of the disc wall at these regions were assessed using uniaxial tensile tests to failure on oblique sagittal bone-annulus-bone samples, prepared such that collagen fibres in half the lamellae were parallel to the direction of the applied load. Following rupture, samples were cryo-sectioned and light microscopy was used to determine the radial thickness of the annulus, confirm fusion of vertebral growth plates, and assess failure mode.

HIT analysis revealed that collagen from the posterior annulus was significantly more thermally stable and indicated a presence of greater crosslinking density compared to the anterior annulus, from L5-6 to L1-2. In DSC, regional variations in thermal stability were less apparent than in HIT analysis. Despite an indication of greater crosslinking density, samples from the posterior annulus has significantly lower ultimate tensile strength compared to those from the anterior annulus. Alongside new contributions to disc structure and mechanics, the findings from this work suggest that the posterior annulus is optimized for a role other than strength, which could have important implications for therapies targeting annular repair.

List of Abbreviations and Symbols Used

AF	Annulus fibrosus
AFM	Atomic force microscopy
AGE	Advanced glycation end-product
ANOVA	Analysis of variance
AR(L)	Axial rotation (left)
AR(R)	Axial rotation (right)
B-A-B	Bone-annulus-bone
cl	Cement line
CEP	Cartilaginous endplate
DIC	Differential interference contrast
DSC	Differential scanning calorimetry
E	Modulus of elasticity
ER	Epiphyseal ring
$FWHM$	Full-width at half-maximum
GP	Growth plate
HIT	Hydrothermal isometric tension
IP	In-plane
k	Slope of load decay during isothermal segment of a HIT experiment
LB	Lateral bending
MTS	Material testing system
$NaBH_4$	Sodium borohydride
NIH	National Institute of Health
OOP	Out-of-plane
PBS	Phosphate buffered saline
R^2	R-squared value
SEM	Scanning electron microscopy
$t_{1/2}$	Half-time of load decay
T_d	Denaturation temperature
tm	Tide mark

T_{onset}	Onset temperature
T_{peak}	Peak temperature
UTS	Ultimate tensile strength
VEP	Vertebral endplate
Δh	Total specific enthalpy
Δh_{left}	Specific enthalpy corresponding to left-hand side of endotherm
Δh_{right}	Specific enthalpy corresponding to right-hand side of endotherm

Acknowledgements

First and foremost, I'd like to thank Dr. Samuel Veres. Thank you for seeing my potential and introducing me to the world of research. The support and enthusiasm you've expressed since the day I first approached you as an undergraduate student with an interest in biomedical research have allowed me to grow beyond what I ever envisioned. I've learned an immense amount over the last five years because of your knowledge and expertise, and I appreciate how you always found time anytime I needed guidance.

I would also like to thank the other people belonging to my supervisory committee. Dr. Michael Lee, thank you for everything you've taught me throughout my academic journey in biomedical engineering. From the role of professor during the classes I took with you to the role of co-supervisor during this project, I've learned an extraordinary amount from you. To Dr. Laurent Kreplak and Dr. Andrew Glennie, thank you for your insightful comments, questions and contributions.

I would also like to express my gratitude to others who helped in completing this project. To Michel Johnson, thank you for your assistance with performing differential scanning calorimetry. To Micheal Isenor, thank you for your cooperation in supplying me with the ovine tissue used throughout this project. To my funding sources – which include The Natural Sciences and Engineering Research Council of Canada and The Dalhousie Faculty of Engineering – thank you for your financial support. To the other members of my lab and to those I've shared an office with throughout this project: thank you for your advice, support, and for the many fun memories we've shared together.

An extra special thanks goes out to my family. To my parents, thank you for providing me with the foundation necessary to complete this project. I could not have achieved what I have if it wasn't for your unwavering love, support and encouragement, and for all of the important lessons you've instilled in me. To my grandmother, thank you for your boundless belief in me and for always being there throughout every step of this journey.

Chapter 1: Introduction

1.1 The Lumbar Spine

The spine – also called the vertebral column – is a structure comprised of two basic elements: vertebrae, which are made of bone, and intervertebral discs, which are soft-tissue structures interposed between the unfused vertebrae.[1–3] The spine extends from the cranium to the apex of the coccyx and is comprised of five distinctive anatomical regions, which are (from superior to inferior): the cervical spine, the thoracic spine, the lumbar spine, the sacrum, and the coccyx (Figure 1.1). The spine serves many important roles within the context of the body, including protection of the spinal cord and providing support for the weight of the body superior to the pelvis.[1–3]

The lumbar spine – which is located between the thorax and the sacrum – consists of five vertebrae, labeled from superior to inferior as L1 through to L5, and four intervertebral discs, which are similarly labelled L1-2 through to L4-5 (Figure 1.1).[1–3] The lumbar spine is a widely-studied anatomical structure due to the global prevalence and burden of low back pain.[4] The L5-S1 disc – located between the lumbar spine and the sacrum – is often included with discussions of the lumbar spine due to its high probability for injury resulting in low back pain.[1]

The lumbar spine can be broken down into basic functional units – often called lumbar motion segments – which are comprised of two adjacent lumbar vertebrae and the intervertebral disc interposed between them (Figure 1.2).[2] Motion segments are named such because they represent the smallest segment of the spine that can be articulated. The anterior elements of a motion segment include the intervertebral disc – which soft tissue structures that allow the spine to be a flexible structure – and the vertebral bodies – which are large, cylindrically-shaped pieces of bone that provide strength and rigidity to the vertebral column. The cross sections of vertebral bodies and intervertebral discs both share a distinctive kidney-bean shape.[1–3] The structure of the intervertebral disc will be explored in detail in Section 1.2. Vertebral bodies consist of a porous core of trabecular

bone enclosed by a thin layer of dense cortical bone.[1–3] The architecture of trabeculae within the vertebral body consists of tall, vertically-aligned struts – ideal for sustaining longitudinal compression – stabilized by short, horizontal struts.[2]

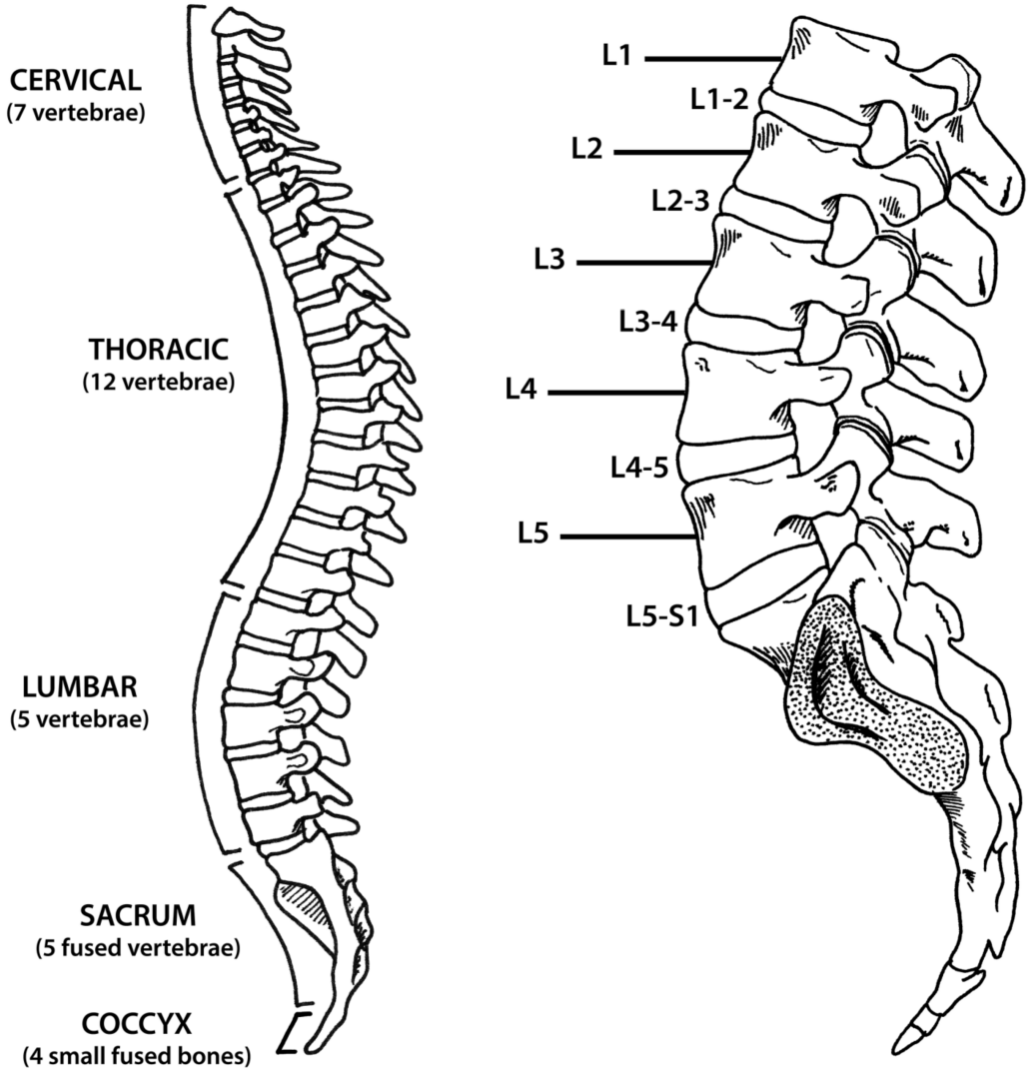

Figure 1.1: An illustration of the vertebral column (left) and the lumbar spine (right). Modified, with permission, from Rodrigues.[5]

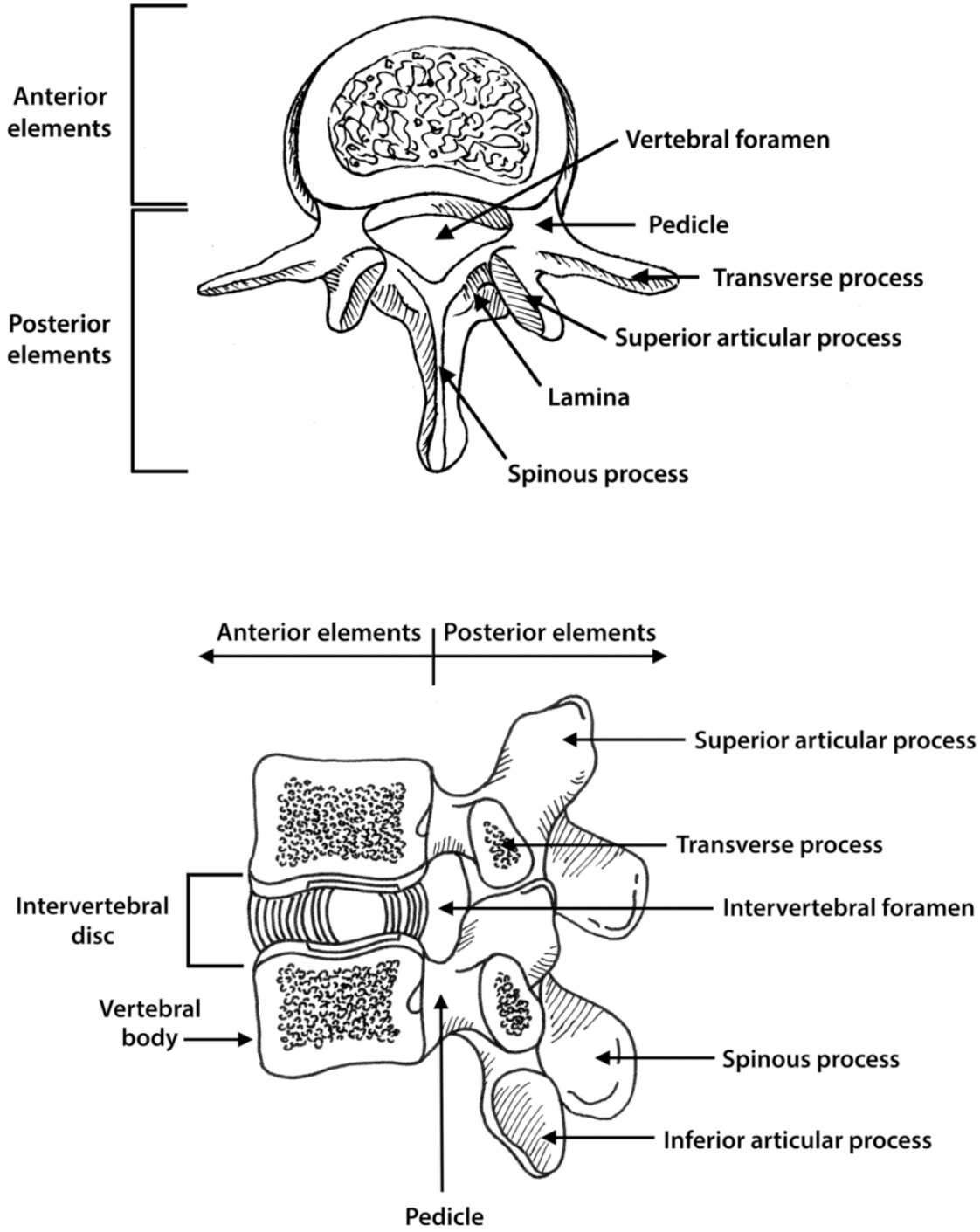

Figure 1.2: Illustrations of a transverse section (top) and a sagittal section (bottom) of a lumbar motion segment. The distinction between anterior and posterior elements is shown in both the top and bottom images by a coronal plane passing through the pedicles. Modified, with permission, from Rodrigues.[5]

The posterior elements of a motion segment – all of which are primarily made of bone – are distinguished from the anterior elements by a coronal plane passing through the pedicles. The pedicles are short projections of bone (often referred to as "processes" – meaning projections of bone from a larger body) originating from the vertebral bodies and extending in the posterior direction.[1–3] The pedicles join with two flat plates of bone called laminae. For each vertebra, the pedicles, the laminae, and the posterior side of the vertebral body all interconnect in such a way that they enclose a space called the vertebral foramen – the canal that shelters the spinal cord. In addition to the pedicles, the posterior elements of each vertebra in a motion segment also include seven processes that project from the surfaces of the pedicles and laminae.[1–3] The four articular processes – two superior and two inferior – are located at the junction of the pedicles and laminae. The articular processes form facet joints with the adjacent articular processes of both superior and inferior vertebrae. Facet joints – also called "zygapophysial joints" or "apophyseal joints" – exhibit features typical of synovial joints.[1–3] The two transverse processes – which project in the posterolateral directions – are also located at the junction of the pedicles and laminae and serve as attachment points for the deep back muscles. The spinous process – which serves a similar role as the transverse processes – projects in the posterior direction from the outer surface of the junction of the laminae.[1–3]

In addition to the intervertebral disc and the vertebrae, lumbar motion segments contain between five to six different ligaments, all of which serve to help stabilize the spine.[1–3] The anterior and posterior longitudinal ligaments cover the anterior and posterior surfaces of both the vertebral bodies and the intervertebral discs (respectively). The range of lengths of fibres within the anterior and posterior longitudinal ligaments varies considerably: shorter fibres span two vertebrae, while longer fibres can span up to four or five vertebrae.[1] The interspinous and supraspinous ligaments connect the spinous process of adjacent vertebrae. While the interspinous ligament is found in all lumbar motion segments, the supraspinous ligament is well developed only in the upper lumbar region.[1] The intertransverse ligament connects the transverse processes of adjacent vertebrae together, while the ligamentum flavum connects the laminae of adjacent vertebrae together.[1–3]

1.2 The Lumbar Intervertebral Disc

1.2.1 Structure

An intervertebral disc consists of three basic structural elements: the nucleus pulposus, the annulus fibrosus, and the cartilaginous endplates (Figure 1.3).[1–3]

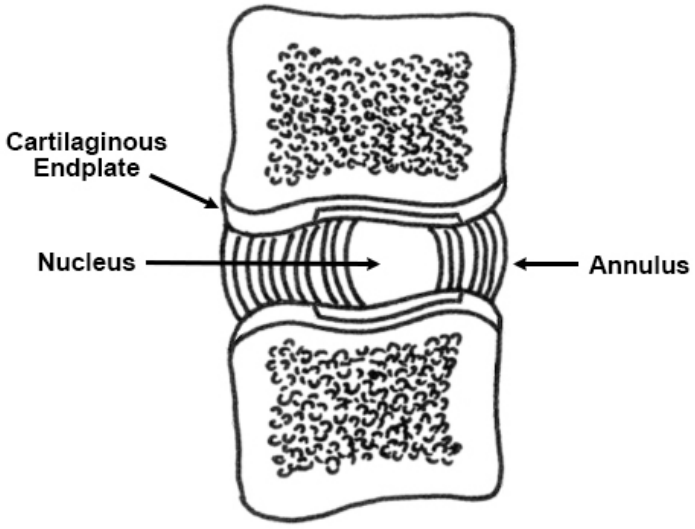

Figure 1.3: An illustration of a sagittal view of an intervertebral disc showing how the annulus encapsulates the nucleus. The cartilaginous endplates (which consist of a calcified layer and an uncalcified layer) border the annulus and nucleus inferiorly and superiorly. Modified, with permission, from Rodrigues.[5]

The Nucleus Pulposus

The nucleus pulposus (referred to hereafter as the nucleus) is a gelatinous material that comprises the central core of an intervertebral disc. The nucleus contains a high concentration of water – approximately 75% to 80% of its wet weight – allowing it to generate hydrostatic pressures when compressed.[6,7] The hydration of the nucleus is achieved by a high concentration of proteoglycans, accounting for approximately 35% to 40% of its dry tissue weight.[6,7] Proteoglycans are entrapped within to an irregular

network of type II collagen,[8] which accounts for approximately 10% of the dry weight of the nucleus.[9–11] While the microstructure of the nucleus has historically been described as a network of collagen fibres with random orientation (when examined in isolation), there is recent evidence suggesting that the fibre-network demonstrates structural continuity from vertebra to vertebra, evident only when the fibres are examined under tension (Figure 1.4).[9,10,12–14]

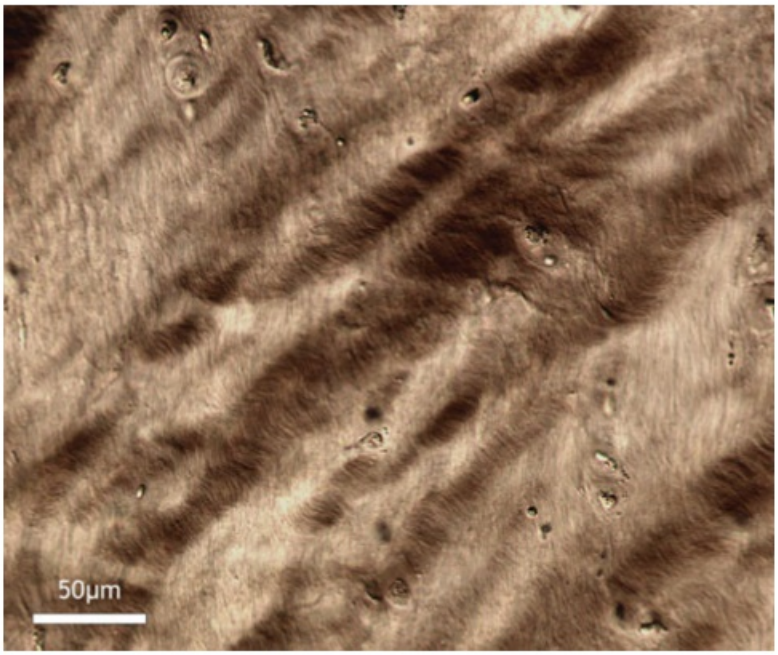

Figure 1.4: The microstructure of an ovine nucleus after being pulled in tension to 350% strain. Image is an unstained cryosection taken using DIC optical microscopy. Modified, with permission, from Wade.[14]

The Annulus Fibrosus

The gelatinous nucleus is encapsulated by a ligamentous structure called the annulus fibrosus (referred to hereafter as the annulus). The annulus can be divided into different circumferential regions (often referred to as "annular regions"), which include the anterior, anterolateral, lateral, posterolateral, and posterior regions (Figure 1.5). Moreover, the radial depth – which originates at the periphery of the disc and measures

the distance to the innermost lamella – is often used to separate the annulus into different radial regions, including inner, mid, and outer regions.

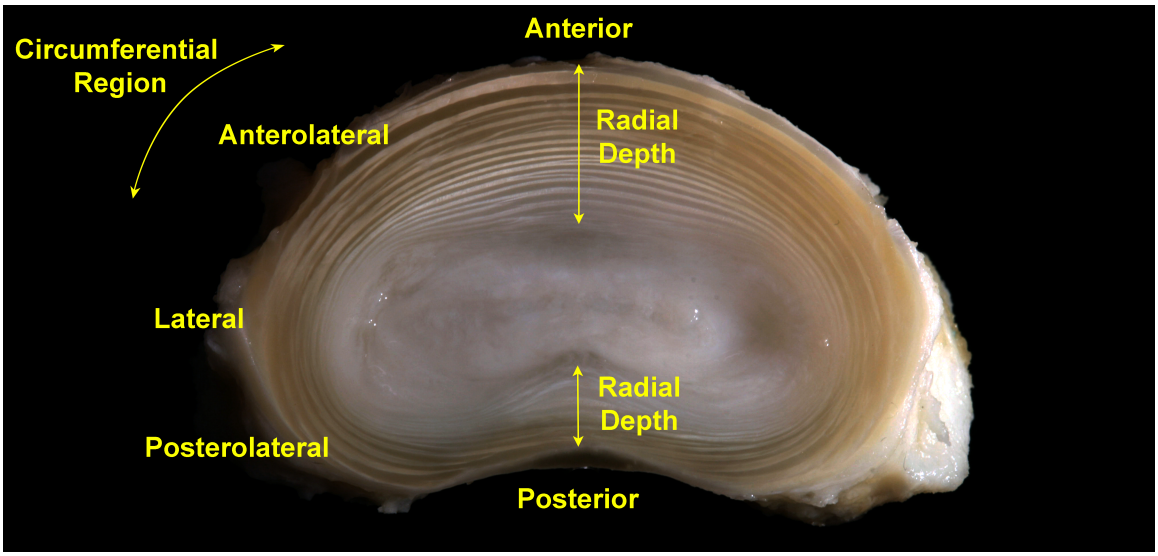

Figure 1.5: A transverse section of an L5-6 disc from a skeletally mature ewe (24+ months old) showing the different circumferential regions. Radial depth, which measures the distance from the periphery of the disc to the innermost lamella, are indicated for the central anterior and central posterior regions. Modified, with permission, from Veres.[15]

Compositionally, the annulus has a lower concentration of proteoglycans than the nucleus – approximately 10% of its dry tissue weight in the outer annulus and as high as 35% in the inner annulus – and accordingly, a lower concentration of water (averaging approximately 70% by wet weight).[6,7] Moreover, collagen comprises a larger percentage of the annulus in comparison to the nucleus, accounting for approximately 70% of the dry weight in the outer annulus and decreasing to 40% in the inner annulus.[11] The type of collagen varies with radial depth: while the outer annulus is made almost exclusively of type I collagen, the relative proportions of type I to type II collagen decreases as radial depth increases until primarily type II collagen is found (representing the nucleus).[11,16] The transition between inner annulus and nucleus has no clear boundary: for this reason, this region is commonly referred to as the transition zone.[1,16,17] Because fibres in the transition zone are not organized into distinct lamellae, they are not included in measurements of the radial depth.

The microstructure of the annulus – in contrast to the nucleus – is a complex, highly ordered structure (Figure 1.6). The collagen fibres of the annulus are contained within sheets called lamellae that form concentric rings around the nucleus. The collagen fibres within the lamellae are oriented in a cross-ply pattern: the oblique fibre-orientation angle alternates between adjacent lamellae (Figure 1.6B).[1,18–20] Measured from the transverse plane, the fibre orientation at the disc's periphery are inclined at 20º within the anterior annulus and 40º within the posterior annulus.[20] The fibre-orientation angle does not vary significantly with increasing radial depth for any annular region.[20] The concentric layers of collagen fibres are not always continuous: approximately 50% of lamellae form incomplete layers (the relative proportions of which do not vary significantly with annular region), and bifurcations are uncommonly observed.[19] Moreover, the number of distinct layers varies with annular region: the anterior annulus has both more lamellae and thicker lamellae than the posterior annulus, making its radial depth approximately 30-40% larger than the posterior annulus.[10,19,21,22] The radial thickness of lamellae is observed to decrease as radial depth increases for all annular regions.[10,22] The annular height (in the superior-inferior direction) also varies: the anterior annulus is approximately 10.5 mm tall, while the posterior annulus is approximately 7.2 mm tall.[23] The lamellar structure of discs, in general, does not change significantly with spinal level.[19]

A series of secondary structures within the lamellar architecture also exists, referred to as "radial bridging elements", "trans-lamellar bridges", or "cross bridges" (Figure 1.7).[24,25] Cross bridges are small branches of collagen fibres that connect lamellae in the radial direction. In addition to connecting adjacent layers, cross bridges also separate the collagen within each lamella into identifiable bundles. While their role is still under investigation, there is evidence suggesting that larger cross bridges are the result of microstructural disruption to lamellar architecture following vascular regression,[24] while smaller cross bridges are structural features that may play a role in resisting lamellar deformation and shear stress.[26,27]

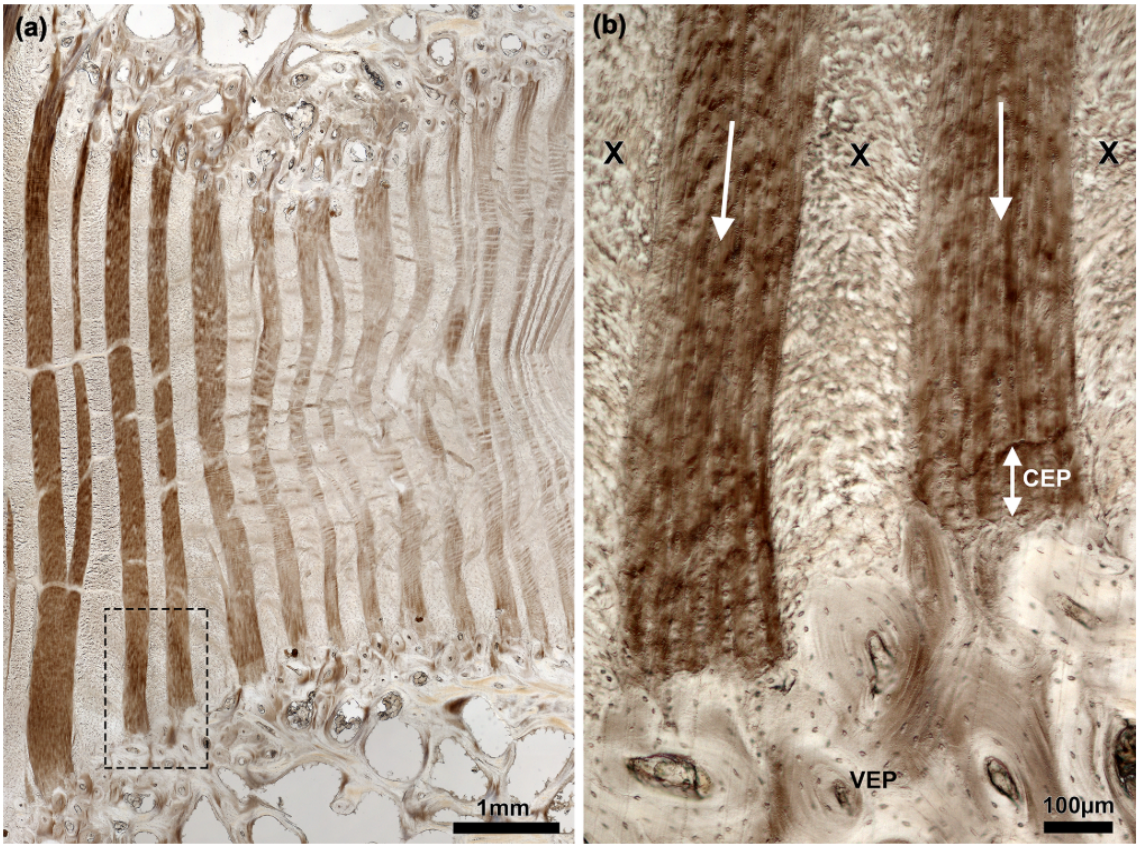

Figure 1.6: The microstructure of the ovine anterior annulus as observed from an oblique section (an inclined sagittal plane parallel to one of the fibre-orientation angles) (a): A low-magnification image illustrating in-plane lamellae (darker) and out-of-plane lamellae (lighter). (b): A higher-magnification image illustrating in-plane lamellae (white arrows) and out-of-plane lamellae (black x's). Out-of-plane lamellae are coming out of the plane of the image at an angle of approximately 65º. CEP = cartilaginous endplate; VEP = vertebral endplate. Images are unstained cryosections taken using DIC optical microscopy. Modified, with permission, from Rodrigues.[5]

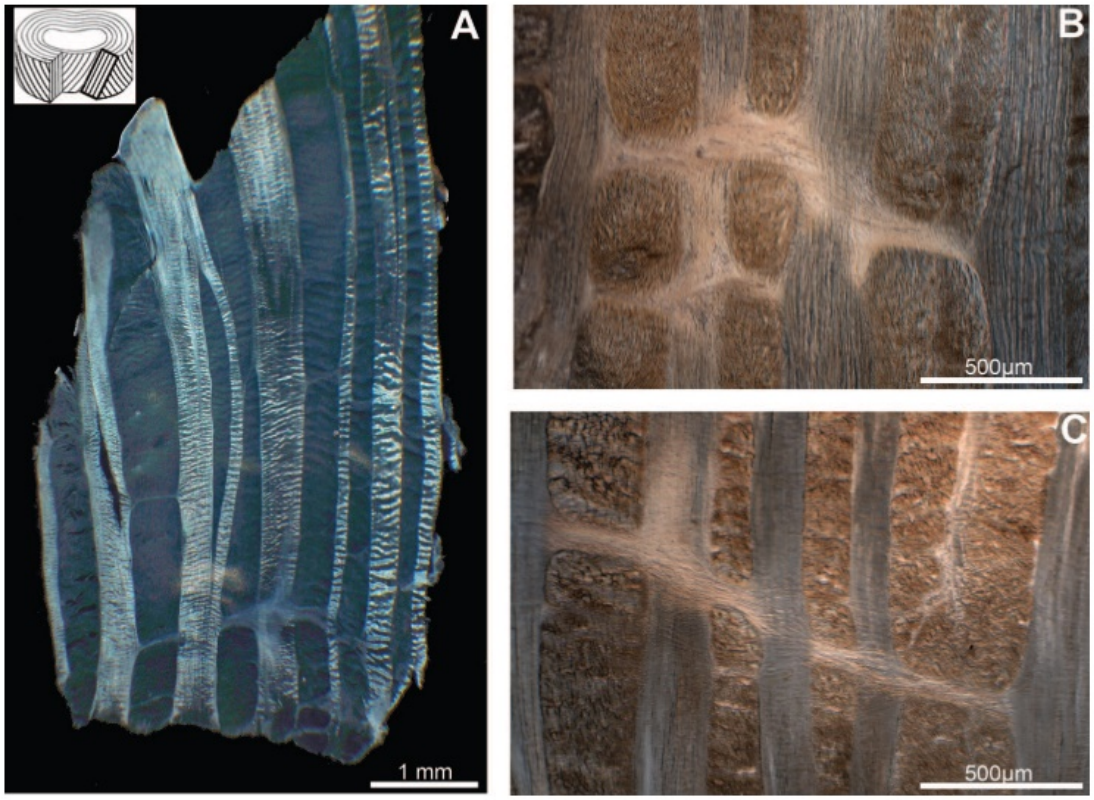

Figure 1.7: Bridging elements, as observed through oblique sections from the anterior region of an ovine disc taken parallel to a fibre-orientation angle. Images are unstained cryosections imaged using DIC optical microscopy. Modified, with permission, from Schollum.[28]

The Cartilaginous Endplates

The cartilaginous endplates, which are approximately 0.6 mm thick (in the superior-inferior direction), cap the disc superiorly and inferiorly.[23] The cartilaginous endplates are comprised of two regions: an uncalcified layer of hyaline cartilage and calcified layer of fibrocartilage (Figure 1.8). There is growing evidence suggesting that the hyaline cartilage layer only covers the nucleus and the inner annulus, extending up to the raised outer rim of the vertebral body (Figure 1.8A).[1,9,25,29,30] In contrast, the calcified layer of cartilage extends to the periphery of the disc.[31] The tidemark marks the point at which the calcified region of cartilage starts (Figure 1.9). The tissue adjacent to the calcified layer is hyaline cartilage at radial depths corresponding to the nucleus and inner annulus, while in

the outer annulus the calcified layer borders directly with the annulus.[23,25,32] The cement line corresponds to the border between calcified cartilage and the vertebral endplate (Figure 1.9).[25,31,33,32] The thickness of the calcified region (measured in the superior-inferior direction) varies radially, being largest within the region that borders annulus and thinnest within the region that borders the nucleus (to such an extent that it can be difficult to distinguish).[23] The collagen fibres from the inner annulus bordering the cartilaginous endplate penetrate through the uncalcified layer and insert directly into the calcified layer.[23,25,34] While the collagen fibres of the nucleus also penetrate into the uncalcified cartilage layer,[23,25] it is unclear whether fibres extend to the calcified region.

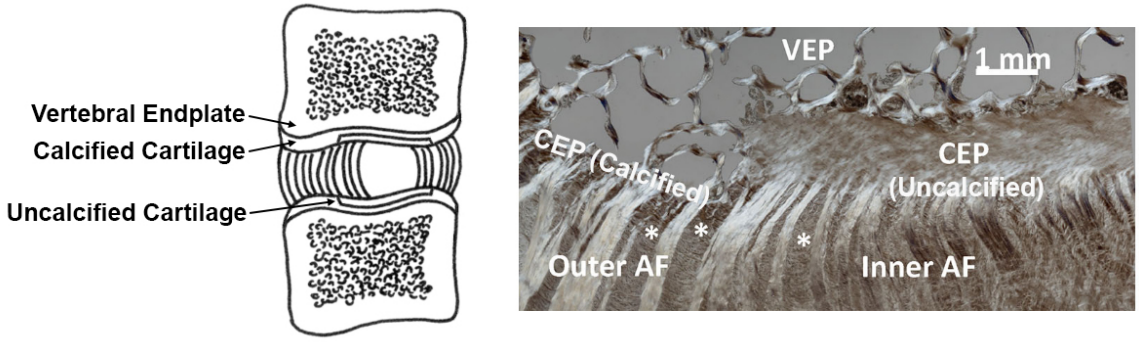

Figure 1.8: An illustration of the different layers of the cartilaginous endplate (left) and a sagittal section of the cartilaginous endplate from a human lumbar disc (right). AF = annulus fibrosus; CEP = cartilaginous endplate. VEP = vertebral endplate. Asterisk = out-of-plane lamellae. Left: Modified, with permission, from Rodrigues.[5] Right: Image is an unstained cryosection taken using DIC optical microscopy. Modified, with permission, from Brown.[25]

Compositionally, the cartilaginous endplates are made up of less proteoglycans than the annulus and, correspondingly, less water.[23] Collagen – which is almost exclusively type II – is more abundant as well: the cartilaginous endplates have approximately 25% more collagen by dry weight relative to the annulus.[23,35] The collagen fibres of the cartilaginous endplate run in parallel with one another across the surface of the endplate.[9,23] Spatial variation in the biochemical constituents exist: the concentration of proteoglycans and water content decreases towards the vertebra, while the collagen content increases.[23] The composition of the cartilaginous endplate does not vary significantly with spinal level.[23]

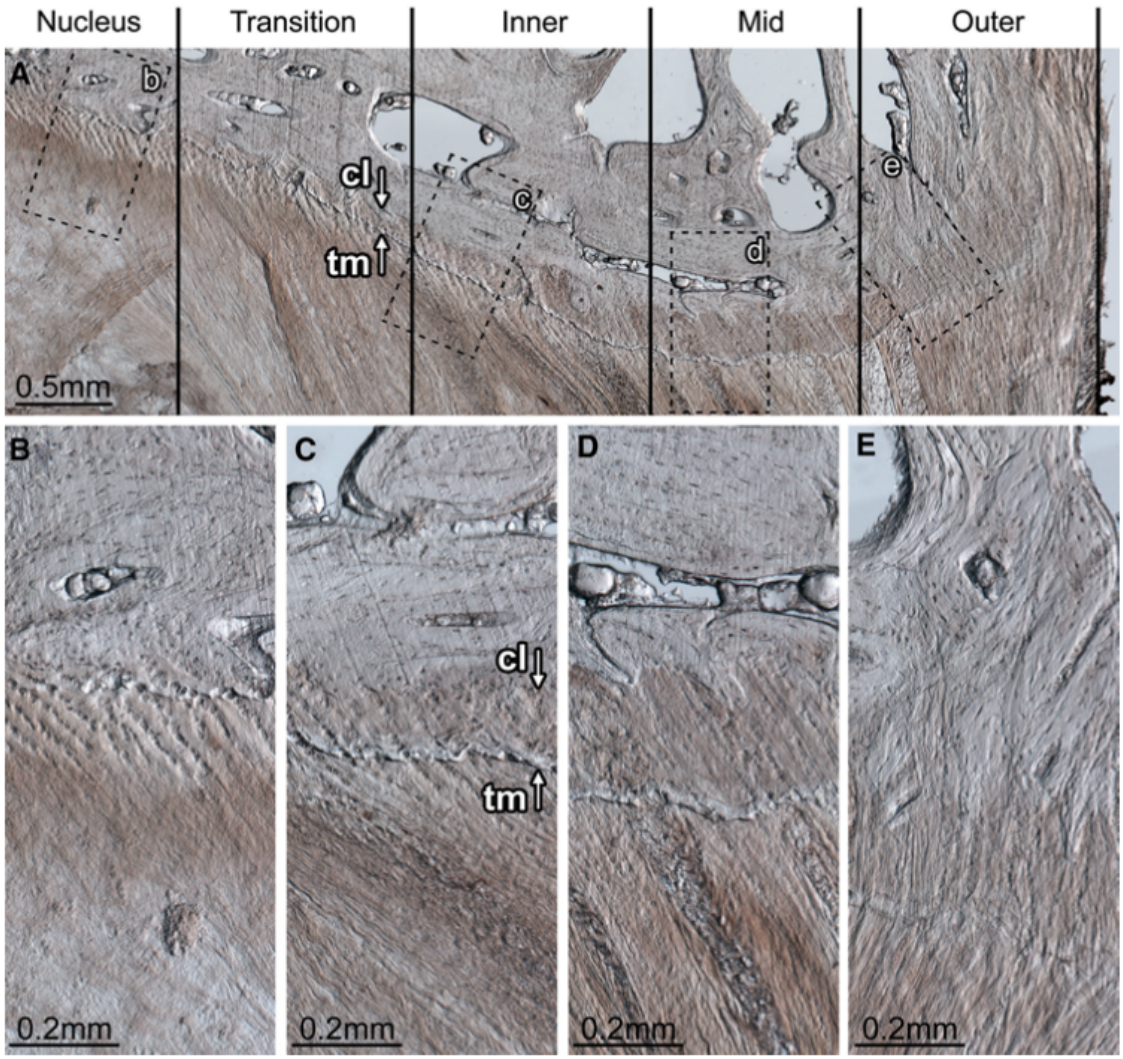

Figure 1.9: A sagittal section of the posterior region of an ovine lumbar disc illustrating the cartilaginous endplate, the cement line (cl) and the tide mark (tm). A: The increase in mineralization of the cartilaginous endplates moving radially outward from the nucleus to the outer annulus. B: The integration of the nucleus with the cartilaginous endplate, where only uncalcified cartilage can readily be observed. C: The start of the inner annulus, as marked by innermost lamella. Both the uncalcified cartilage and calcified cartilage layers can be distinguished, as well as the tide mark and the cement line. D: The mid annulus, marked by the full calcification of the cartilaginous endplate. E: The outer annulus, again reflecting full calcification of the cartilaginous endplate. Image is an unstained cryosection taken using oblique illumination microscopy. Modified, with permission, from Veres.[32]

The Vertebral Endplates

A fourth component often included in discussions of the intervertebral disc are the vertebral endplates, which cap the intervertebral disc superiorly and inferiorly (Figure 1.8). The vertebral endplates are technically part of the vertebrae within a motion segment – not the intervertebral disc. Because they are involved with anchoring both the annulus and the cartilaginous endplate, however, their structure will be reviewed. The vertebral endplates are composed of dense subchondral bone made primarily of type I collagen.[22,35] The raised outer rim of the vertebral endplate is often distinguished from the rest of the structure and is termed the apophyseal ring (historically – and incorrectly – referred to as the epiphyseal ring).[25,36]

The vertebral endplates border the intervertebral disc in several different ways. At the outer annulus, collagen fibres penetrate through the calcified cartilage,[22,31,29,34] anchoring directly to bone within the vertebral endplate.[22,25] Collagen fibres at the periphery of the annulus have also been observed to curve around the cement line, attaching directly to the vertebra.[34] In addition to interacting with fibres from the outer annulus, the vertebral endplates also interact with the cartilaginous endplate, reportedly interlocking with it.[25] The inner surface of the apophyseal ring serves as a strong anchor point for the cartilaginous endplate, while the remainder of the vertebral endplate is loosely cemented to the cartilaginous endplate via a thin layer of calcium.[29,30]

1.2.2 Mechanical Function and In Vivo Loading

The primary functions of lumbar intervertebral discs are to allow the spine to be a flexible structure and to participate in the weight-bearing responsibilities of the vertebral column. While weight-bearing subjects the spine to compressive loads, the movements associated with day-to-day activities – including flexion and axial rotation – can place the spine under more complex loading.[1]

Compression

Lumbar intervertebral discs are passively subjected to compressive loading when standing or sitting. The magnitude of compressive loads generated during physiological loading is surprisingly large: the L3-4 disc, for example, has been shown to experience a load equal to 1.2x the individuals body weight when standing and 2x body weight when sitting without back support.[37] The ability for lumbar intervertebral discs to sustain such large compressive loads results from the annulus and the nucleus working in cooperation with one another. When an intervertebral disc is compressed, the nucleus responds by expanding in the radial direction, which in turn applies pressure to the inner walls of the annulus. This, in turn, causes the annulus to radially bulge outward, producing a multiaxial set of stresses within the annulus that includes both compressive and tensile stresses.[2,38,39] If the annulus is treated as two distinct materials, being: (i) the fibrillar matrix (consisting of collagen fibres), and (ii) the extrafibrillar matrix (consisting of non-collagenous proteins including proteoglycans), the tensile and compressive stresses experienced by the annulus can be separated by material.[40] While the extrafibrillar matrix functions to sustain the compressive load mostly through osmotic pressure, its deformation is limited by the collagen fibres of the annulus, which are placed in tension. Prolonged loading can result in water flowing out of the disc through the annulus if the internal hydrostatic pressure is sufficiently large.[41–43] The water loss from the nucleus as a result of prolonged compressive loading results in a transfer of load: as the hydrostatic pressure decreases (due to fluid loss), the magnitude of compressive loading experienced by the annulus increases.[42,44] Water will flow back into the disc when the prolonged load applied to the disc is lessened – a process that primarily occurs during bedrest when the spine is placed in a supine posture.[45]

Intradiscal pressures during weight bearing have been measured *in vivo* through the use of pressure transducers inserted into the nucleus: in one study, the intradiscal pressure within the L4-5 disc was reported to be 0.5 MPa when standing.[46] Measurements of the multiaxial stress environment of the annulus have been explored primarily through finite elemental modeling.[2,38,39,47] Through such studies, it has been shown that the stresses

experienced by the extrafibrillar matrix in the axial, radial, and circumferential directions are compressive, while collagen fibres within lamellae experience tensile stress.[2,38] The maximum tensile and compressive stresses occurs at the innermost lamella and decrease continuously towards the outer layers.[2,38,37] Lu *et al* demonstrated that the tensile stress experienced by collagen fibres in response to compression varies not only with radial depth, but also with annular region: the inner annulus experiences a tensile stress approximately twice the magnitude of the outer annulus, and the posterior annulus experiences tensile stress in the range of three to four times the magnitude of the anterior annulus.[47] The axial and circumferential compressive stresses in the annulus predicted by modeling studies have been validated *in vitro* using a technique called stress profilometry.[42,48,49] Here, a pressure transducer is pulled through a cadaveric motion segment to measure the compressive stresses perpendicular to the surface of the transducer. Such studies have measured axial and circumferential stresses of approximately 0.5 MPa throughout the annulus, where posterior stresses are slightly higher than anterior stresses, and inner annulus stresses are larger relative to the stresses in the outer annulus.[42,48,49]

Flexion

Flexion of the lumbar spine results in the anterior annulus being compressed while the posterior annulus is stretched in tension. Measurements *in vivo* show that when the spine is placed at its physiological limit of flexion, the percentage change in disc height for the anterior and posterior regions of the annulus are approximately -30% and +50%, respectively.[50] The nucleus is also reported to respond to flexion by shifting posteriorly (most pronounced in the L4-5 and L5-S1 discs), thus creating a larger tensile stress within the inner posterior annulus relative to the inner anterior annulus.[51,52] The increase in posterior disc height combined with the posterior shift in the nucleus place the posterior annulus under considerable stress in flexion – a problematic loading regime given that the posterior annulus is the thinnest region of the annulus.[10,19,21,22]

Flexion of the lumbar spine results in changes to the intradiscal pressure. In one study, the intradiscal pressure was shown to increase by almost five times – from 0.5 MPa to 2.3 MPa – when lifting a 20 kg weight off the ground with a rounded back (relative to standing with no flexion).[46] The changes in the compressive stresses in the annulus wall in response to flexion have also been explored with stress profilometry, showing that when the anterior annulus is loaded to its elastic limit, compressive stresses can grow as large as 1.1 MPa (an increase of over 50% relative to standing upright).[48]

Axial Rotation (Torsion)

Axial rotation of the lumbar spine refers to the twisting of one vertebra relative to an adjacent vertebra. The cross-ply arrangement of collagen fibres implies that regardless of the twist direction, half of the lamellae (those with collagen fibres in alignment with the direction of twist) will actively resist the applied rotation. However, the collagen fibres not in alignment with the direction of twist will be relaxed, and will therefore not contribute to resisting the applied rotation.[1] These observations have been confirmed *in vitro* by dissecting all of the collagen fibres oriented in one fibre-orientation angle and evaluating the change in resistance to torsion.[53] *In vitro* biomechanical studies have also shown that torsion can significantly increase risk for injury when combined with flexion (relative to flexion alone).[54]

1.2.3 Loading-Induced Damage

Intervertebral discs are susceptible to structural alteration resulting from a variety of different causes. Damage can be inflicted through day-to-day activities, leading to injuries such as disc herniation or internal disc disruption. In addition, disc degeneration disease can result from loading-induced damage, leading to progressive structural failure. While all of these processes are distinct from one another, they are all suspected to be the result of some form of loading-induced damage to the intervertebral disc.

Internal Disc Disruption

Internal disc disruption is defined as the disorganization of structures within the intervertebral disc space in the form of radial fissures and circumferential tears (Figure 1.10).[55,56] Internal disc disruption – unlike a disc herniation – does not result in displacement of material beyond the intervertebral disc space (Figure 1.11A). Radial fissures are classified by three grades: grade 1 fissures are contained within the inner third of the annulus, grade 2 fissures extend as far as the inner two-thirds of the annulus, and grade 3 fissures extend as far as the outer third of the annulus (Figure 1.10).[1,57] A fourth grade (grade 4) is sometimes recognized, which describes a grade 3 fissure that terminates in a circumferential tear within the outer third of the annulus (Figure 1.10D).[1,57] Radial fissures are more likely to form in the posterior annulus in comparison to the anterior annulus.[58]

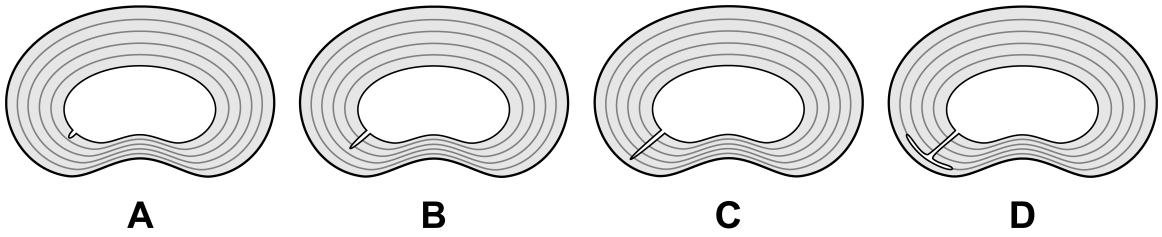

Figure 1.10: Classification of radial fissures (as defined by Bogduk[1]) by the extent to which they penetrate the annulus. Grade 1 fissures (A) extend only as far as the inner third of the annulus. Grade 2 fissures (B) extend as far as the inner two-thirds of the annulus. Grade 3 fissures (C) extend as far as the outer third of the annulus. Grade 4 fissures (D) are grade 3 fissures with evidence of fissures extending circumferentially within the outer annulus.

Internal disc disruption in the form of grade 3 or grade 4 fissures have been shown to be a determinant of nociceptive back pain, which refers to pain resulting from stimulation of structures in the lumbar spine.[55,59] Pain caused by radial fissures is often attributed to stimulation of the nerve endings in the intervertebral disc, which are located only within the outer-third of the annulus.[60–62]

Disc Herniation

Disc herniation is defined as the localized displacement of intervertebral disc tissue beyond the perimeter of the apophyseal rim (Figure 1.11A).[56] While disc herniations are commonly associated with displacement of the nuclear material through the annulus, the displacement can also be caused by fragmented cartilage, bone or annular tissue.[56] In fact, in a study that considered 120 lumbar disc herniations, while 98% contained some nuclear material, 62.5% also had presence of the annulus, bone or cartilage (or any combination thereof).[63] Disc herniations can be classified by their relative size: a focal herniation involves less than 25% of the disc circumference (Figure 1.11B), while a broad-based herniation involves between 25% and 50% of the disc circumference (Figure 1.11C).[56] Disc herniations favor particular annular regions and disc levels: approximately 80% occur in the paracentral region, while approximately 90% occur in either the L4-5 disc or the L5-S1 disc.[64,65] Several different postures have been linked to an increased susceptibility of disc herniation, such as sudden loading of the spine in flexed postures.[66] The combination of flexion and axial rotation has also been shown to lead to high localized stresses in the posterior annulus, leading to an increased susceptibility for disc herniation.[54,67] Disc herniation can lead to pain due to irritation to a spinal dorsal root or its ganglion due to extruded disc material.[1,68] Herniation can also cause pain by radial fissures in the same fashion as those described for internal disc disruption.[68]

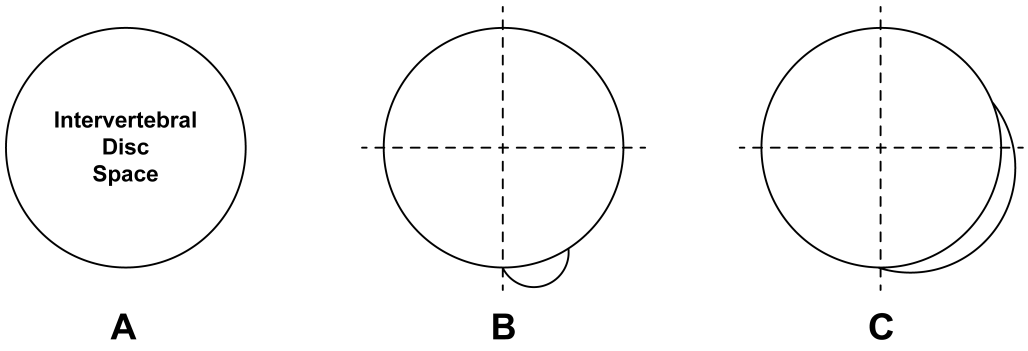

Figure 1.11: Classification of disc herniations (as defined by Fardon[56] *et al*) by relative size to the intervertebral disc space (A), defined as the space encapsulated by the outer perimeter of the apophyseal rim. Focal herniations (B) involve a displacement of material contained within 25% of the disc circumference, while broad-based herniations (C) involves material displaced between 25% and 50% of the disc circumference.

Degenerative Disc Disease

Degenerative disc disease is defined as the abnormal and irreversible cell-mediated response to structural defects that results in accelerated aging of the disc and progressive structural failure.[8] Some of the structural defects that can initiate the process of disc degeneration include endplate fracture, radial fissures, and annular punctures. The magnitude of such injuries often leads to nuclear depressurization because the nucleus is allowed to expand into the space created by the defect. The decrease in hydrostatic pressure places the annulus under greater compressive stress, resulting in permanent changes to the local mechanical environment that disc cells experience.[8] The cell-mediated response that occurs with degenerative disc disease leads to a decrease in proteoglycan concentration and water content – particularly in the nucleus.[8,69] Later stages of degenerative disc disease are characterized by annular delamination, ultimately resulting in structural failure of the annulus.[70] Disc degeneration is closely tied to pain due to its dependency on structural failure.[8]

Several different scales have historically been using to grade macroscopic disc degeneration, the most common being the Pfirrmann 5-point grading scheme, which uses MRI to grade the extent of degeneration.[71–73] These grading schemes, however, have been criticized for missing important inter-individual variability and intra-individual variability, as well as demonstrating suboptimal reliability in measurements.[74,75] Continual research into new and improved methods for grading disc degeneration are still being proposed today.[74,75]

1.3 Factors Contributing to Annular Damage

Many different factors ultimately contribute the susceptibility of the annulus to damage, including regional variations in mechanical loading, structure, and tensile mechanics. Damage to the disc is commonly associated with the posterior region, which is thinner (radially) relative to other annular regions.

1.3.1 Regional Variations in Mechanical Loading

Regional variations in how the annulus responds to different types of applied loads have largely been demonstrated through modeling studies. For example, the regional variations in tensile strain and shear strain of fibres in the annulus in response to an applied moment of 7.5 N·m that caused: (i) flexion, (ii) extension, (iii) lateral bending, (iv) axial rotation, or (v) any two combinations of (i) through (iv) was explored by Schmidt *et al* (Figure 1.12).[76] The maximum tensile strain resulting from single rotations (i.e., conditions i through iv) occurred in response to axial rotation, which led to a tensile strain of 11.9% occurring in the posterolateral region of the annulus. In contrast, the maximum shear strain resulting from single rotations occurred in response to lateral bending, which led to a shear strain of 39.7% occurring in the lateral region of the annulus. Interestingly, the maximum tensile strain and shear strain in response to combined rotations occurred posterolaterally for nearly all combinations.[76]

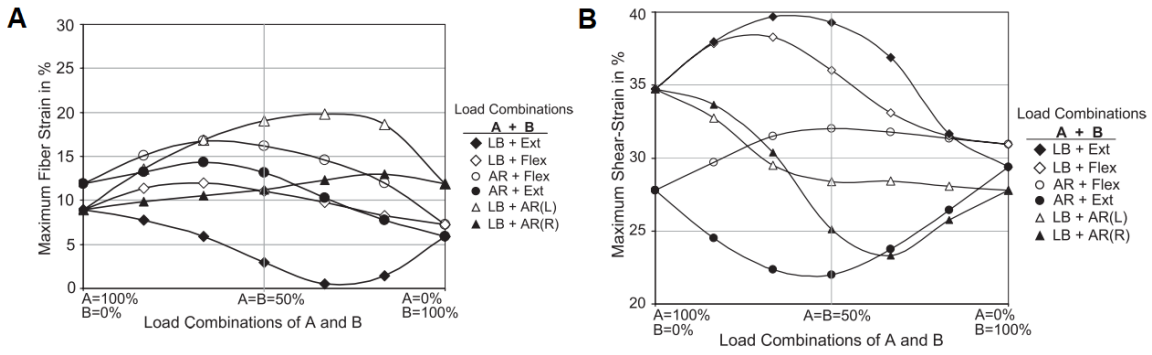

Figure 1.12: The maximum fibre strain (a) and the maximum shear strain (b) that occurs within the lumbar annulus in response to lateral bending (LB), extension (Ext), flexion (Flex), and axial rotation (AR(L) for axial rotation – left, and AR(R) for axial rotation – right). Modified, with permission, from Schmidt.[76]

The regional variations in tensile stress under similar loading conditions has also been reported. In general, the maximum tensile stresses occur within the posterior and posterolateral region under complex loads that include axial compression, axial rotation, lateral bending and/or flexion.[77] The tensile stresses developed in the posterior region

(measured in the superior-inferior direction) in response to an applied moment of 7.5 N·m causing pure flexion, axial rotation, or lateral bending, were 7 MPa, 1.8 MPa and 1 MPa, respectively.[77] When flexion was combined with axial rotation or lateral bending, the tensile stresses in the posterior region grew to 11 MPa and 10 MPa, respectively.

1.3.2 Regional Variations in Annular Structure

The majority of studies that have explored whether regional variations in annular structure exist have focused on variations in microscopic structure. The number of lamellae and radial thickness of individual lamella are known to vary between the anterior and posterior region, where the anterior annulus has more lamellae and thicker lamellae, making its radial depth approximately 30-40% larger than the posterior annulus.[10,19,21,22] The fibre-orientation angle is also known to vary between the anterior and posterior annulus: measured from the transverse plane, the orientation of the fibres at the disc's periphery are inclined at 20º within the anterior annulus and 40º within the posterior annulus.[20]

While annular variations in certain microstructural features such as collagen bundle size and bridging element distribution have not yet been studied, even less is known about variations within the annulus at the ultrastructural level. There is currently no information available on whether regional variations exist in collagen crosslinking or collagen molecule stability. These may be important structural characteristics related to the discs ability to accumulate damage, given that crosslinking is a significant determinant of collagen load-bearing ability,[78] and molecular stability has been shown to be related to the susceptibility of collagen fibrils to loading-induced disruption.[79,80]

1.3.3 Regional Variations in Mechanical Properties

Several cadaveric studies have explored whether the tensile mechanics of the human annulus varies regionally. Of these studies, most have utilized small pieces of annulus cut away from the intervertebral disc.[81–86] For those that considered changes with annular

region, only comparisons between the anterior and the posterolateral have been explored using human discs.[81] For samples cut from the disc parallel to the transverse plane (i.e. not in alignment with a fibre-orientation angle), outer anterior samples failed at approximately 2.5 MPa while outer posterolateral samples failed at approximately 1 MPa.[83,84] Interestingly, when samples are prepared parallel to a fibre-orientation angle, the strengths of the samples appears to increase. Skaggs *et al* showed that outer anterior samples failed at approximately 10 MPa, while outer posterolateral samples failed at approximately 5 MPa.[85] In contrast, Shan *et al* reported smaller values of strength for both regions, where outer anterior samples failed at 3.5 MPa and outer posterolateral samples failed at 3.10 MPa.[82] In terms of radial depth, studies have concluded that in general, the inner annulus – regardless of region – is weaker than the outer annulus.[81–86] How the mechanical properties of samples from the posterior region (prepared in similar ways to the studies summarized) would compare to the anterior region remains unclear.

While pieces of annulus have successfully been used to explore regional variations in tensile mechanics, these studies fail to capture the structural role that the vertebral endplate plays in anchoring collagen fibres from the annulus. To address this limitation, some studies have utilized bone-annulus-bone samples mounted in dental stone and directly compared the anterior and posterior regions of the annulus.[87,88] These studies, however, prepared vertically oriented samples (i.e. with the loading axis oriented in the superior-inferior direction), resulting in the development of large shear stresses in addition to tensile stresses. The results from these studies have produced conflicting reports. Zak and Pezowicz, who used a porcine model, reported that posterior samples failed at 4.5 MPa, while anterior samples failed at 7.5 MPa.[88] In contrast, Green *et al*, who used cadaveric samples, reported that posterior samples failed at 3.8 MPa and while anterior samples failed at 1.7 MPa.[87] Whether the actual tensile strength of collagen in bone-annulus-bone samples (i.e. with the applied load parallel to a fibre-orientation angle) varies regionally remains to be seen.

Chapter 2: Research Objectives and Hypotheses

2.1 Overview

Despite the prevalence of lumbar intervertebral disc related pathologies, fundamental aspects of the structure and mechanics of healthy discs remains unexplored. While microstructural variations in the annulus with circumferential location have been investigated, it is completely unknown whether microstructural variations are accompanied by variations in collagen structure at the molecular level. Meanwhile, while some studies have investigated variations in the mechanics of the annulus, none have assessed the tensile properties of the entire disc wall using bone-disc-bone samples to preserve annulus/endplate/vertebrae integrations while also aligning the loading axis parallel to one of the fibre-orientation angles.

The objectives of the research presented were to investigate: (i) whether molecular-level regional variations exist between the anterior and posterior regions of the annulus, and (ii) whether potential differences in thermomechanical responses are accompanied by differences in tensile mechanics of the disc wall.

2.2 Experiment I: Hydrothermal Isometric Tension Testing

Rationale: Hydrothermal isometric tension (HIT) analysis in conjunction with sodium borohydride ($NaBH_4$) crosslink stabilization treatment allows for an assessment of thermal stability and intermolecular crosslinking for the collagen molecules that contribute to the development of tension within a tissue during heating. For crosslinking, HIT analysis can provide information on the relative proportions of heat labile vs. heat stable crosslinks present, as well as provide a comparative indication of crosslink density. HIT analysis has previously been used to show differences in collagen stability and crosslinking with tissue development,[89] and between functionally distinct tissues of the same age.[90] Testing different annular regions with HIT analysis will allow for assessment

of whether molecular-level regional variations in the annulus' tension-bearing collagen structure are present.

Objective: To characterize the thermal stability and crosslinking of collagen molecules within lumbar intervertebral discs with annular region and disc level.

Hypothesis 1: Differences in thermal stability and crosslinking of collagen molecules will be revealed for annular region due to the higher extent of physiological loading the posterior annulus is subjected to.[51,52] Collagen molecules in the posterior annulus will correspondingly have a higher thermal stability (as indicated by T_d through HIT analysis) and a higher density of thermally stable crosslinks (as indicated by $t_{1/2}$ in HIT analysis) when compared to the anterior annulus.[90]

Hypothesis 2: Differences in thermal stability and crosslinking of collagen molecules will not be revealed for disc level because disc level does not have a profound effect on lumbar disc mechanics.[91] Collagen molecules in the anterior and posterior annulus will correspondingly have similar values of T_d and $t_{1/2}$ when comparing between L5-6 and L1-2 discs for each respective annular region.

Hypothesis 3: Collagen molecules in the anterior and posterior annular regions will not have a significantly higher amount of stable crosslinks when treated with $NaBH_4$ because the annulus has low cellularity (which implies a low rate of collagen remodelling).[92]

2.3 Experiment II: Differential Scanning Calorimetry

Rationale: Like HIT analysis, DSC can also be used to assess the thermal stability of collagen within a tissue. Unlike HIT analysis, DSC can provide information on the distribution of molecular stabilities present within a tissue, with the least stable collagen molecules being captured by the endotherm onset temperature, and presence of molecules with greater stability captured through peak temperature and full-width at half-maximum. For assessment of annular structure, DSC therefore provides additional information not

able to be captured by HIT analysis. DSC also assesses all material present within the tested sample, not just the collagen contributing to tension generation like in HIT analysis, possibly an important feature for annular characterization given the presence of radial bridging elements. Finally, sample preparation differences will allow variations in annular structure with radial depth to be more easily assessed than would be possible through using HIT analysis.

Objective: To characterize the thermal stability of collagen molecules within lumbar intervertebral discs with annular region and radial depth.

Hypothesis 1: Collagen molecules in the posterior annulus will have a higher thermal stability as indicated by T_{onset} and T_{peak} due to the higher extent of physiological loading the posterior annulus is subjected to.[51,52]

Hypothesis 2: Collagen molecules in the outer annulus will have a smaller range of thermal stabilities as indicated by $FWHM$ due to the outer annulus being composed primarily of a smaller variety of collagen types relative to the inner annulus.[17]

2.4 Experiment III: Mechanical Testing and Light Microscopy

Rationale: While regional variations in the strength of the annulus of lumbar intervertebral discs have been explored in other studies,[81–86] there remains a lack of understanding regarding how the tensile strength of collagen fibres varies between the anterior and posterior region of the annulus. No studies have explored the tensile properties of the annulus while preserving annulus/endplate/vertebrae integrations, the disruption of which could significantly alter mechanical response. By aligning bone-annulus-bone samples such that one of the fibre-orientation angles is parallel to the applied tensile load, the tensile strength of the collagen fibres of the annular wall from the anterior and posterior regions can be more accurately assessed.

Objective: To determine whether potential molecular-level variations in collagen molecules with annular region in lumbar intervertebral discs are accompanied by collagen fibres with differing tensile properties.

Hypothesis: Mechanical testing will reveal that samples from the posterior annulus will have a higher ultimate tensile strength based on the larger tensile stress the posterior annulus is subjected to physiologically as a result of compression and flexion.[42,48–52]

Chapter 3: Materials and Methods

3.1 The Ovine Lumbar Spine Model

While human lumbar spines would have been the ideal tissue for the research performed, the difficulties associated with acquiring the necessary volume of lumbar spines from healthy, young individuals ruled out the use of human tissue for this project. The ovine lumbar spine serves as an appropriate model of the human lumbar spine.

3.1.1 Tissue Collection and Dissection

Lumbar spines from mature ewes (24+ months old) were collected from a local abattoir (Northumberlambs Lamb Marketing Co-Op Ltd, Nova Scotia, Canada) within 24 hours of slaughter. Slaughtered ewes were stored in an industrial refrigerator until the time of collection. The lumbar spines were transported back to the laboratory in a chilled cooler and then stored in a refrigerator until processing. Lumbar spines were dissected into vertebra-disc-vertebra segments within 24 hours of retrieval. In order to obtain the desired segments, a cut was made in the transverse plane of each lumbar vertebra to break the spine down into smaller segments (Figure 3.1A). Next, the posterior elements – including the spinal cord – were removed from each dissected segment by making a single cut in the coronal plane at the pedicles (Figure 3.1B), producing the desired vertebra-disc-vertebra segments (Figure 3.1C). These segments were then wrapped in phosphate-buffered saline-soaked gauze and then stored at -86 ºC in freezer bags.

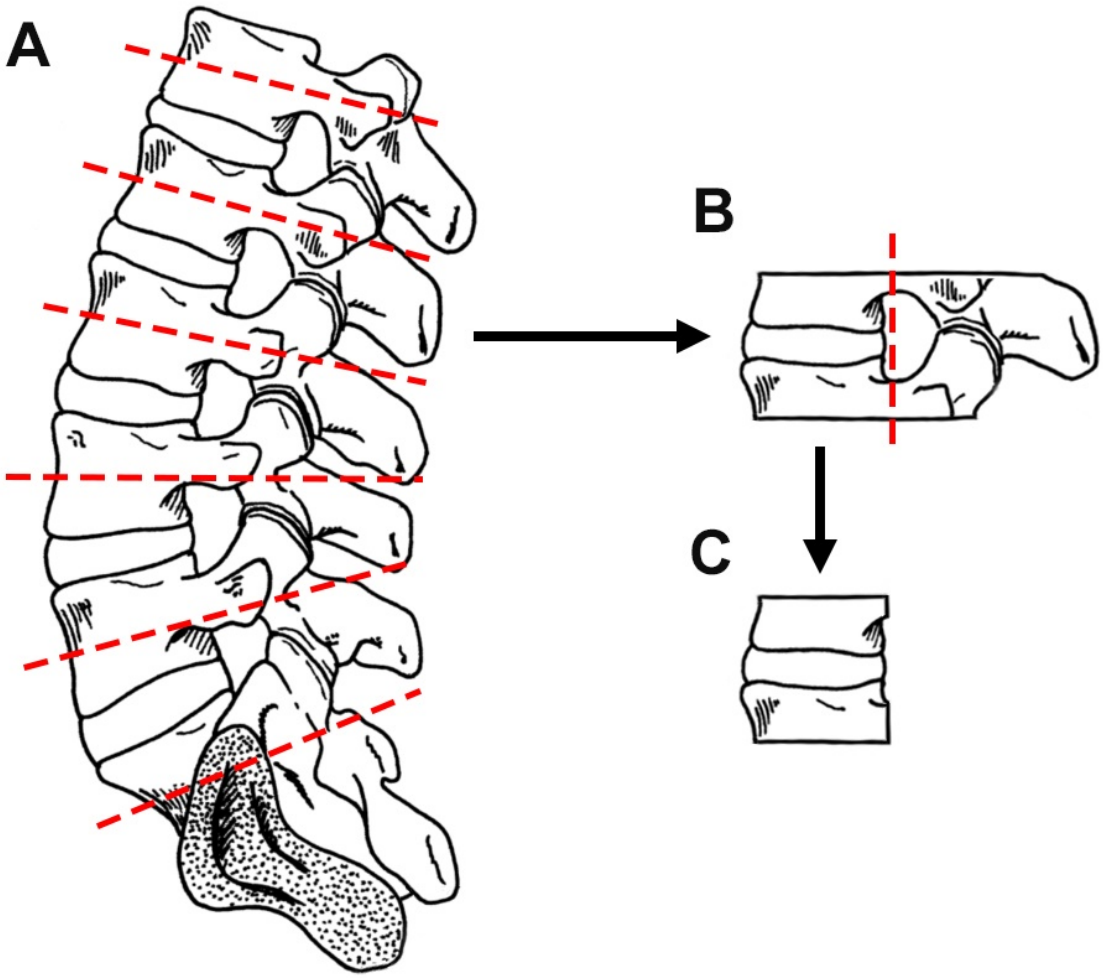

Figure 3.1: The method of dissecting vertebra-disc-vertebra segments from lumbar spines for storage at -86 ºC. A: A cut was made in the transverse plane of each lumbar vertebra in order to break the spine down into smaller segments. B: A second cut was made, this time in the coronal plane at the pedicles, in order to remove the posterior elements. C: The resulting vertebra-disc-vertebra segment stored at -86 ºC. Modified, with permission, from Rodrigues.[5]

3.1.2 Comparison of Ovine and Human Lumbar Spines

The ovine lumbar spine is commonly used as a model for the human cadaveric spine for spinal research due to many similarities existing in both species.[93–95] Although the ovine lumbar spine commonly contain either six or seven lumbar vertebrae (in contrast to the five vertebrae that make up the human lumbar spine) the spines of both species otherwise

share comparable gross anatomy and biomechanical performance.[96,97] While the human spine is loaded primarily in axial compression – much like a vertical column – quadrupedal animals have lumbar spines that are aligned horizontally. Yet, despite the difference in alignment, the lumbar spine of a quadrupedal animal is also primarily loaded in axial compression.[98] This can be explained by considering the tensile forces from the muscles and ligaments of the trunk, which stabilize the spine by placing it in axial compression so that it is able to resist bending from the force of gravity.[98] These observations have been confirmed by evaluating the structure of trabecular bone in the vertebral bodies of quadrupedal animals. The structure of bone remodels over time in response to the mechanical stress it is exposed to – a phenomenon described by Wolff's Law.[99] The trabecular bone in the vertebrae of quadruped animals consists of tall, vertically-aligned struts that span from endplate to endplate – as found in human vertebrae[2] – thus confirming that they are subjected to axial compression.[98]

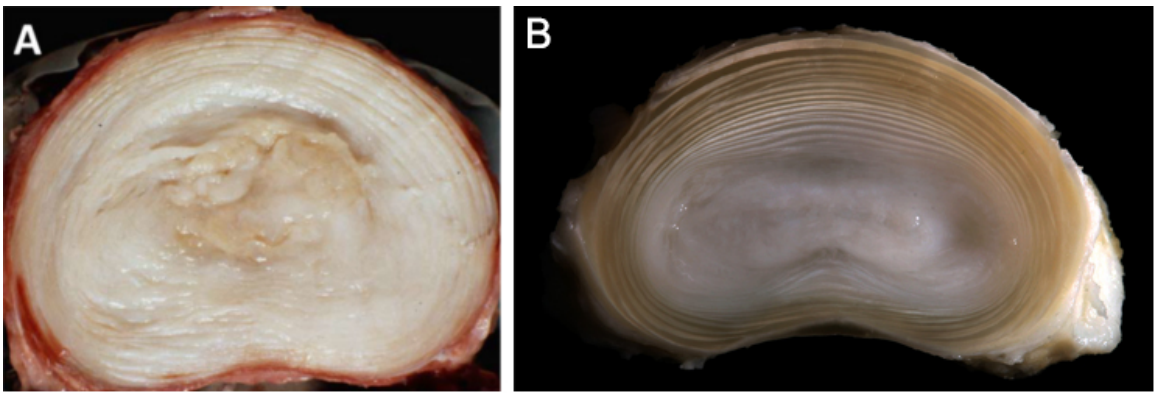

Figure 3.2: Transverse sections of: a middle-aged human lumbar disc (level not specified) (A) and a skeletally-mature L5-6 ovine lumbar disc (B) illustrating the shared kidney-bean shape. A: Modified, with permission, from Adams.[100] B: Modified, with permission, from Veres.[15]

In terms of microstructure, the ovine lumbar intervertebral disc is largely comparable to the human lumbar disc. Although the ovine lumbar disc is smaller than the human disc, both discs share the same distinct kidney-bean shape (Figure 3.2).[96,101] The anterior annulus of both species contain more lamellae and thicker lamellae when compared to their posterior sides, and both species exhibit incomplete lamellae throughout their

annulus.[15] Moreover, the orientation of collagen fibres within lamellae in the ovine lumbar disc are similar to the values reported for the human lumbar disc.[102] Cross bridges are also observed within the ovine annulus, sharing resemblance to those found in the human annulus (Figure 3.3A).[103] In terms of the cartilaginous endplate, both species share similar features (Figure 3.3B and Figure 3.4).[5,25,84] The calcified cartilage layer of the ovine cartilaginous endplate decreases in thickness as the radial depth decreases, and the uncalcified layer does not cover the entirety of the annulus, as observed within human intervertebral discs.[25] Moreover, annulus fibres in the outer annulus anchor directly with subchondral bone within the vertebral endplate in both species (Figure 3.3C and Figure 3.4). In addition to the cartilaginous endplates, the vertebral endplates of both are also similar (Figure 3.3B and Figure 3.3C).[5,25,84] The biochemical composition of the skeletally-mature ovine disc also compares favorably to the mature human lumbar disc in terms of collagen content, glycosaminoglycan content, and water content for both the annulus and the nucleus.[102,104,105]

An important difference exists between species related to the development of the vertebral bodies. Unlike in the human vertebral body, where the growth plate is located between the cartilaginous endplate and the vertebral endplate,[106,107] the ovine growth plate is located within the vertebral body, and is thus offset from the vertebral endplate by a layer of trabecular bone.[15,107] The growth plates of both species are remodelled over time and fuse with the rest of the vertebral bodies once skeletal maturity is reached. For sheep, this age corresponds to approximately 24 months old.[15] In humans, growth plate remodelling gives rise to the apophyseal ring – the raised rim at the periphery of the vertebral endplate.[36] Despite these differences during development, the topography of the ovine vertebral endplate shares a raised rim much like the apophyseal ring found in human discs, making them comparable.[15] It has, however, been shown that an unfused or partially fused ovine growth plate (i.e. skeletally immature) can significantly alter the failure mode in response to excessive loading, illustrating the importance of ensuring skeletal maturity has been reached in both species.[15]

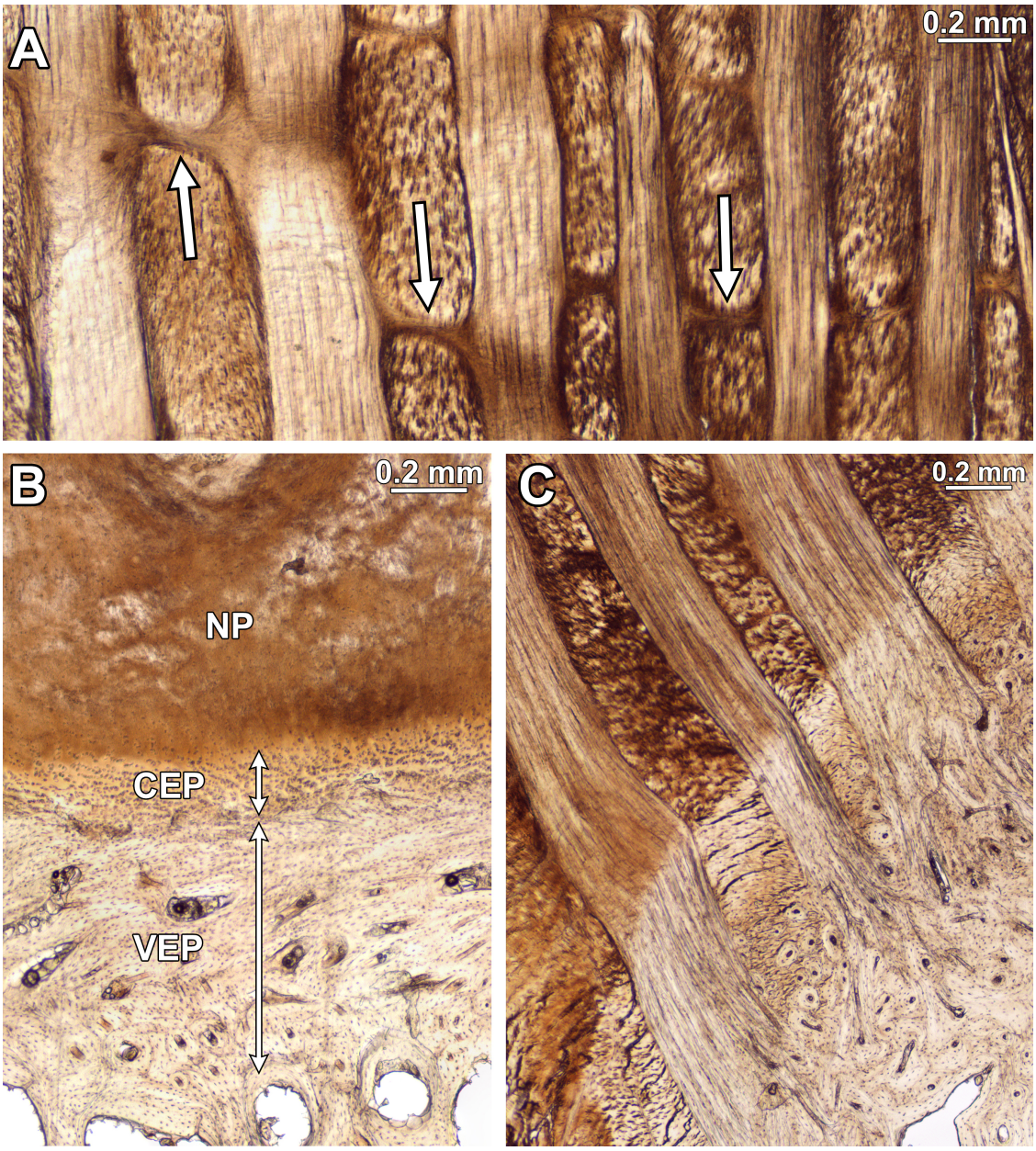

Figure 3.3: Microstructure of the ovine intervertebral disc. A: Differentiation between in-plane lamellae (fibres parallel to the plane of the image), out-of-plane lamellae (fibres oriented at a steep angle out of the plane of the image), and cross-bridges (indicated by arrows). B: The interface between (i) the nucleus (NP) and the cartilaginous endplate (CEP), and (ii) the interface between the CEP and the vertebral endplate (VEP). C: Anchoring of lamellae in the outer annulus with the CEP. Images are unstained cryosections from L6-7 discs taken using transmission light microscopy.

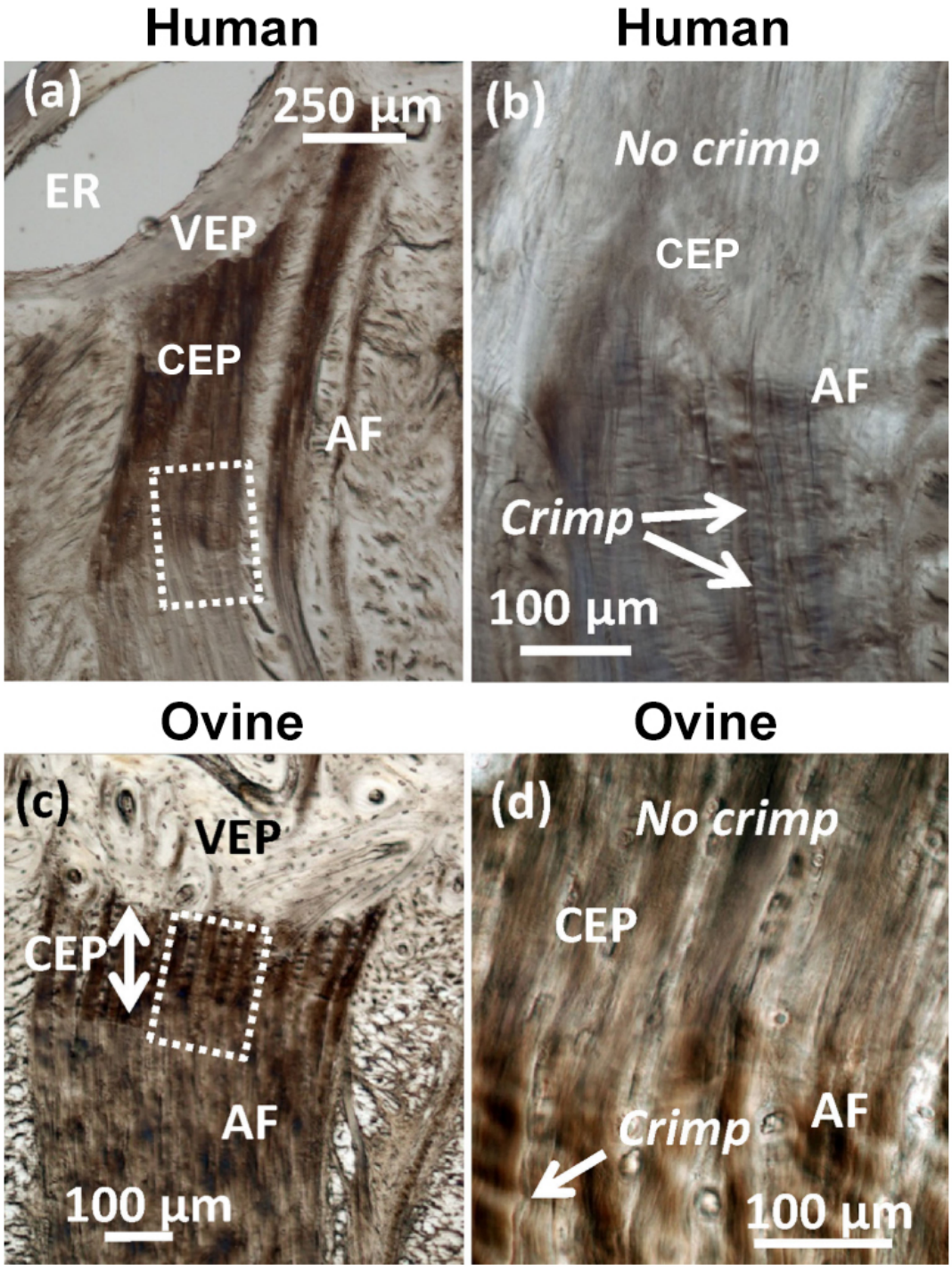

Figure 3.4: The anchorage of collagen fibres from the outer annulus with the vertebral endplate in the human disc (top row) and the ovine disc (bottom row). Both species result in a loss of crimp as collagen fibres enter the calcified region of cartilage. AF = annulus fibrosus; CEP = cartilaginous endplate; ER = epiphyseal ring; VEP = vertebral endplate. Images are unstained cryosections taken using DIC optical microscopy. Modified, with permission, from Brown.[25]

3.2 Hydrothermal Isometric Tension Testing

3.2.1 Untreated Samples

Vertebra-disc-vertebra segments were retrieved from storage at -86 ºC, taken out of their sealed bags, and thawed to room temperature (Figure 3.5A). Ten spines were tested using matched-pair L1-2 and L5-6 discs. All soft tissues from the anterior and posterior region of the segment were removed, including the posterior longitudinal ligament. A mini hacksaw was used to cut small rectangular bone-annulus-bone samples from the anterior and posterior regions of each segment at an oblique angle (measured using a digital bevel) parallel to one of the fibre-orientation angles (Figure 3.5). The angle of the oblique cut was 32° ± 5° from the transverse plane for anterior samples, and 39° ± 5° from the transverse plane for posterior samples, and were based on previously reported values for the annular fibre inclination at the discs periphery.[102] The average dimensions of the cross section for samples prepared (grouping anterior and posterior samples together) was 3.22 ± 0.54 mm in the circumferential direction and 5.21 ± 1.15 mm in the radial direction, as measured using digital calipers.

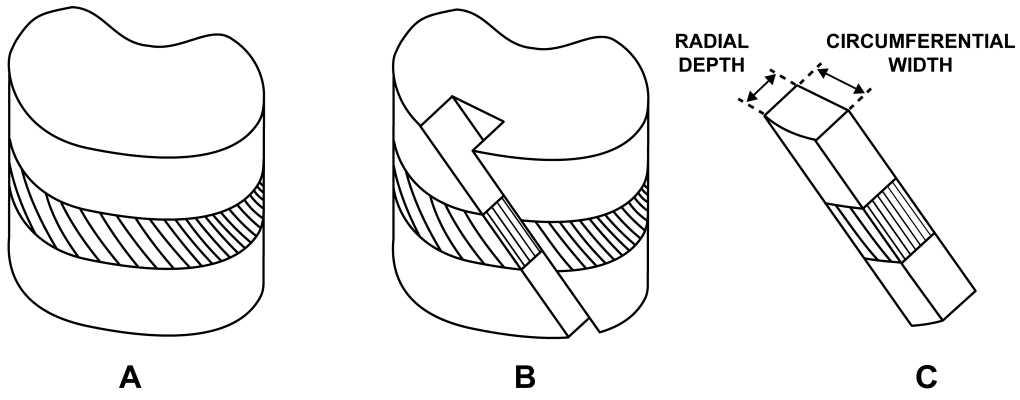

Figure 3.5: The method of preparing an anterior bone-annulus-bone sample for HIT analysis. A: The vertebra-disc-vertebra segment thawed to room temperature. B: The vertebra-disc-vertebra segment after cutting the rectangular bone-annulus-bone segment from the anterior region. A similar sample was also removed from the posterior portion of the segment. C: The bone-annulus-bone segment used for HIT testing.

HIT analysis was performed using a custom apparatus, as described previously.[108–110] Briefly, the samples were isometrically mounted longitudinally between a load cell and fixed support, and then submerged in a bath of room temperature distilled, deionized water. A tensile preload of 60 g was applied to each sample for a 10-minute period. Following the preload, the water was heated to 90 ºC using a hot plate, and then maintained at 90 ºC for five hours. During the temperature climb, the rate of temperature increase was approximately 1.6 ºC/min from 22 ºC to 75 ºC and 0.4 ºC/min from 75 ºC to 90 ºC. During the test, time, temperature, and load data were recorded at 0.2 Hz using LabVIEW (2010 Edition, National Instruments, USA).

Following testing, the acquired data was analyzed using Microsoft Excel (Version 1901, Microsoft, USA). Each sample's denaturation temperature (T_d) and half-time of load decay ($t_{1/2}$) were determined (Figure 3.6). The denaturation temperature is taken as the temperature corresponding to the initial onset of the continuous increase in force. To identify the half-time of load decay, the five-hour isothermal segment is first assumed to follow a Maxwell decay, as described previously.[108] The natural logarithm of the load divided by the maximum load is plotted against time, and a best-fit line is applied to a 5000-second data interval between 2,000 seconds and 17,000 seconds, where the average starting time for the 5000-second interval was 6474 ± 2765 seconds. The slope of the line (k) is then measured to allow for direct calculation of $t_{1/2}$ using the Maxwell Decay equation.[108] Statistical analysis was conducted using JMP (Version 14, SAS Institute, USA). Outlier analysis was used to exclude any samples that lay outside of the upper and lower quartiles by greater than ± 1.5x the inter-quartile range. Statistical differences between disc level and annular region for both T_d and $t_{1/2}$ were first tested using a two-way mixed model ANOVA with main effects (disc level and annular region), interaction effect, and random effect for spine included. For $t_{1/2}$, the data were rank transformed prior to the ANOVA to improve normality. Following the two-way ANOVA, a matched-pair t-test was performed on T_d data, while a Wilcoxon Sign Ranked test was performed on $t_{1/2}$ data.

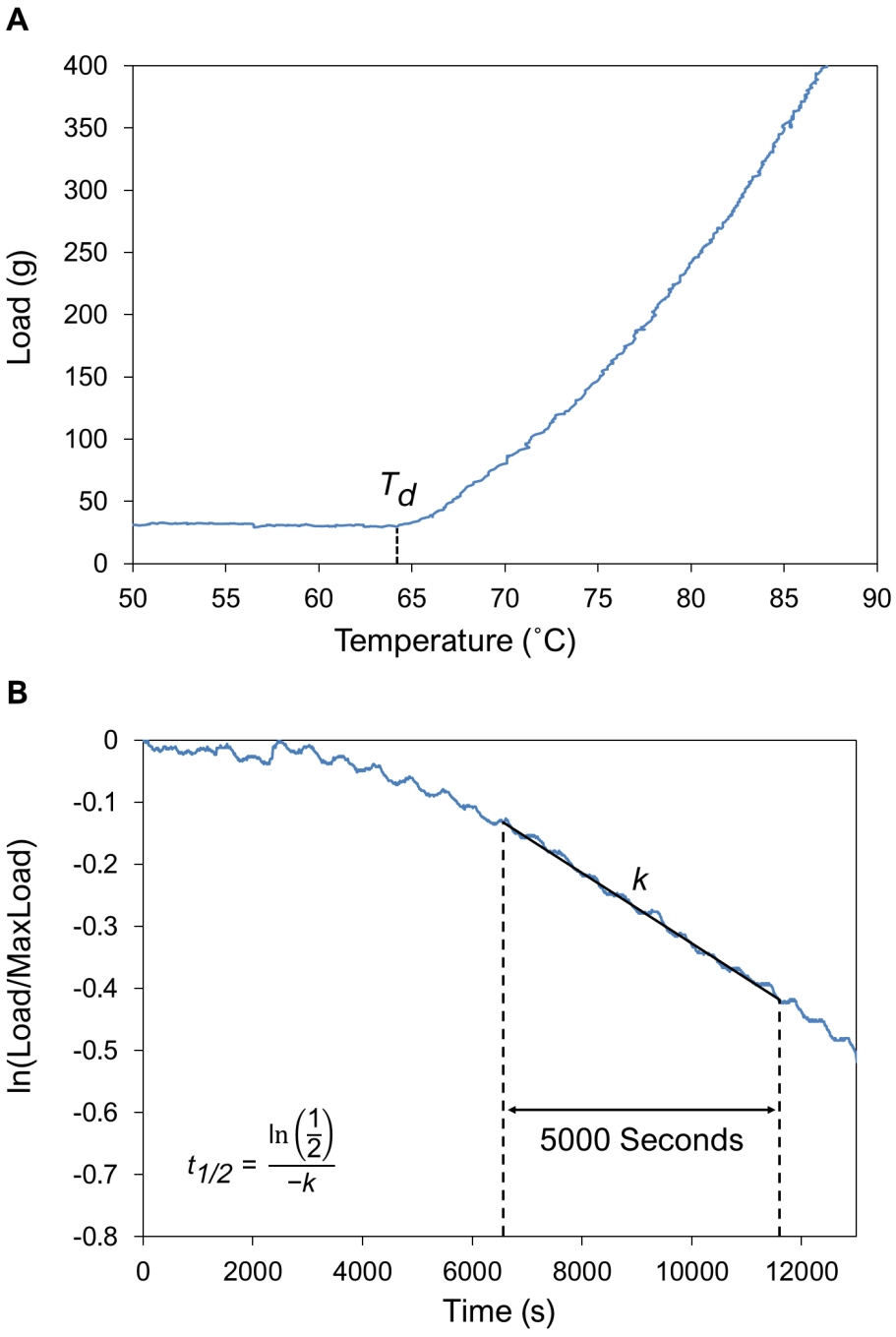

Figure 3.6: A depiction of the denaturation temperature (A) and the measurement of slope used in calculating the half-time of load decay (B). Data taken from the anterior region of an L1-2 disc.

3.2.2 $NaBH_4$ Treated Samples

Vertebra-disc-vertebra segments were retrieved from storage at -86 ºC and thawed to room temperature to prepare bone-annulus-bone samples using the method described in Section 3.2.1. For samples allocated to the sodium borohydride ($NaBH_4$) experiment, five spines were tested using matched-pair L1-2 and L2-3 discs. The average dimensions of the cross section for samples prepared (grouping anterior and posterior samples together) was 3.50 ± 0.56 mm in the circumferential direction and 4.40 ± 0.49 mm in the radial direction, as measured using digital calipers.

Following sample dissection, crosslink stabilization was conducted using sodium borohydride, as described previously.[89] Briefly, anterior and posterior samples from each L1-2 disc underwent four 15-minute treatments in fresh 100 mL borate buffer solution containing 0.1 mg/mL $NaBH_4$ (pH = 9.0) with constant agitation at 4 ºC, followed by three 10-minute agitated rinses in distilled, deionized water at 4 ºC. The matching anterior and posterior samples from the L2-3 disc of the same spine – used as controls – underwent four 15-minute rinses in fresh 100 mL borate buffer solution (pH = 9.0) with constant agitation at 4 ºC, followed by using three 10-minute agitated rinses in distilled, deionized water at 4 ºC. HIT tests were then performed to determine the samples $t_{1/2}$ values using the method described in Section 3.2.1. To ensure that the $NaBH_4$ treatment was working as intended, samples from bovine forelimb extensor tendons, known to contain predominantly thermally-labile crosslinks, were used to validate the treatment process. The extensor tendon samples included with the $NaBH_4$ treatments confirmed the efficacy of the treatment process, showing stabilization of the heat labile crosslinks, consistent with previously reported results.[90] Statistical analysis was conducted using JMP. Outlier analysis was used to exclude any samples that lay outside of the upper and lower quartiles by greater than ± 1.5x the inter-quartile range. Statistical differences between disc region and $NaBH_4$ treatment were first tested using two-way mixed model ANOVA with main effects (annular region and treatment), interaction effect, and random effect for spine included, followed by matched-pair t-tests.

3.3 Differential Scanning Calorimetry

Vertebra-disc-vertebra segments were retrieved from storage at -86 ºC, taken out of their sealed bags, and thawed to room temperature (Figure 3.7A). Nine spines were tested, using one disc per spine (four L4-5 discs and five L5-6 discs). All soft tissues from the anterior and posterior region of the segment were removed, including the posterior longitudinal ligament. A mini hacksaw was used to cut small rectangular bone-annulus-bone samples from the anterior and posterior regions of each segment (Figure 3.7) as described in Section 3.2. The average dimensions of the cross section of posterior samples were 4.77 mm in the circumferential direction and 5.16 mm in the radial direction, while the average dimensions of anterior samples were 4.78 mm in the circumferential direction and 6.89 mm in the radial direction (as measured using digital calipers). Samples were then stored overnight at 4 ºC in fresh distilled, deionized water (using 50 mL Falcon tubes). The next day, the annulus from each sample was separated from the bone using a razor blade (Figure 3.7D). The posterior annulus was subdivided into two radial categories (outer and inner) while the anterior annulus was subdivided into three radial categories (outer, mid, and inner). For both regions, two samples from the inner and outer regions were taken for subsequent testing. Hermetic aluminum pans (DSC Consumables) were used for testing and were weighed prior to sample preparation. Excess water was removed from the surface of the samples by dragging samples lightly across a cutting board. Each sample was weighed (average wet weight: 10.43 ± 1.33 mg) and then gently pressed into the bottom of the aluminum pan to maximize the pan/sample contact area. Pans containing samples were then hermetically sealed.

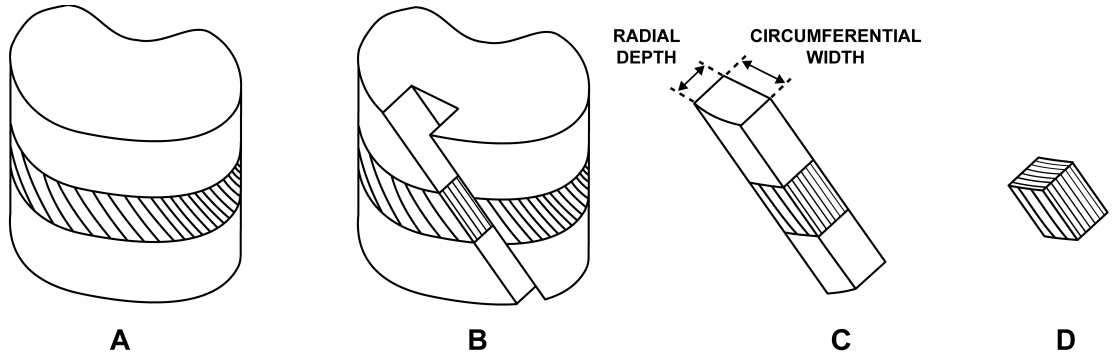

Figure 3.7: The method of preparing the annulus for DSC. A: The vertebra-disc-vertebra segment thawed to room temperature. B: The vertebra-disc-vertebra segment after cutting the rectangular bone-annulus-bone segment from the anterior region. A similar sample was also removed from the posterior portion of the disc. C: The bone-annulus-bone segment cut from the vertebra-disc-vertebra segment. D: The annulus separated from the bone-annulus-bone segment.

A Q200 differential scanning calorimeter (TA Instruments) was used for testing. An Indium standard was used for calibration prior to testing. Sample pans were tested alongside an empty hermetically sealed aluminum pan. Samples were equilibrated at 30 ºC, and then ramped to 90 ºC at a rate of 5 ºC/min. Following testing, sample pans were pierced (to allow moisture to escape) and placed in a vacuum desiccator. The mass of each pan was measured every 24 hours in order to determine the dry weight of the sample (which was concluded once the mass of the pan remained constant between measurements).

Endotherms were analyzed between 55 ºC and 85 ºC using Universal Analysis 2000 software (Version 4.5A, TA Instruments, USA), as shown in Figure 3.8. The onset temperature (T_{onset}), peak temperature (T_{peak}), full-width at half-maximum ($FWHM$), the total specific enthalpy of denaturation ($\Delta h = \Delta h_{left} + \Delta h_{right}$) based on dry sample weight, and the water content of each sample (using the sample's wet mass and dry mass) were determined. To quantify the behavior on the right-hand side of the endotherm, two additional parameters were determined – the specific enthalpy corresponding to the right-hand side of the endotherm (Δh_{right}), and the skewness index. The onset temperature is taken as the temperature corresponding to the intersection of (i)

the tangent line to the inflection point of the curve corresponding to the steep increase in differential heat flow segment, and (ii) the linear baseline drawn between 55 ºC and 85 ºC. The peak temperature is taken as the temperature corresponding to the maximum heat flow. The full-width at half-maximum measures the temperature difference at the half-peak height of differential heat flow relative to the baseline. The specific enthalpy measures the area under the linear baseline between 55 ºC and 85 ºC. The area corresponding to the specific enthalpy was split in half by inserting a line perpendicular to the linear baseline at the temperature correspond to the peak temperature, allowing for calculation of the specific enthalpy corresponding to the right-hand side of the endotherm. The skewness index of the endotherm[111] was taken by dividing the specific enthalpy of the right-hand side by the total enthalpy. Statistical analysis was conducted using JMP software. Data for replicate subsamples tested (for each combination of annular region and radial depth) were averaged. Outlier analysis was used to exclude any samples that lay outside of the upper and lower quartiles by greater than ± 1.5x the inter-quartile range. Statistical differences between annular region and radial depth were tested using two-way mixed model ANOVA's (after T_{onset}, T_{peak}, and $FWHM$ were rank transformed) with main effects (annular region and radial depth), interaction effect, and random effect for spine included. Matched-pair t-tests were then used on $FWHM$, water content and the skewness index.

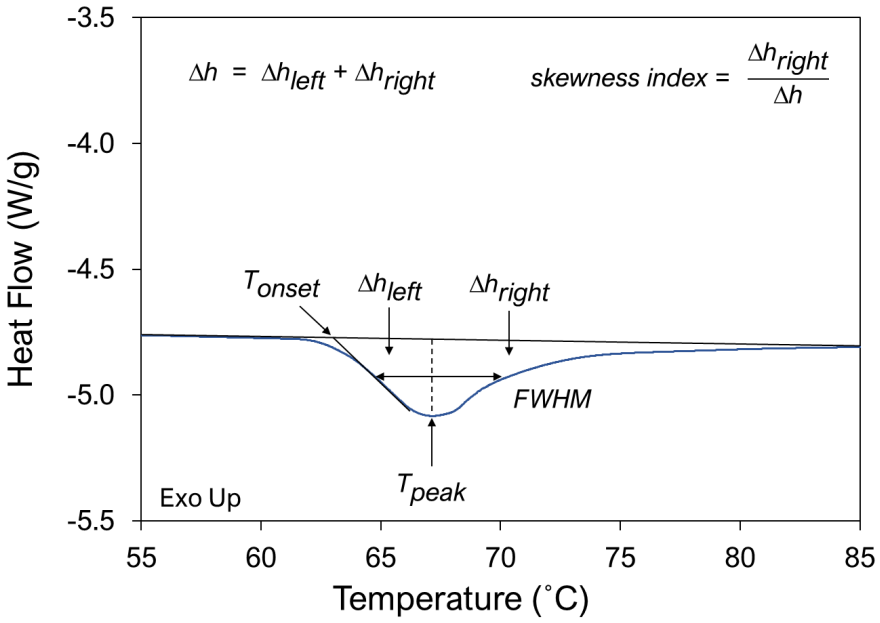

Figure 3.8: A depiction of the parameters measured from the endotherms produced from DSC. Data taken from the outer anterior region of an L4-5 disc.

3.4 Mechanical Testing and Light Microscopy

Vertebra-disc-vertebra segments were retrieved from storage at -86 ºC, removed from their sealed bags, and thawed to room temperature (Figure 3.9A). 13 discs – each from a different spine – were used for testing (totaling five L5-6 discs and eight L6-7 discs). Throughout preparation, the hydration of samples was maintained using a spray-bottle containing room-temperature PBS. All soft tissues were carefully removed from the anterior and posterior regions of the segment, including the posterior longitudinal ligament. A mini hacksaw was used to make a cut in the coronal plane to separate the anterior from the posterior (Figure 3.9B). Two 9/16" holes were drilled through the superior and inferior vertebral bodies – oriented in alignment with one of the fibre-orientation angles[102] – for subsequent mounting (Figure 3.9C). Once the holes had been created, the lateral sides of the annulus were severed using a razor to isolate the annulus located between the drilled holes (Figure 3.9C).

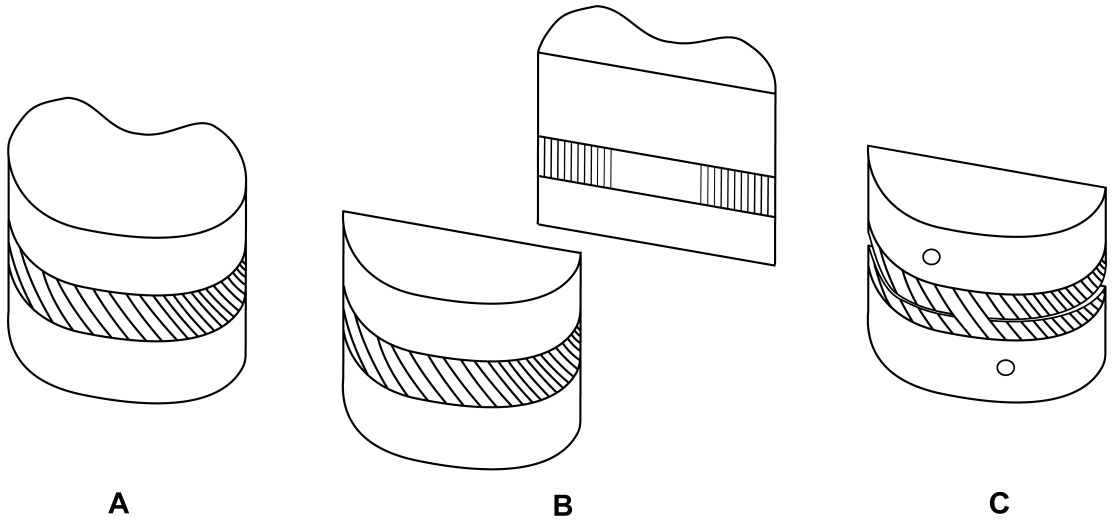

Figure 3.9: The method of preparing a sample for mechanical testing. A: The vertebra-disc-vertebra segment thawed to room temperature. B: The vertebra-disc-vertebra segment after making a cut in the coronal plane to separate the anterior region from the posterior region. C: The anterior sample after drilling a hole in each vertebra and severing the lateral sides of the annulus. The posterior sample retrieved from the vertebra-disc-vertebra segment was prepared in a similar way.

Using digital calipers, the radial depth – taken at the center of the anterior and posterior region (Figure 3.10A and Figure 3.10B) – as well as the circumferential width (Figure 3.10C) were measured. The average radial depth was 5.06 ± 1.13 mm for posterior samples and 13.45 ± 1.37 mm for anterior samples, while the average circumferential width was 2.03 ± 0.18 mm for anterior samples and 3.15 ± 0.42 mm for posterior samples.

A servo-hydraulic hydraulic material testing system (MTS) controlled using LabVIEW was used for mechanical testing. Samples were mounted to custom grips using screws. The screws were tightened only to the initial point of contact with the vertebral bodies, allowing the samples to rotate during testing. The load cell was zeroed prior to sample mounting. A video capture system was used to record all tests performed. Samples were pulled to failure at a slow displacement rate of 0.01 mm/sec. Time, displacement, and force data were recorded using LabVIEW. Samples were kept hydrated using a drip-feed of room-temperature PBS throughout testing.

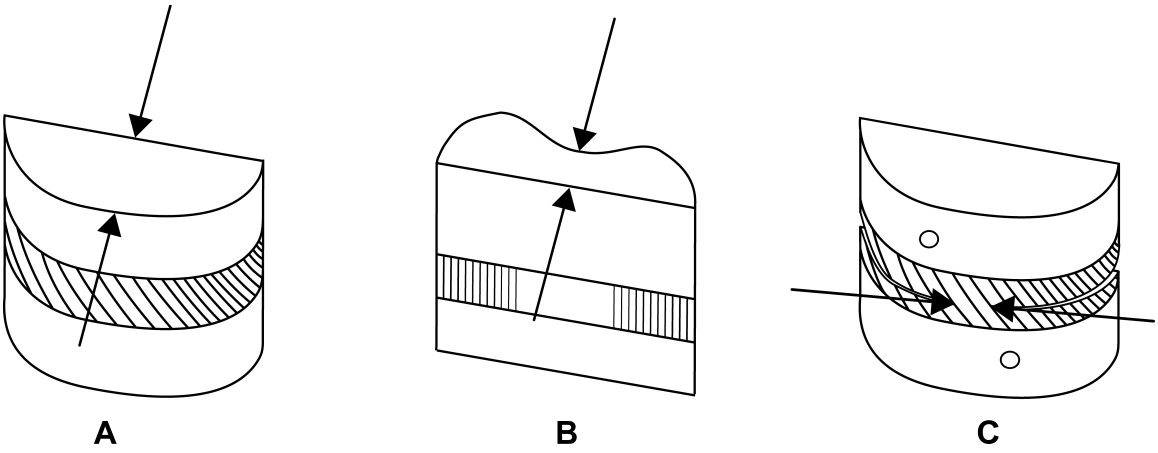

Figure 3.10: The measurements of radial depth for anterior samples (A) and posterior samples (B), as well as the measurement of circumferential width (C) for samples allocated to mechanical testing.

Following mechanical testing, samples immediately underwent chemical fixation for seven days using 10% neutral-buffered formalin. Following fixation, samples were decalcified by being placed in 10% formic acid under agitation for two weeks. Once samples were decalcified, they were stored in 10% formalin for a maximum of eight weeks.

To prepare samples for optical microscopy, cryogenic sectioning was performed. Samples were trimmed using a razor blade to isolate the region of the sample located between the holes that had been drilled into the vertebral bodies (Figure 3.11B). A small amount of the region containing the severed annulus on the lateral sides of each sample was kept intact in order to distinguish the damaged region from the undamaged region. Samples were mounted to a metal platform using optimal cutting temperature compound and placed in liquid nitrogen for up to 30 seconds to freeze the sample. Once frozen, samples were cut into approximately 30 μm thick sections using a sliding microtome (Figure 3.11C). The sectioned samples were cut on an oblique angle (measured using a digital bevel) parallel to one of the fibre-orientation angles.[102] Sectioned samples were wet-mounted on glass slides, covered using a cover slip, and imaged using a Nikon Eclipse E600 light microscope (Nikon) equipped with a 10-megapixel digital camera

(AmScope) within 24 hours of cryo-sectioning. For each slice, overlapping images at 4x magnification were taken until the entire surface of the sample had been captured.

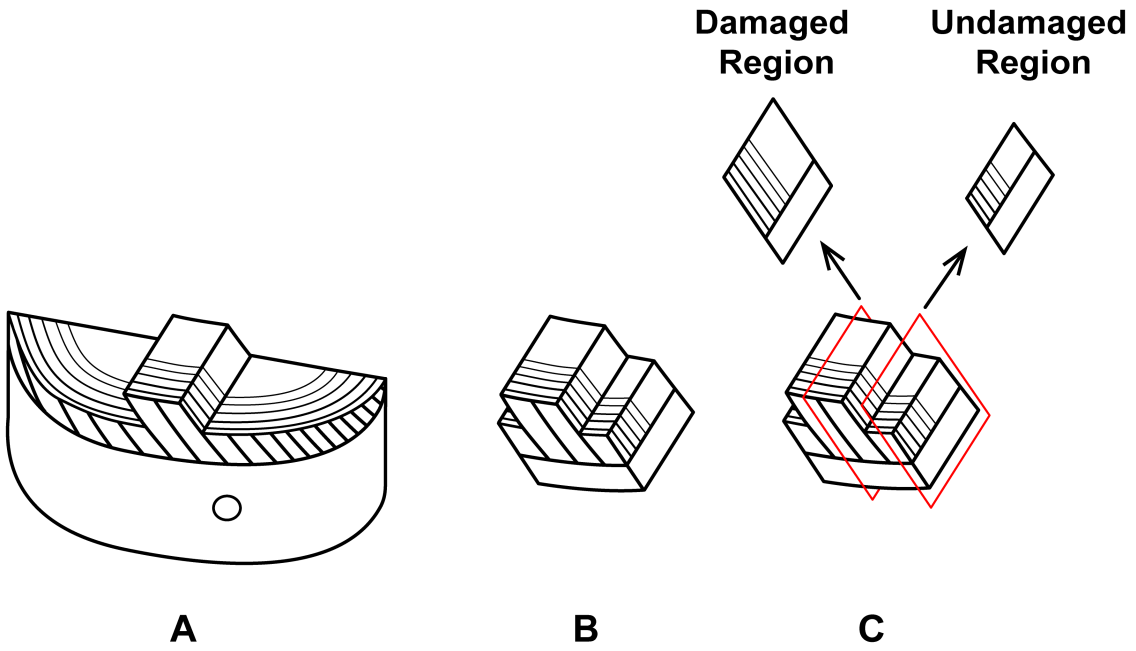

Figure 3.11: The method of preparing samples for light microscopy. A: One-half of a ruptured sample following mechanical testing which underwent chemical fixation using 10% formalin and decalcification using 10% formic acid. B: Following decalcification, the sample was trimmed in preparation for sectioning using a sliding microtome. C: 30 µm thick sections were taken from the damaged region (corresponding to the tissue that was ruptured) and the undamaged region (corresponding to the tissue that was severed using a razor blade)

A panoramic of each imaged cryosection was assembled from the individual micrographs using PTGui (Version 10.0.15 Pro, New House Internet Services BV, Netherlands). The annular radial thickness for each slice free of damage (obtained from the lateral sides of the sample, see Figure 3.11C) was measured using ImageJ (Version 1.51j8, National Institutes of Health, USA). The line used to measure the annular radial thickness bordered the cartilaginous endplate such that it was perpendicular to the largest number of lamellae (Figure 3.12). For each sample, the annular radial thickness was then determined by averaging together all measured slices free of damage for that sample.

The stiffness, stress-displacement slope, ultimate tensile strength of the annulus (omitting the area contributed by the nucleus) and the tension strength of the annulus wall were calculated using Microsoft Excel. The stiffness was taken as the slope corresponding to the linear portion of the force-displacement plot. The stress-displacement slope was taken as the slope corresponding to the linear portion of the stress-displacement plot. The ultimate tensile strength was taken as the maximum force obtained during testing divided by the product of (i) the annular radial thickness measured using ImageJ, and (ii) the circumferential width (Figure 3.10C). The tension strength of the annulus wall was taken as the maximum force obtained during testing divided by the circumferential width (Figure 3.10C). Statistical analysis was conducted using JMP software. Outlier analysis was used to exclude any samples that were ± 1.5x the inter-quartile range. Statistical differences between the anterior and posterior annular regions were determined using matched-pair t-tests. Samples containing an unfused or partially-fused growth-plate (a sign that the animal had not reached skeletal maturity[15]) – as well as samples that failed due to cracks developing within the vertebral body – were omitted from statistical analyses related to the calculations of mechanical properties. The proportions of different categories of damage observed in anterior and posterior samples were compared using Fisher's exact test (2-tail). For the Fisher's exact tests performed, samples that had growth plates that hadn't completed fused (which had been excluded from the mechanical properties' analyses) were included for this assessment of failure morphology. Only the samples that had failed due to cracks that had developed in their vertebral bodies (a sign of early failure) were omitted from the Fisher's exact tests performed.

Figure 3.12: Representative measurements of the annular radial thickness for anterior samples (A) and posterior samples (B) for samples allocated to mechanical testing. Measurements are taken only counting lamellae that are clearly integrated with the cartilaginous endplate. Images are unstained cryosections taken from the same L6-7 disc using transmission light microscopy.

Chapter 4: Results

For all results (including figures and tables), numerical data are presented as mean ± standard deviation.

4.1 Hydrothermal Isometric Tension Testing

4.1.1 Untreated Samples

In order to assess crosslinking of collagen molecules with annular region and disc level, HIT analysis was performed on untreated anterior and posterior samples from L5-6 and L1-2 discs. Of the ten spines prepared, several samples were lost due to testing errors and problems encountered during sample preparation. The number of samples with T_d and $t_{1/2}$ parameters successfully measured with respect to annular region and disc level are listed in Table 4.1. Representative HIT responses are shown in Figure 4.1.

Table 4.1: The number of samples successfully measured for each HIT analysis parameter

Parameter	Disc Level	Anterior	Posterior
T_d	L5-6	n = 9	n = 8
	L1-2	n = 10	n = 9
$t_{1/2}$	L5-6	n = 6	n = 8
	L1-2	n = 9	n = 9

For T_d, ANOVA results revealed that annular region was a significant factor ($p < 0.0001$, Figure 4.2A), while disc level was not ($p = 0.1391$). The same was true for $t_{1/2}$: annular region was a significant factor ($p = 0.0025$, Figure 4.2B), while disc level was not ($p = 0.2943$). Based on the ANOVA results, the disc levels were pooled (Table 4.2), and the paired differences between the anterior and posterior regions of each disc for T_d and $t_{1/2}$ data were calculated. Paired differences were then averaged across disc level (when both

levels were present) to yield only one value for T_d and $t_{1/2}$ per spine. A matched-pair t-test was performed on T_d while a Wilcoxon Signed Rank test was performed on $t_{1/2}$, revealing that both T_d and $t_{1/2}$ were significantly greater for the posterior annulus compared to the anterior annulus (Table 4.2).

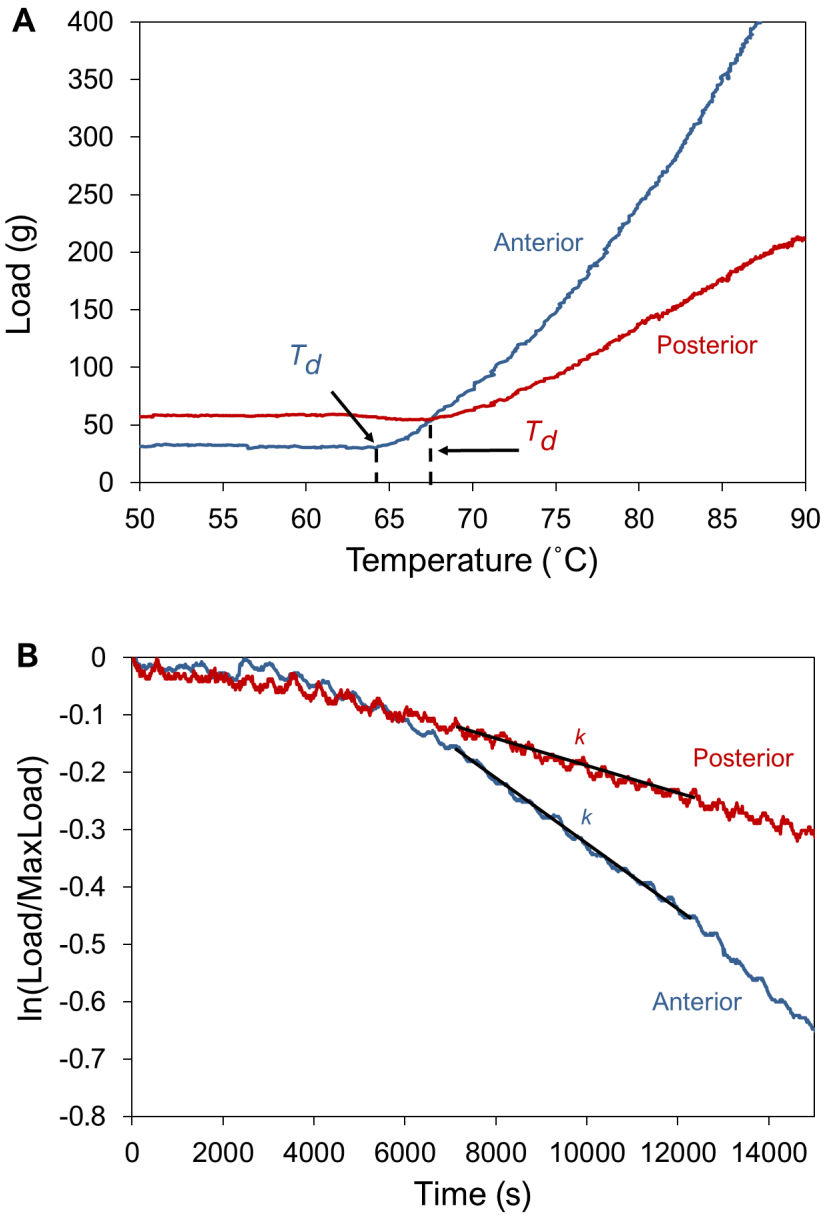

Figure 4.1: Representative HIT responses during the temperature rise to 90 ºC (A) and the five-hour isothermal segment (B) for anterior and posterior samples taken from the same L1-2 disc.

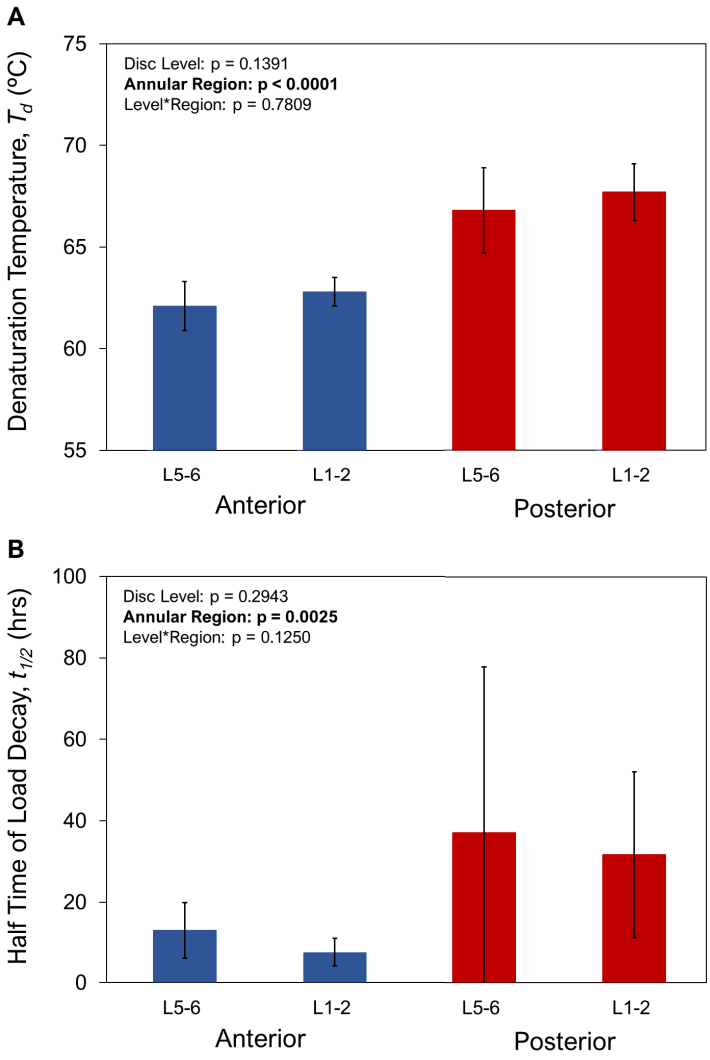

Figure 4.2: The variations in the denaturation temperature (A) and the half-time of load decay (B) for untreated samples when grouped by annular region and disc level.

Table 4.2: The variations in the denaturation temperature and the half-time of load decay for untreated samples when disc levels are pooled together.

	Anterior (L5-6 & L1-2)	Posterior (L5-6 & L1-2)	
T_d (˚C)	62.6 ± 0.7 (n = 10)	67.2 ± 1.2 (n = 9)	$p < 0.0001$
$t_{1/2}$ (hrs)	9.4 ± 4.6 (n = 8)	32.7 ± 23.7 (n = 9)	$p = 0.0156$

4.1.2 Sodium Borohydride Experiment

In order to assess total crosslinking, HIT analysis was repeated using samples from L1-2 discs treated with $NaBH_4$ and untreated samples from L2-3 discs (from the same spines as the matching L1-2 discs) that served as controls. ANOVA results revealed that annular region was a significant factor ($p < 0.0001$), while treatment was not ($p = 0.5004$). As an additional confirmation, paired differences in $t_{1/2}$ between $NaBH_4$-treated samples and untreated samples were calculated for both the anterior and posterior regions. Matched-pair t-tests were then performed, confirming that neither annular region was affected by treatment ($p = 0.1854$ for the anterior and $p = 0.7791$ for the posterior). The results obtained from the $NaBH_4$ HIT experiment are summarized in Figure 4.3.

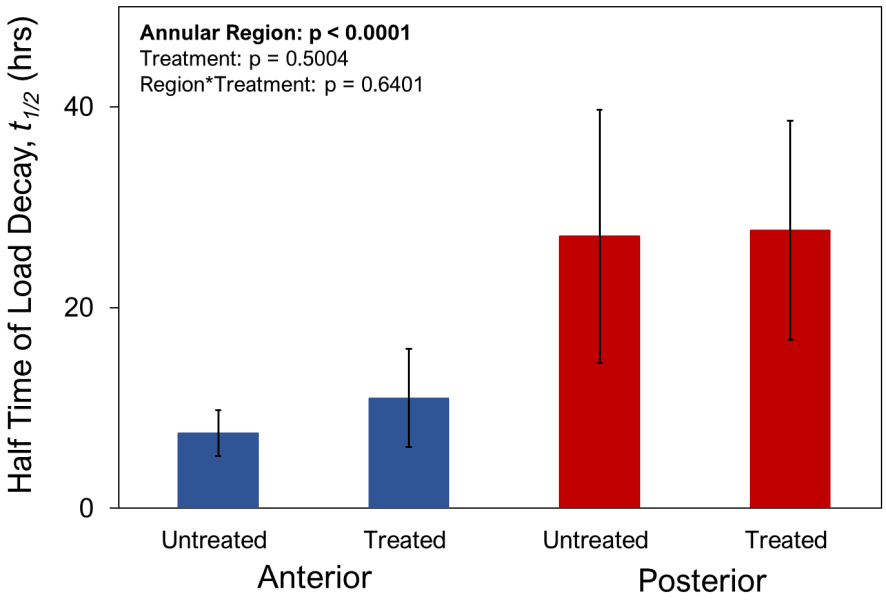

Figure 4.3: The variations with annular region and treatment in the parameters measured from the $NaBH_4$ HIT experiment.

4.2 Differential Scanning Calorimetry

In order to assess the thermal stability of collagen molecules with annular region and radial depth, DSC was performed. Samples were taken from L4-5 and L5-6 discs, with only one of these discs used per spine. Of the nine spines prepared for DSC, each spine had one or more samples that had data omitted due to errors encountered in the endotherms produced. After averaging replicate subsamples, the number of successful measurements for each DSC parameter with respect to annular region and radial depth are listed in Table 4.3. Representative DSC responses are shown in Figure 4.4.

Table 4.3: The number of samples successfully measured for each DSC parameter.

Parameter	Radial Depth	Anterior	Posterior
T_{onset}	Outer	n = 8	n = 8
	Inner	n = 8	n = 9
T_{peak}	Outer	n = 8	n = 8
	Inner	n = 8	n = 9
$FWHM$	Outer	n = 8	n = 8
	Inner	n = 8	n = 9
Δh	Outer	n = 8	n = 8
	Inner	n = 7	n = 8
Δh_{right}	Outer	n = 8	n = 8
	Inner	n = 7	n = 7
Skewness Index	Outer	n = 8	n = 8
	Inner	n = 7	n = 7
Water Content	Outer	n = 8	n = 8
	Inner	n = 7	n = 8

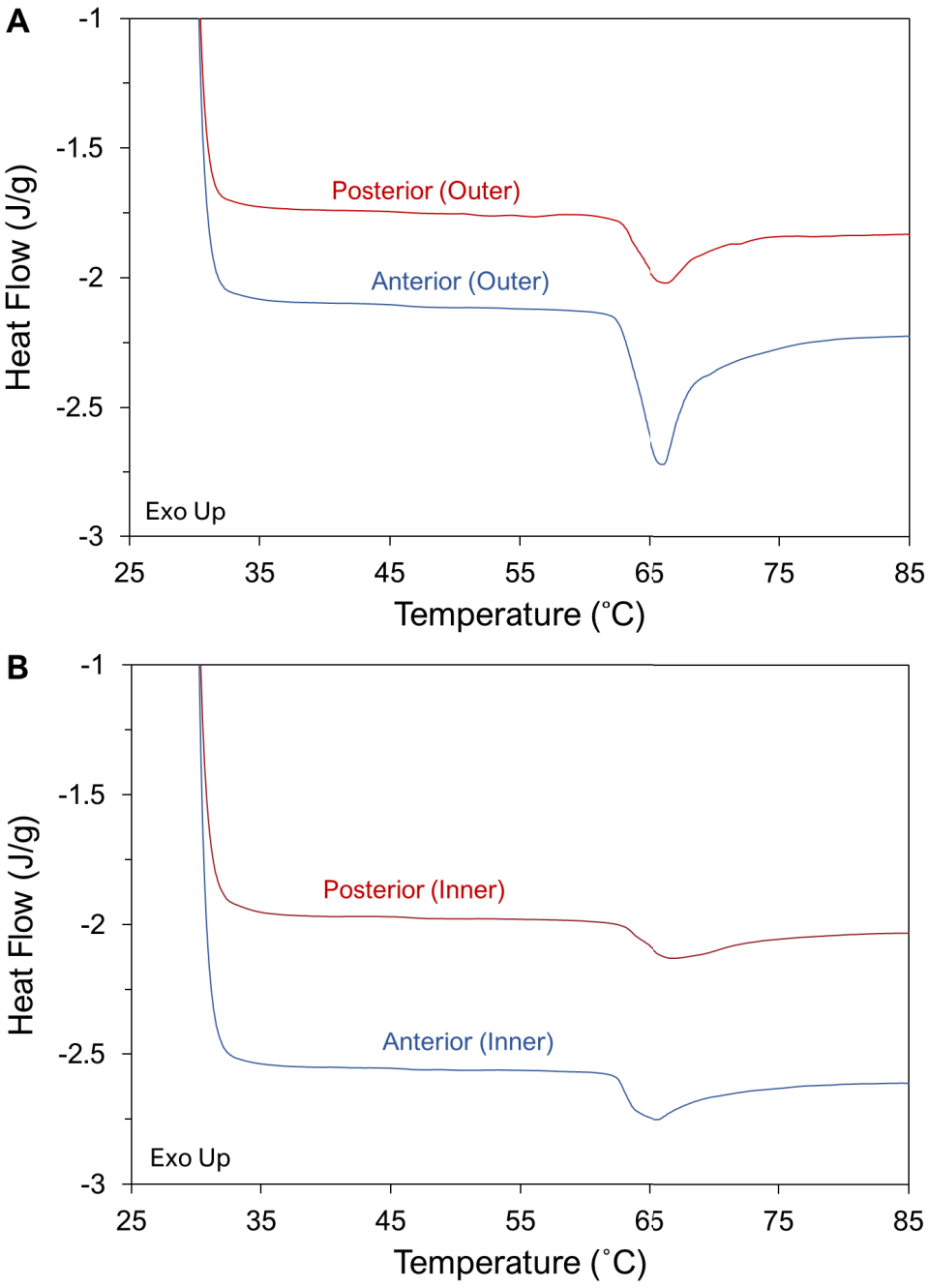

Figure 4.4: Representative endotherms for the outer annulus (A) and the inner annulus (B) for samples allocated to the DSC experiment. Data taken from the same L5-6 disc.

For T_{onset}, ANOVA results revealed that while annular region was not significant (p = 0.5806), radial depth was much closer to reaching significance (p = 0.0607, Figure 4.5A). In contrast, while radial depth was not a significant factor for T_{peak} (p = 0.9108), annular region was closer to reaching significance (p = 0.0731, Figure 4.5B). The ANOVA results for $FWHM$ revealed that annular region, radial depth, and the interaction between annular region and radial depth were all significant (p = 0.0202, p = 0.0068, and p = 0.0196, respectively – see Figure 4.5C and Figure 4.6). For Δh, ANOVA results revealed that neither annular region or radial depth were significant (p = 0.9390 and p = 0.5696, respectively, see Figure 4.5D). For the skewness index, however, while annular region was not a significant factor (p = 0.1345), radial depth was (p = 0.0080, Figure 4.5E). Based on the ANOVA results, the annular regions were pooled, and the paired differences between the inner annulus and the outer annulus for the skewness index were calculated. Paired differences were then averaged across annular region to yield only one value of the skewness index per spine. The matched-pair t-test subsequently performed showed that skewness index was close to being significantly larger in the outer annulus (p = 0.0704, Table 4.4). For water content, the ANOVA results revealed that radial depth was a significant factor (p = 0.0003), but annular region was not (p = 0.0650, Figure 4.5F). When the paired differences were calculated and then averaged across annular region, the matched-pair t-test performed revealed that the water content of the inner annulus was significantly greater than the outer annulus (p = 0.0110, Table 4.4).

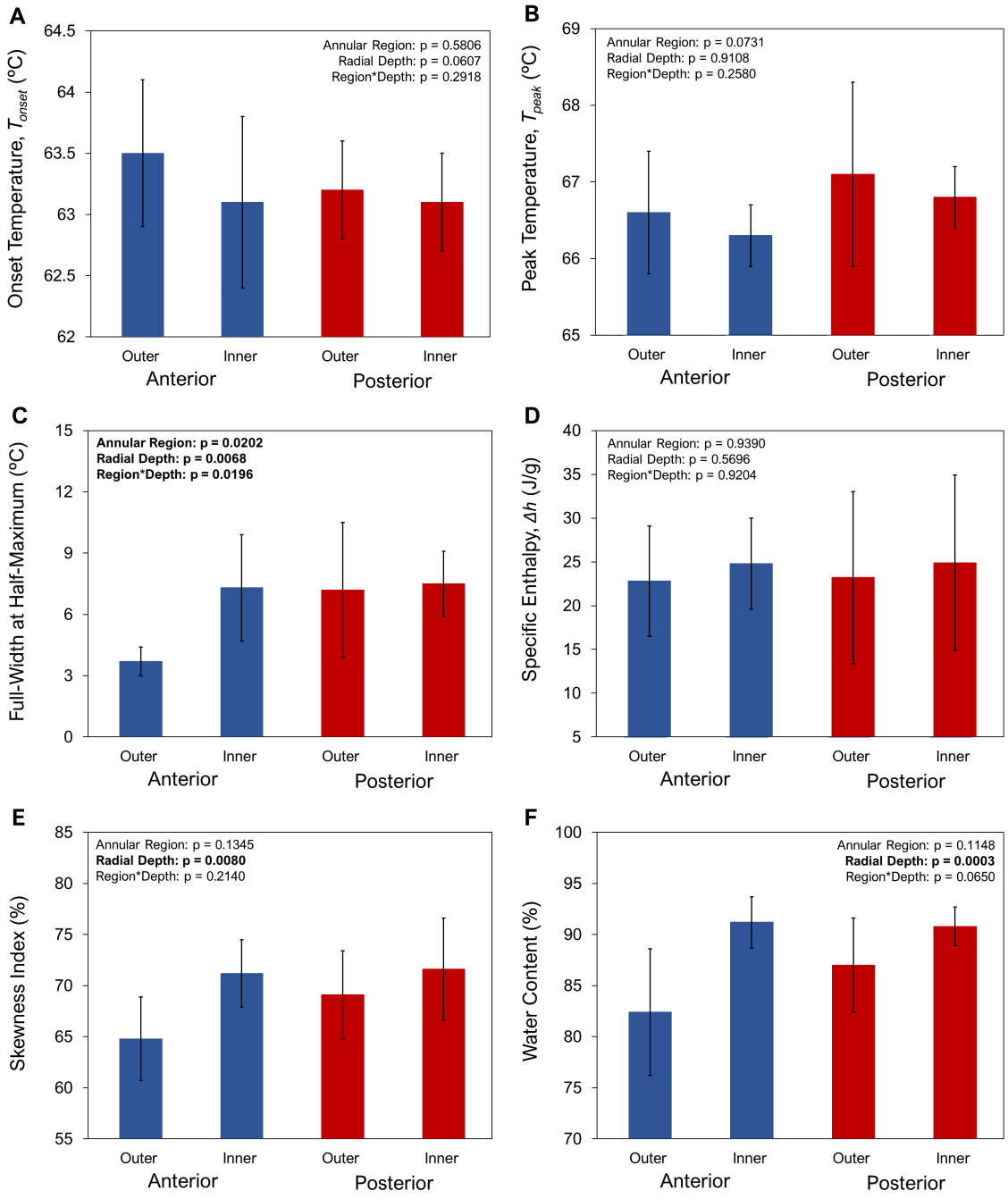

Figure 4.5: The values in the onset temperature (A), the peak temperature (B), the full-width at half-maximum (C), the specific enthalpy (D), the skewness index (E), and the water content (F) with annular region and radial depth for samples allocated to the DSC experiment.

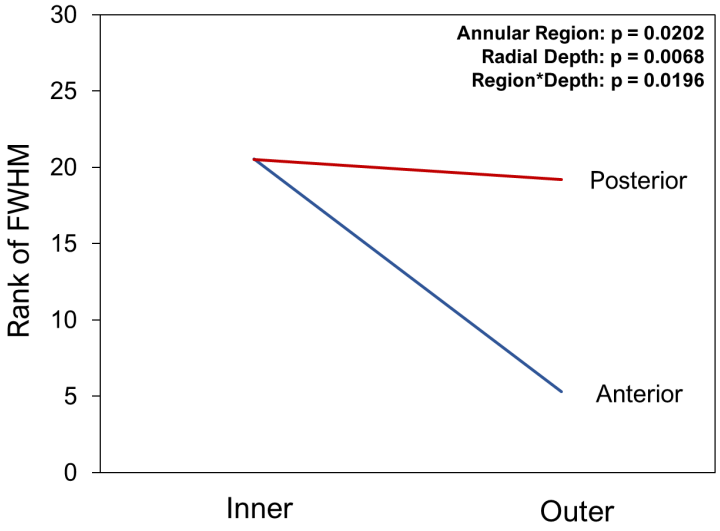

Figure 4.6: Interaction plot from the two-way ANOVA performed on rank-transformed full-width at half-maximum data. Annular region, radial depth, and the interaction between region and depth were all significant.

Table 4.4: The variations in skewness index and water content when annular regions are pooled together.

	Outer (Anterior + Posterior)	Inner (Anterior + Posterior)	
Skewness Index (%)	71.6 ± 5.0 (n = 8)	69.1 ± 4.3 (n = 8)	$p = 0.0704$
Water Content (%)	84.7 ± 4.6 (n = 8)	90.9 ± 1.9 (n = 8)	$p = 0.0110$

4.3 Mechanical Testing and Light Microscopy

4.3.1 Mechanical Testing

In order to determine whether the tensile properties of the annulus vary with annular region, matched-pair anterior and posterior samples from 13 discs were prepared for mechanical testing. Samples were taken from either L5-6 or L6-7 discs, with each disc taken from a different spine. Of the 13 spines prepared for mechanical testing, 5 were

omitted. Two samples (one posterior, one anterior, each from a different spine) failed early into testing due to a crack that developed within one of the vertebral bodies at the hole for the support screw. The other three spines excluded were due to the presence of partially fused growth plates (Figure 4.7). The number of samples with mechanical properties successfully measured with respect to annular region are listed in Table 4.5. Representative stress-displacement curves are shown in Figure 4.8. The values of annular radial thickness (measured with ImageJ, see Figure 3.12) were, in general, much smaller than the values of radial depth (measured with digital calipers, see Figure 3.10), as described by Table 4.6.

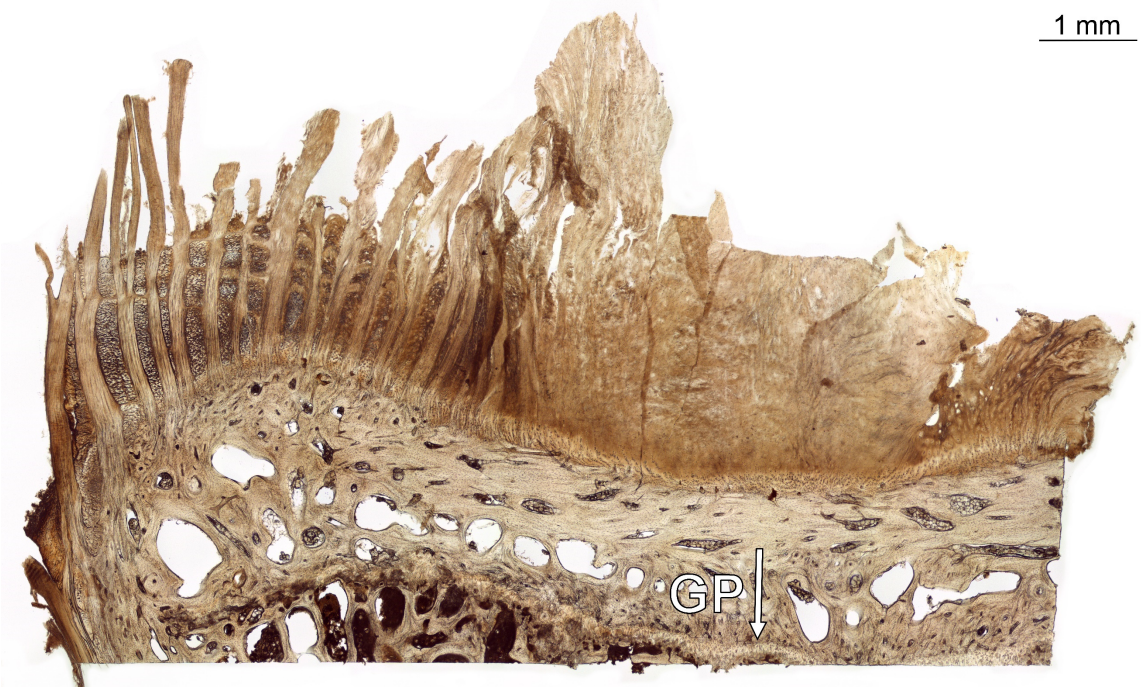

Figure 4.7: A partially fused growth plate (GP) found in a sample that underwent mechanical testing. Samples containing partially fused growth plates were excluded from measurements of the mechanical properties. Image is an unstained cryosection of an L5-6 disc taken using transmission light microscopy.

Table 4.5: The number of samples successfully measured for each parameter calculated from mechanical testing data

Parameter	Anterior	Posterior
Stiffness (N/m)	n = 8	n = 8
Stress-Displacement Slope (MPa/mm)	n = 8	n = 8
Ultimate Tensile Strength, Annulus (MPa)	n = 8	n = 8
Tension Strength of Annulus Wall (N/m)	n = 8	n = 8

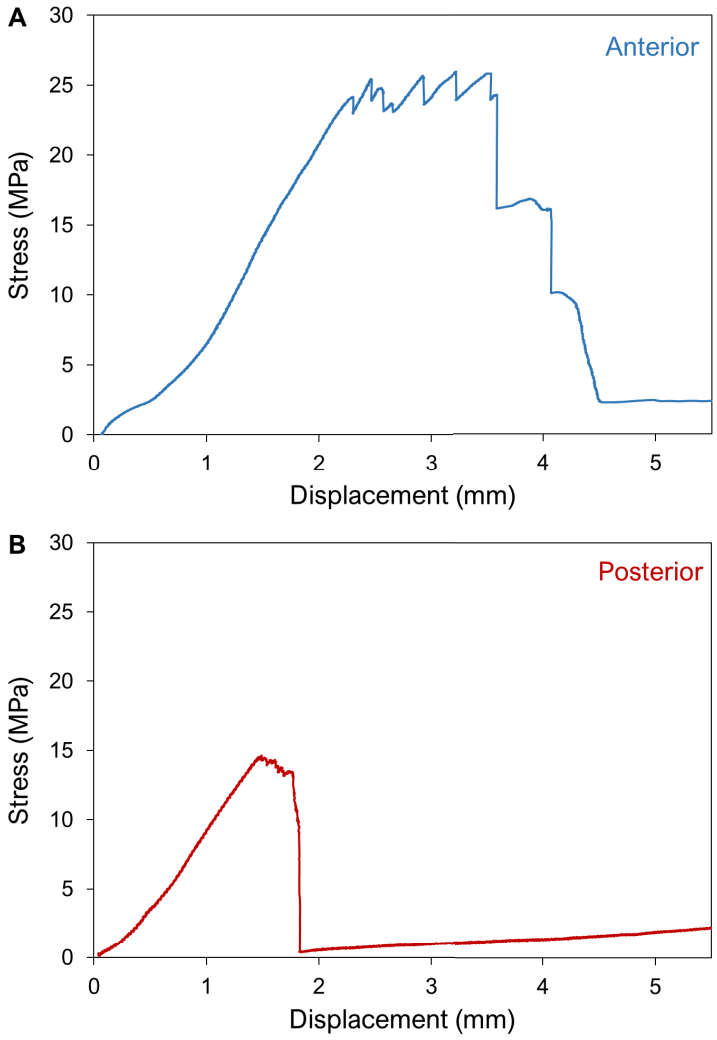

Figure 4.8: Representative pull-to-rupture responses for anterior samples (A) and posterior samples (B). Individual rupture events of lamellae can be distinguished by jagged peaks at the top of the stress-displacement curve. Data taken from the same L5-6 disc.

Table 4.6: The sample radial depth measurements (measured with calipers) and the annular radial thickness measurements (measured with ImageJ, see Figure 3.12) for the anterior and posterior annular regions for samples allocated to mechanical testing.

	Anterior	Posterior
Sample Radial Depth (mm)	13.2 ± 1.6 (n = 8)	5.3 ± 1.0 (n = 8)
Annular Radial Thickness (mm)	5.9 ± 0.5 (n = 8)	4.1 ± 0.5 (n = 8)

The resulting matched-pair t-tests revealed that both the ultimate tensile strength of the annulus and the tension strength of the annulus wall were significantly larger in the anterior annulus when compared to the posterior annulus ($p = 0.0063$ and $p = 0.0005$, respectively). In contrast, the stiffness and the stress-displacement slope did not vary with annular region ($p = 0.8690$ and $p = 0.2160$, respectively). The results of the parameters measured through mechanical testing are summarized in Table 4.7.

Table 4.7: The variations in the mechanical properties measured for the anterior and posterior regions.

	Anterior	Posterior	
Stiffness (N/m)	190.1 ± 48.0	175.3 ± 20.1	$p > 0.8$
Stress-Displacement Slope (MPa/mm)	17.0 ± 4.5	13.6 ± 4.0	$p > 0.2$
Ultimate Tensile Strength, Annulus (MPa)	27.0 ± 7.1	12.8 ± 3.6	$p = 0.0063$
Tension Strength of Annulus Wall (N/m)	158.0 ± 38.4	51.4 ± 11.7	$p = 0.0005$

4.3.2 Light Microscopy

Following mechanical testing, ruptured samples were cryosectioned and viewed using light microscopy in order to assess the microstructure of ruptured anterior and posterior samples. The cryosections were taken parallel to the fibre-orientation angles so that in-plane lamellae (those loaded in pure tension) would be parallel to the plane of the image. Due to the cross-ply pattern of the annulus, the sectioned cuts taken resulted in the fibres of lamellae between in-plane lamellae being oriented out-of-plane at an angle of approximately 70º (measured from the plane of the image). Representative anterior and posterior sections taken from outside the damaged region are shown in Figure 4.9A and Figure 4.10A, respectively. The undamaged region (i.e. the region outside of the tested region where the annulus has been severed with a razor cut) can be clearly distinguished by a lack of splitting/fraying at the cut-ends of lamellae, as well as a lack of interlamellar disruption.

The most prevalent damage observed was lamellae rupture near mid-disc height, resulting in samples being torn into two roughly equivalent halves. The ruptured ends of in-plane lamellae – the lamellae that were loaded in pure tension – generally showed signs of splitting or fraying (Figure 4.9B and Figure 4.10B for anterior and posterior examples, respectively). Of the samples tested that ruptured via annular failure (including those omitted from the statistical analysis for the mechanical properties due to having incompletely fused growth plates), all 12 anterior and posterior samples demonstrated extensive lamellae rupture at mid-disc height (Table 4.8).

Evidence of disruption to the integration between in-plane and out-of-plane lamellae accompanied lamellae rupture at mid-disc height. Different types of interlamellar disruption were observed. Most common were out-of-plane lamellae with missing pieces close to the rupture location interposed between longer in-plane lamellae, effectively creating gaps between lamellae throughout the sectioned sample (Figure 4.11A and Figure 4.10B for anterior and posterior examples, respectively). Interlamellar damage of this type was found in all anterior and and posterior samples that ruptured via annular

failure and hence did not vary with region (Table 4.8). Another type of interlamellar disruption was observed where large pieces of out-of-plane lamellae were missing distant to the rupture location while the lengths towards both the ruptured end and the cartilaginous endplate remainded – termed "mid-gaps" (Figure 4.11A). Mid-gaps were found exclusively in anterior samples and were relatively common (Table 4.8). In more severe cases of disruption to interlamellar integration, disruption between lamellae resulted in damage to the cartilaginous endplate (Figure 4.11B and Figure 4.10C for representative anterior and posterior samples, respectively). Although interlamellar disruption extending to the endplate appeared to be more commonly observed in posterior samples, it was not statistically significant ($p = 0.2377$, Table 4.8).

Less common were instances of in-plane lamellae (the lamellae loaded in tension) causing fracture at the interface between the calcified cartilaginous endplate (CEP) and the vertebral endplate (VEP), which tended to occur near the apex of the vertebral endplate. Representative anterior and posterior samples with CEP-VEP damage are shown in Figure 4.11C and Figure 4.12, respectively. Damage occuring at the CEP-VEP interface commonly resulted in pieces of the CEP still bound to the lamellae being pulled away from the VEP. While CEP-VEP fractures were more commonly observed in anterior samples, this was not statistically significant ($p = 0.3783$, Table 4.8).

Table 4.8: The prevalence of the different types of damage with annular region for samples that were allocated to mechanical testing.

	Anterior	Posterior	
Lamellae rupture at mid-disc height	12 of 12	12 of 12	
Interlamellar damage at rupture	12 of 12	12 of 12	
Interlamellar damage distant to rupture	7 of 12	0 of 12	$p = 0.0052$
Interlamellar damage at endplate	5 of 12	9 of 12	$p = 0.2377$
Damage at CEP-VEP interface	5 of 12	2 of 12	$p = 0.3783$

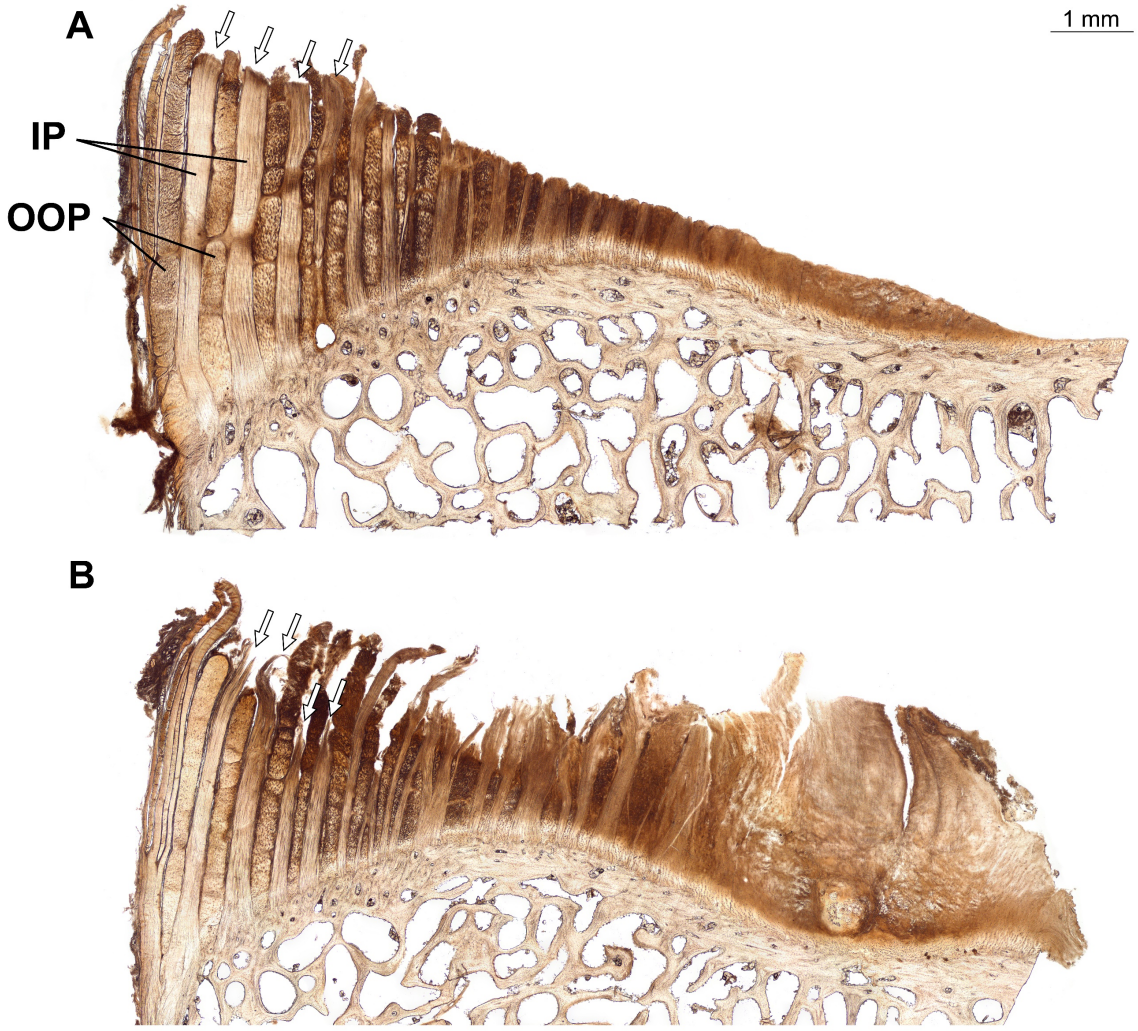

Figure 4.9: Representative anterior samples taken from the same L6-7 disc showing an undamaged region (A) and a damaged region (B). Fibres within in-plane (IP) lamellae were parallel to the direction of the applied load, while fibres within out-of-plane lamellae (OOP) were at an angle of approximately 80º away from the direction of the applied load. Arrows point at the same in-plane lamellae in order to distinguish the ends of lamellae from the undamaged (top) and the damaged region (bottom). In general, in-plane lamellae from the damaged region showed signs of splitting in response to tensile overload. Images are unstained cryosections taken using transmission light microscopy.

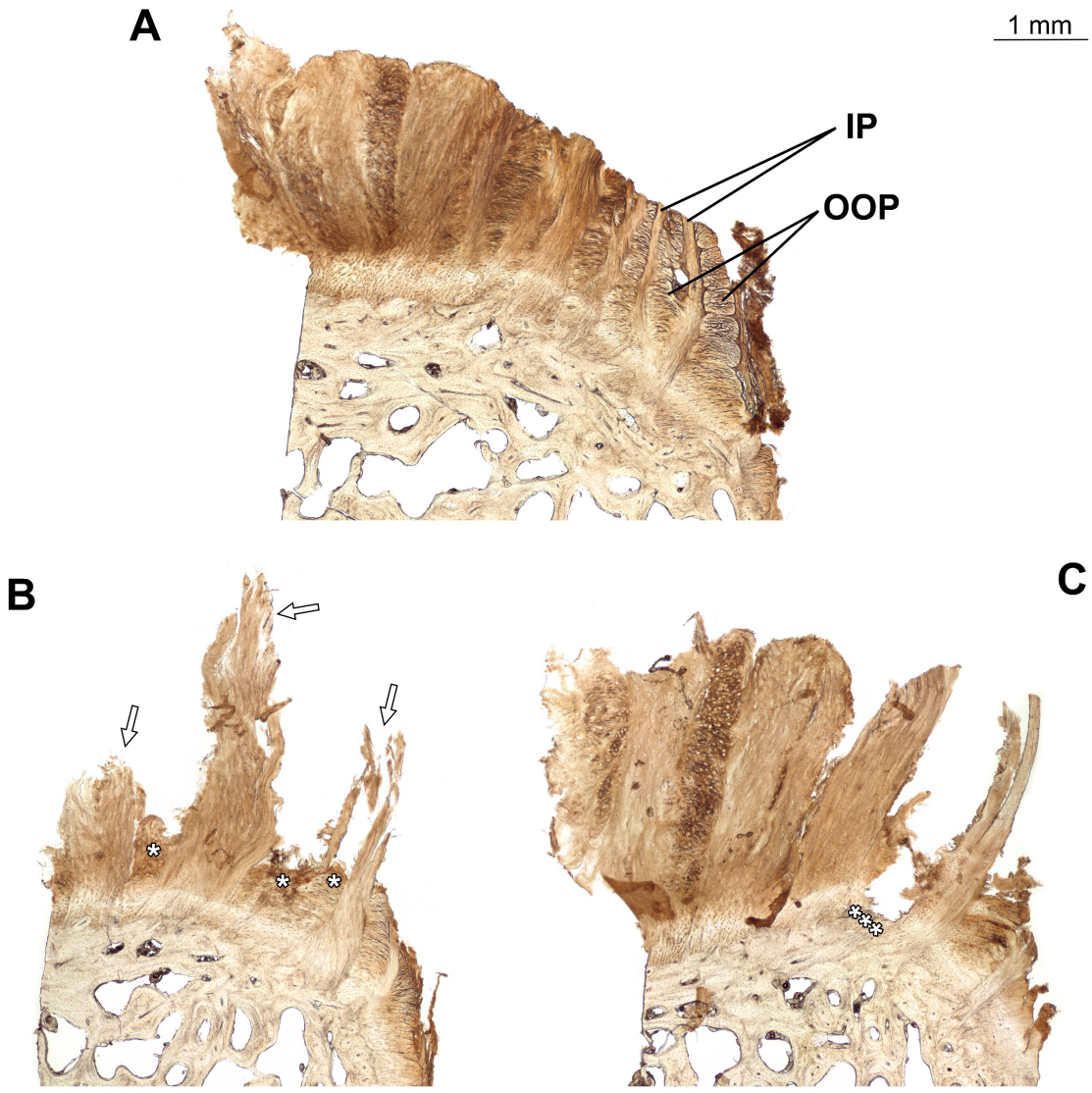

Figure 4.10: Representative posterior samples taken from the same L6-7 disc showing an undamaged region (A) and damaged regions (B and C). Fibres within in-plane (IP) lamellae were loaded in pure tension, while the direction of load application in out-of-plane (OOP) lamellae was at an angle of approximately 65º relative to the fibre direction. Arrows point at examples of in-plane lamellae splitting. Interlamellar damage is observed in B and C. Examples of lamellae with missing ends interposed between longer lamellae (marked by *) are observed in B, while an example of interlamellar disruption extending to the cartilaginous endplate (marked by ***) is observed C. Images are unstained cryosections taken using transmission light microscopy.

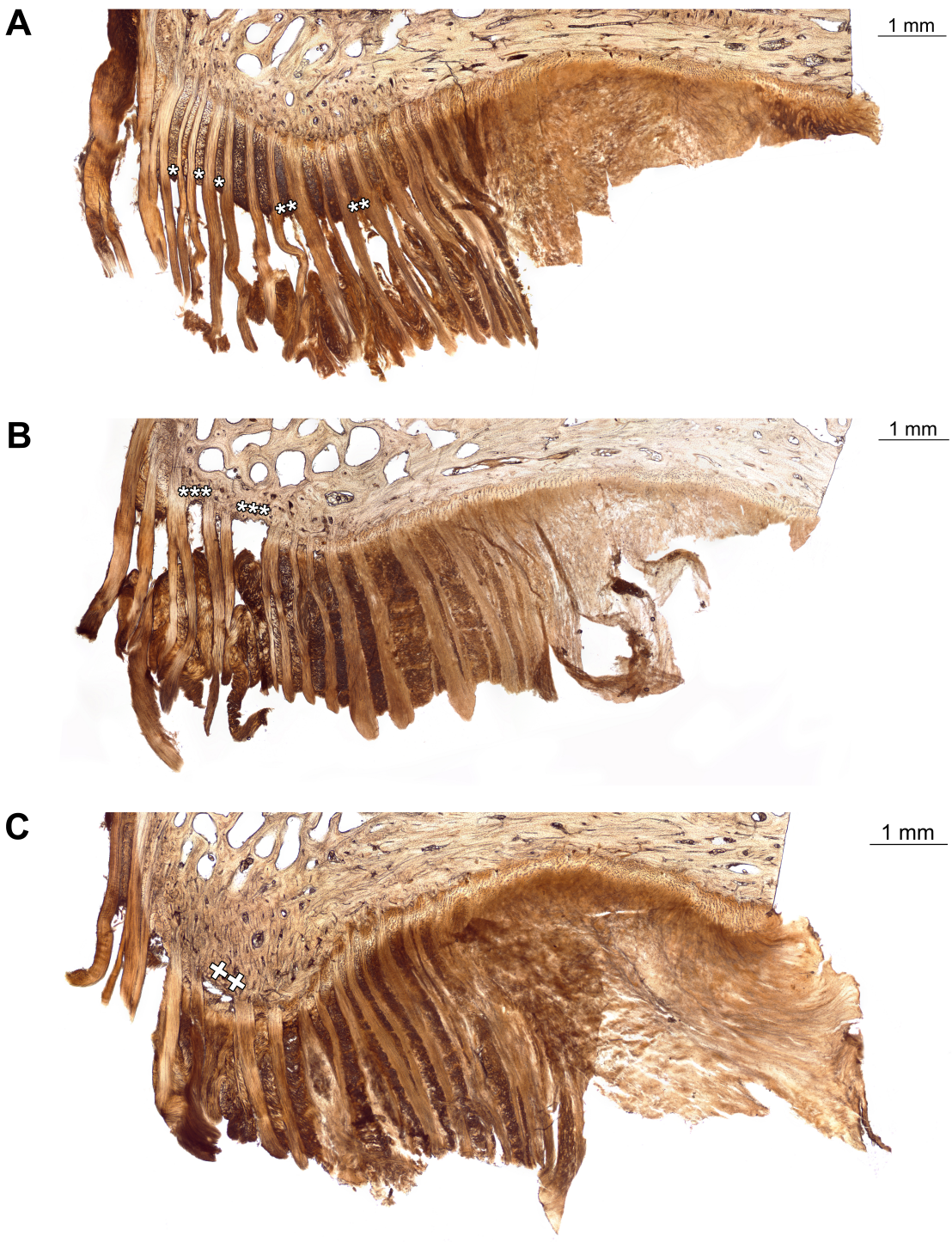

Figure 4.11: Representative anterior samples showing interlamellar disruption (A and B) and damage at the CEP-VEP interface (C, marked by ++). Examples of missing ends (marked by *) and "mid-gaps" (marked by **) can be observed in A, while interlamellar disruption resulting in damage to the cartilaginous endplate (marked by ***) can be observed in B. L6-7 discs are featured in B and C, while an L5-6 disc is featured in A. Images are unstained cryosections taken using transmission light microscopy.

Figure 4.12: A representative posterior sample showing damage at the CEP-VEP interface (marked by ++). Arrows point at instances of the cartilaginous endplate embedded to in-plane lamallae. Image is an unstained cryosection of an L6-7 disc taken using transmission light microscopy.

Chapter 5: Discussion

5.1 Contributions to Disc Structure and Mechanics

Thermal Stability and Crosslinking of Collagen Molecules

The results obtained from HIT analysis and DSC work show, for the first time, that significant regional variations exist in the collagen structure of the annulus within lumbar intervertebral discs at the molecular level. HIT analysis indicated that collagen molecules from the posterior annulus have greater thermal stability and a higher density of intermolecular crosslinking than those from the anterior annulus, as illustrated by having larger values of denaturation temperature (T_d) and half-time of load decay ($t_{1/2}$), respectively. Similar differences with annular region exist throughout the lumbar spine, from L5-6 to L1-2. The use of $NaBH_4$ revealed that both the anterior and posterior annulus contain insignificant populations of immature thermally labile crosslinks, as reflected by minimal differences in $t_{1/2}$ between treated and untreated samples. The results from DSC further revealed that variations in the thermal stability of collagen also exists with radial depth for the anterior region, where the inner annulus was found to have a greater range of thermal stabilities relative to the outer annulus, as indicated by a higher value of $FWHM$.

Crosslinks – which provide strength[78] and stability[112] to collagen molecules – are formed during biosynthesis by the enzyme lysyl oxidase.[113] Initially, these enzymatically-derived crosslinks are divalent, joining two collagen molecules together. With time, these crosslinks spontaneously react to form trivalent crosslinks.[113] Divalent and trivalent crosslinks are commonly referred to as immature and mature crosslinks, respectively. Many different types of enzymatic crosslinks exist, showing variance between different types of tissues.[90,113,114] In addition to the enzymatically-derived crosslinks formed during biosynthesis, new crosslinks are formed throughout aging through a spontaneous (non-enzymatic) process called glycation, resulting in the formation of advanced glycation

end-products (AGEs).[113,115] Like enzymatic crosslinks, many different types of AGEs exist. While enzymatic crosslinks are limited to forming at the terminal domains of collagen molecules, AGEs can form at multiple locations along the length of collagen.[116]

From the HIT experiments performed, samples from both the anterior and posterior regions (from both L5-6 and L1-2 discs) displayed linear increases in tension with temperature past T_d up to 90 ºC, indicating that both annular regions contain heat-stable crosslinks throughout the lumbar spine.[113] These findings suggest that the enzymatic crosslinks in both regions are either immature keto-amine crosslinks or mature crosslinks, both of which are heat stable.[113] While HIT analysis cannot discriminate between thermally stable divalent crosslinks and trivalent crosslinks, others studies have reported that the annulus contains mature, trivalent pyridinoline crosslinks.[114,117,118] Although samples from both annular regions demonstrated linear increases in tension to 90 ºC, their denaturation temperatures varied considerably: posterior samples denatured at a significantly higher temperature (independent of disc level). T_d corresponds to the temperature at which the intramolecular hydrogen bonds of the triple helix structure of collagen molecules begin to rupture. Differences in T_d – as observed between annular regions – are explained by the "polymer-in-a-box" theory, which states that the thermal stability of collagen molecules increases as the proximity of neighboring molecules increases due to the restriction in conformational freedom.[108,112] It is likely that the samples from the posterior annulus have a larger T_d due to a tighter packing of collagen molecules within the collagen fibrils at this location.

During the isothermal phase of the HIT experiment, the load decay seen for anterior and posterior samples is attributable to gradual hydrolysis of peptide bonds within the α-chains of collagen molecules.[108] The rate of decay in load is slowed by heat-stable crosslinks: thus, $t_{1/2}$ is an indicator of the relative density of heat-stable crosslinks within the sample.[74,108] $t_{1/2}$ values differed between samples from the anterior and posterior annulus, with the rate of load decay being significantly slower in posterior samples (independent of disc level). Moreover, $t_{1/2}$ values did not significantly change when samples from both regions were treated with sodium borohydride ($NaBH_4$). Because

$NaBH_4$ converts enzymatic heat labile crosslinks to a heat stable form, it allows for determination of total crosslinking: heat-labile and heat-stable combined. The $t_{1/2}$ results indicate that both the anterior and posterior annulus contain insignificant populations of heat-labile crosslinks relative to heat-stable crosslinks,[90,108,113] and that the posterior annulus is more heavily crosslinked than the anterior annulus. A higher density of intermolecular crosslinks will effectively lower the number of configurations the molecule can achieve, consistent with the higher values of T_d observed for the posterior annulus.[108,112,119] While no comparable studies were identified that considered changes in crosslinking with annular region in human lumbar discs, Tan *et al* reported on differences in crosslinking in human thoracic intervertebral discs.[117] It was shown in this study that the posterior anulus had significantly higher amounts of heat-stable pyridinoline crosslinks relative to the anterior annulus. These findings – in combination with the results from this experiment – suggest that human lumbar intervertebral discs may show similar regional variations in thermal stability and crosslinking of collagen molecules to the results presented here for ovine lumbar discs.

Given that T_d and $t_{1/2}$ are larger for the posterior annulus, these findings together confirm the first hypothesis for the HIT experiment: the posterior annulus does, in fact, have a higher thermal stability and a higher density of thermally stable crosslinks. These molecular-level structural differences are likely tied to the differences in physiological loading that the posterior annulus is subjected to relative to the anterior annulus. For example, flexion of the lumbar spine – a frequent posture during daily living – places the anterior and the posterior annulus under considerably different loads: while the anterior annulus is compressed, the posterior annulus is placed under additional tension.[2,50] Moreover, the nucleus shifts posteriorly, increasing the stress on the posterior annulus.[51,52] It is likely that these physiologic differences in mechanical loading have resulted in significant changes to the molecular-level collagen architecture between regions. Because T_d and $t_{1/2}$ did not vary with disc level, the second hypothesis for the HIT experiment – that molecular-level structural differences would not vary with disc level – was also confirmed. These findings are also likely tied to *in vivo* loading. Although inferior lumbar disc levels experience larger loads relative to superior disc

levels,[1] they are also larger,[120–123] which could imply that the stresses are comparable. Lastly, the third hypothesis for the HIT experiment – that collagen molecules in both annular regions would not have a significantly higher amount of heat stable crosslinks – was confirmed. For both anterior and posterior samples, $NaBH_4$ treatment did not significantly slow the rate of load decay compared to their match-pair untreated samples, as reflected by insignificant changes in $t_{1/2}$. From these results, it can be concluded that both the anterior and posterior annulus contain an insignificant population of immature aldimine crosslinks, which are thermally labile. Previous research has shown that a high ratio of immature crosslinks to mature crosslinks may indicate a high rate of collagen turnover.[108,124] Tissues that exhibit a high rate of collagen turnover continuously synthesize new collagen, which implies that there are large proportions of immature crosslinks present in the tissue (regardless of age). Given that matrix synthesis and degradation is dependent in part on the cell density of the tissue, a low density of immature crosslinks within the annulus is not surprising: adult intervertebral discs have been shown to have an extremely low cell density relative to other tissues.[125–127] This, in part, is because intervertebral discs are largely avascular, which limits metabolite transport.[76,112] Moreover, annular tears show minimal signs of healing, which suggests that matrix turnover is very low.[8,129] The low rate of collagen turnover, in turn, highlights a vulnerability to accumulated damage, such as from repetitive loading. If damage occurs, it will not be remodeled at a fast rate, which can compromise the structure of the annulus and lead to further damage or early degeneration.[114]

In addition to HIT analysis, DSC was also used to assess how the thermal stability of collagen molecules varies with both annular region and radial depth. This was accomplished primarily through measures of the onset temperature (T_{onset}), the peak temperature (T_{peak}), and the full-width at half-maximum ($FWHM$). T_{onset} is a measure of the kinetic energy of initial α-chain uncoiling, while T_{peak} is a measure of the point of maximum energy absorption during denaturation.[119,130] For T_{onset}, only radial depth came close to reaching significance, with the outer annulus having a higher value relative to the inner annulus. In contrast, for T_{peak}, only annular region came close to reaching significance, with the posterior annulus having a higher value relative to the anterior

annulus. Given that the first hypothesis for the DSC experiment stated that the posterior annulus would have a higher thermal stability – as indicated by T_{onset} and T_{peak} – the first hypothesis was not verified, as neither parameter varied in a statistically significant manner with region. While T_{onset} and T_{peak} both describe aspects of the thermal stability of collagen molecules, there are important differences to consider between these parameters and the denaturation temperature, T_d, measured in HIT analysis. In DSC, the onset of denaturation is detected as it occurs by a change in heat flow; in contrast, during HIT analysis, the onset of denaturation must first generate a measurable change in tension before being detected.[109,131] Previous research has shown that T_d values align better with T_{peak} as opposed to T_{onset}.[109,131] It is interesting that regional variation in T_{peak} failed to reach significance in DSC ($p = 0.0731$ for circumferential region) given the significant difference seen in T_d for HIT analysis ($p < 0.0001$). This discrepancy may be explained by the relative differences in how HIT analysis and DSC measure thermal stability. For samples mounted in the HIT apparatus, only the collagen that is oriented in-line with the grips (i.e. the in-plane lamellae) will produce a substantial signal, as collagen fibres oriented in other directions will not meaningfully contribute to the tensile load due to their orientation relative to the load cell. In contrast, all of the collagen in the samples prepared for DSC (in-plane lamellae, out-of-plane lamellae, and other structural elements like radial bridging elements) will collectively produce a response that is captured by the heat flow measured. It is therefore possible that measurements made through DSC are capturing other responses not measured with HIT analysis that are influencing the measurements of T_{peak} to some extent. In terms of T_{onset}, the fact that it did not vary with annular region suggests that the least-stable collagen molecules in both regions have comparable thermal stability, while the near-significance of a higher T_{onset} in the outer vs. inner annulus suggests that differences with radial depth may exist.

The heterogeneity in the thermal stability of collagen molecules in the anterior and posterior regions was captured by the full-width at half-maximum ($FWHM$), where larger values correspond to greater heterogeneity relative to smaller values.[90,130] The results obtained show that annular region, radial depth, and the interaction between these factors were significant: the outer anterior annulus had a significantly smaller value of $FWHM$

relative to both the inner anterior annulus and the outer posterior annulus. These findings have several important implications regarding differences in the structure of collagen within the annulus. First, they reinforce that the posterior annulus contains collagen that is more thermally stable than the anterior annulus: while both regions had similar values of T_{onset}, the posterior region had a larger value of $FWHM$, indicating the presence of collagen molecules with greater thermal stability. Second, they show that greater heterogeneity in the thermal stability of collagen molecules exists in the inner annulus relative to the outer annulus. Given that the second hypothesis for DSC predicted that collagen molecules in the outer annulus will have a smaller range of thermal stabilities relative to collagen from the inner annulus, this hypothesis was only partially verified, as the change in $FWHM$ with radial depth was significant only for the anterior region. These trends in $FWHM$ likely reflect the different types of collagen present in the annulus: studies have reported that the inner annulus contains a mix of type I and type II collagen, while the outer annulus contains primarily type II collagen.[11,16] These differences in collagen type may lead to differences in molecular packing, and hence thermal stability.

Tensile Mechanics

The results obtained from mechanical testing showed that samples from the anterior annulus were significantly stronger than those from the posterior annulus. These results can be compared to other studies that have explored regional variations in the tensile properties of the annulus (Table 5.1), though it should be noted that no other studies have tested mechanical properties using bone-annulus-bone samples loaded parallel to the collagen fibre direction, as in the current study. Zak and Pezowicz also showed that the anterior region was stronger than the posterior region using bone-annulus-bone samples from pigs.[88] Moreover, several authors have reported that the anterior region is significantly stronger than the posterolateral region (which is adjacent to the posterior) in human discs.[81–85] Yet, while many other studies have reported similar trends in the regional variations of the tensile mechanics of the annulus, the strengths measured in these studies were *significantly* smaller compared to those measured in this experiment.

Although it is important to note that cross-sectional areas were calculated in the current work using radial depth measurements made on formalin-fixed tissue, which may have experienced some shrinkage, it is unlikely that this would account for the magnitude of the difference seen between the current values and those reported previously.

Table 5.1: The measurements of ultimate tensile strength with annular region measured in the current work compared to other applicable studies.

Tissue	Method of Sample Preparation	Load Parallel to Collagen Fibre Direction?	*UTS*, Anterior (MPa)	*UTS*, Posterior (MPa)	*UTS*, Posterolateral (MPa)
Human[83]	Annulus Only	No	1.6†	-	0.7†
Human[84]	Annulus Only	No	2.0†	-	1.1†
Human[82]	Annulus Only	Yes	3.5†	-	3.1†
Human[85]	Annulus Only	Yes	10.3†	-	5.6†
Human[87]	B-A-B	No	1.7	3.8	-
Pig[88]	B-A-B	No	7.5	4.5	-
Sheep*	**B-A-B**	**Yes**	**27**	**12.8**	**-**

B-A-B = Bone-annulus-bone. †*UTS* taken from the outer annulus. *From the current study.

Because the goal of mechanical testing in the current work was to assess the tensile strength of collagen fibres within lamellae, the applied load was oriented parallel to one of the fibre-orientation angles so that that collagen fibres in half the lamellae were loaded in pure tension. Yet, given that only half of the lamellae were oriented in the direction of the applied load, the measurements obtained underestimate the true strength of collagen fibres. To correct for this, the cross-sectional area measured should be halved, which would double the ultimate tensile strengths measured. These calculations can then be compared to the other studies that aligned the applied load parallel to one of the fibre-orientation angles (Table 5.2).

Table 5.2: The measured strength of the annulus wall and the calculated true strength of collagen fibres within the annulus obtained from the current work compared to other applicable studies

Structure Assessed	Anterior (MPa)	Posterior (MPa)	Posterolateral (MPa)
Human, Annular Collagen Fibres[82]	7.0†	-	6.2†
Human, Annular Collagen Fibres[85]	10.3*	-	5.6*
Sheep, Annular Collagen Fibres	54.0†	25.6†	-

† *UTS* was multiplied by two to correct for out-of-plane lamellae. * *UTS* was measured from tensile tests performed on samples containing only one lamella

The large discrepancies in strength observed may be explained by differences in sample preparation. Several of these studies, for example, tested pieces of isolated annulus cut from the disc,[81–85] which do not account for the structural role of the endplate in anchoring the collagen fibres of the annulus. Of the studies that tested isolated pieces of annulus, the failure stress of the anterior region ranged from 1.6 MPa to 10.3 MPa, while the failure stress of the posterolateral region ranged from 0.7 MPa to 5.6 MPa. The variation in strength amongst these studies was likely influenced by the direction of the applied load: studies that chose not to align the applied load in the direction of one of the fibre-orientation angles were weakest (Figure 5.1A).[83,84] These observations likely reflect how collagen fibres within lamellae did not cross the gauge region, which would have reduced their ability to withstand tension. In contrast, the studies that did align the applied load parallel to one of the fibre-orientation angles (Figure 5.1B)[82,85] led to increases in the measured strengths for both the anterior and posterior regions.

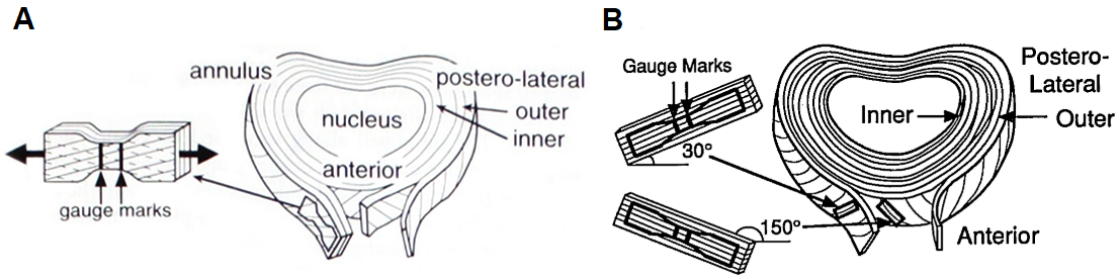

Figure 5.1: Two examples of isolated annulus samples prepared by other studies for tensile testing. A: A study that cut their samples parallel to the circumferential direction of the disc. B: A study that cut their samples parallel to one of the fibre-orientation angles. A: Modified, with permission, from Ebara.[84] B: Modified, with permission, from Skaggs.[85]

The two studies that utilized bone-annulus-bone samples each prepared their samples in unique ways (Figure 5.2). The samples prepared by Green *et al* (Figure 5.2A) were quite large, having an average cross section of 15 mm by 5 mm.[87] The direction of the applied load was in alignment with the inferior-superior axis and thus not parallel to one of the fibre-orientation angles. Anterior samples were found to fail at 1.7 MPa, while posterior samples failed at 3.8 MPa. While these results may seem conflicting with the other results presented, several potential problems were identified with this experiment, including questionable means of measuring the cross-sectional area and unspecified means of hydration during testing. Moreover, because fibres from the anterior annulus were closer to the horizontal, they would have experienced greater levels of shear stress relative to posterior samples, which likely contributed to the lower strength observed in anterior samples. In contrast, Zak and Pezowicz used smaller rectangular bone-annulus-bone samples relative to Green *et al* (Figure 5.2B), having an average cross section of 6 mm by 4 mm.[88] The direction of the applied load was again in alignment with the inferior-superior axis and thus not parallel to one of the fibre-orientation angles. Anterior samples had an average failure stress of 7.5 MPa while posterior samples had an average failure stress of 4.5 MPa. The discrepancy in measured strengths between other studies that utilized bone-annulus-bone samples and the results from the current work likely reflect the importance of aligning the applied load parallel to one of the fibre-orientation angles.

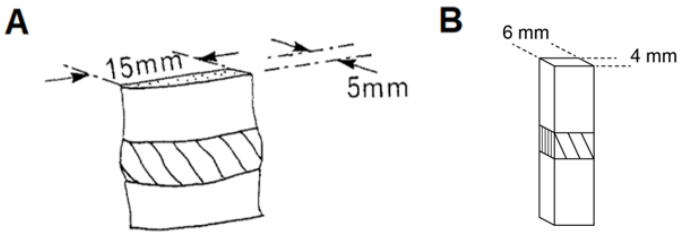

Figure 5.2: Two examples of bone-annulus-bone samples prepared by other studies for tensile testing. A: Modified, with permission, from Green.[87] B: Drawing based on samples used by Zak and Pezowicz.[88]

Table 5.1 illustrates just how sensitive the measured tensile properties of the annulus are to sample preparation. The role of aligning the applied load parallel to one of the fibre-orientation angles is likely a key factor in the high strengths reported for the current work, as it enabled collagen fibres (in half the lamellae) to be recruited in pure tension. Moreover, having the cartilaginous endplates and vertebral endplates present in the samples preserves the integration of the annulus with bone, which likely plays an important structural role. These results have important implications for studies that aim to model the biomechanical behavior of lumbar intervertebral discs.[39] Because models are often validated using *in vitro* tests (such as those cited in Table 5.1), the mechanical testing data obtained from the current work suggests that *UTS* values currently used for collagen fibres in models may significantly underestimate their true strength.

5.2 Comparison of Thermal Stability, Crosslinking, and Mechanics of the Annulus to Other Collagenous Tissues

The parameters measured through HIT analysis and mechanical testing for the anterior and posterior ovine lumbar annulus can be compared to several other collagenous tissues that have been investigated using comparable techniques (Table 5.3). Because samples in the current work were oriented such that the applied load was parallel to one of the fibre-orientation angles, they can be directly compared to tendon, given that both types of tissue test uniaxially aligned collagen fibres. The steer tail tendons referenced in Table 5.3 are from two age groups (~2 years old and ~5 years old) while the bovine forelimb

tendons are from animals approximately 2 years old.[90,131] In contrast, the human sartorius tendon are from male donors between the ages of 20 and 60 years old.[132]

Table 5.3: The half-time of load decay, denaturation temperature, and the ultimate tensile strength measured in the current work compared to other applicable studies.

Tissue	$t_{1/2}$† (hrs)	T_d (ºC)	*UTS* (MPa)
Young Steer Tail Tendon[131]	~0††	64.5 ± 1.0	36 ± 5.6*
Old Steer Tail Tendon[131]	-	65.0 ± 1.0	47 ± 10*
Bovine Extensor Tendon[90]	3.5 ± 1.0	62.7 ± 0.4	36 ± 5
Ovine Anterior Annulus	**11.0 ± 4.9**	**62.6 ± 0.7**	**54 ± 14****
Bovine Flexor Tendon[90]	11.5 ± 1.9	65.4 ± 0.7	25 ± 30
Ovine Posterior Annulus	**32.7 ± 23.7**	**67.2 ± 1.2**	**26 ± 7****
Human Sartorius Tendon[132]	55.2 ± 54.9	66.5 ± 0.4	32 ± 9

†Values taken from $NaBH_4$-treated samples for comparisons of *total* crosslinking. ††Samples failed too early into the isotherm to allow for $t_{1/2}$ to be measured. *UTS solved for by converting true strain to engineering strain and assuming that the engineering strain at failure was 18%. **UTS was multiplied by two to correct for out-of-plane lamellae.

In terms of the parameters measured through HIT analysis, Table 5.3 illustrates that the thermal stability of the posterior annulus – as reflected by T_d – is larger than all other collagenous tissues listed, including the energy storing bovine flexor tendon and the human sartorius tendon. The lower thermal stability of the anterior annulus, in contrast, is approximately the same as the adult bovine forelimb extensor tendon. Perhaps most interesting, however, is consideration for the magnitude of difference in T_d between anterior and posterior annulus. The study that compared the bovine forelimb extensor and flexor tendons showed that a difference of ~3.0 ºC in T_d between flexor and extensor tendons was accompanied by significant differences in tensile strength, toughness, and susceptibility of collagen fibrils to both tensile overload and fatigue damage.[90] Given that samples from the anterior and posterior annulus had significantly different measurements of T_d (~5.0 ºC) and *UTS*, these findings may allude to similar differences in terms of toughness and susceptibility to fatigue damage as well. The values of $t_{1/2}$ for both annular regions reveal that the annulus, overall, retained tension significantly longer than

all other collagenous tissues of similar age listed, illustrating just how densely crosslinked samples from both regions are. The only tissue that had a larger $t_{1/2}$ – the human sartorius tendon – came from tissue that was significantly older than the ovine tissue, and thus had more AGE's contributing to crosslinking density.[132] The relative contributions of non-enzymatic crosslinks in the animal tissues listed in Table 5.3, in contrast to the human sartorius tendon, are likely negligible. Willett *et al*[131] explored the effects of aging on crosslinking in animal tissue by quantifying the crosslinks present in a young group (~2 years) and an old group (~5 years) of bovine tail tendons and measuring the change in T_d between these groups. The results obtained found that T_d did not change between age groups and that pentsosidine – an AGE marker – was only present in trace amounts in the old group. In terms of strength, the anterior annulus interestingly was the strongest tissue while also having the least-stable collagen molecules (as indicated by T_d). The posterior annulus, in contrast, was comparable to the strength of sartorius tendon, which also shared comparable measurements of thermal stability. While increases in the loading rate can lead to modest increases in strength,[133,134] all of the tests performed were slow enough to likely not be influenced by the relative differences in loading rate (ranging from 0.01 mm/sec to 1%/sec).[90,131,132]

To further explore the relationships between T_d, $t_{1/2}$, and UTS, bivariate linear regression was used (Figure 5.3). While the strong relationship between T_d and $t_{1/2}$ was anticipated based on previous research connecting an increase in total crosslinking density to an increase in thermal stability,[108,112,119] more interesting were the relationships involving UTS. For example, comparing UTS with $t_{1/2}$ (Figure 5.3B) suggests that UTS does not depend on total crosslinking density for the tissues referenced in Table 5.3, which is a surprising result given that previous research has shown that an increase in the total crosslinking density can lead to an increase in tensile strength.[78,113,135] Moreover, comparing UTS with T_d (Figure 5.3C) suggests that decreases in thermal stability lead to increases in strength. These findings illustrate that the strength of collagenous tissues may not necessarily depend on an increase in total crosslinking density, which is particularly interesting given that T_d and $t_{1/2}$ appear to be related.

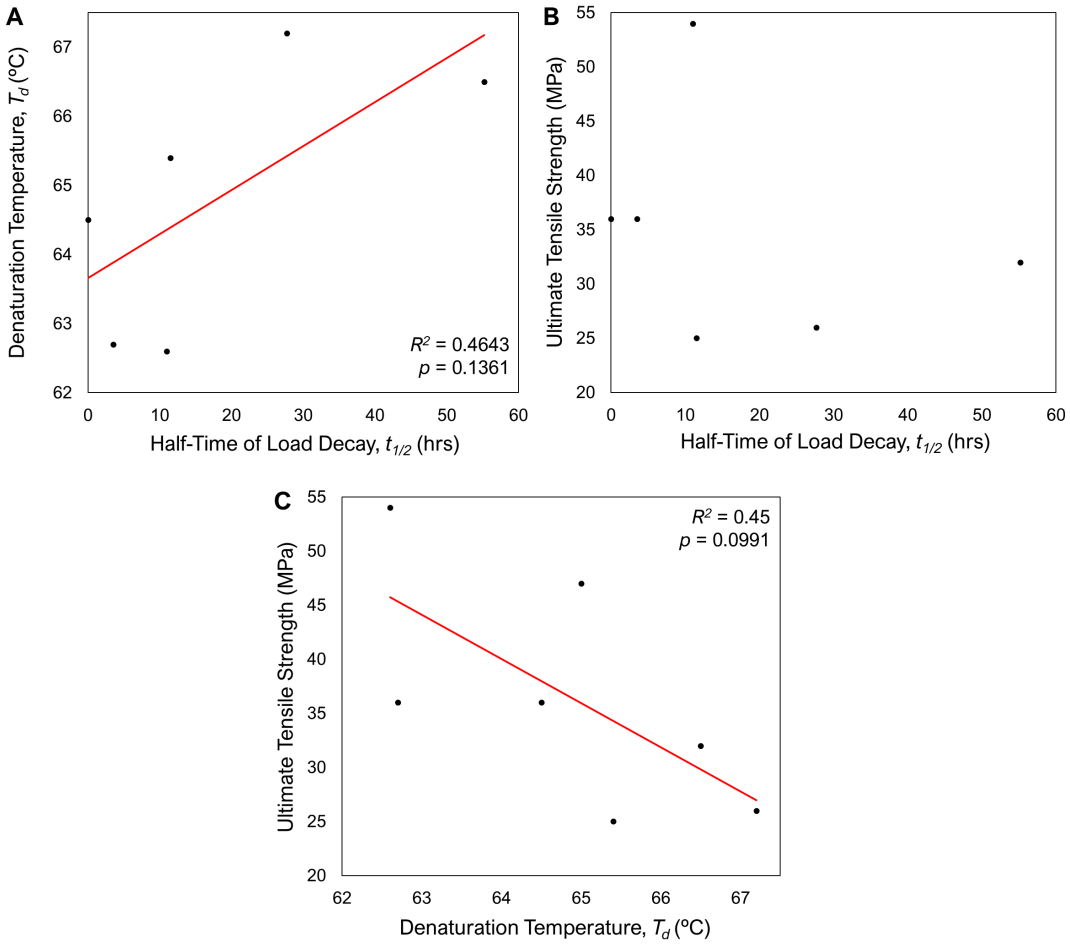

Figure 5.3: Bivariate linear regression between: the denaturation temperature and the half-time of load decay (A), the ultimate tensile strength and the half-time of load decay (B), and the ultimate tensile strength and the denaturation temperature (C).

5.3 Relationships Between Collagen Fibril Structure and Mechanical Properties

While the mechanical testing performed in the current work revealed that the anterior annulus is significantly stronger than the posterior annulus (which is in agreement with several other studies[83,84,88]), the hypothesis for this experiment was that the posterior annulus would be the stronger region – not the anterior annulus. This hypothesis was based on the assumption that the posterior annulus would have a higher density of thermally-stable crosslinks (per the first hypothesis for the HIT experiment, which was

confirmed), given that previous research has shown that increased crosslinking can significantly strengthen collagenous tissues.[113] For example, it has been shown that increasing exogeneous crosslinking in rat tail tendons using glutaraldehyde significantly increases their tensile strength.[135] Similarly, inhibition of enzymatic crosslinking in rat tail tendons using dietary lathyrogens has been shown to significantly decrease the ultimate tensile strength.[78] These findings are also supported by atomistic modeling that describe the mechanical properties of collagen fibrils based on crosslinking type and crosslinking density.[136] Given that the total crosslinking density of the posterior annulus was significantly larger than the anterior annulus, it would follow that the posterior annulus should be stronger than the anterior annulus – not weaker. Yet, studies have shown that greater enzymatic crosslinking density does not necessarily result in greater tissue strength, as revealed through the mechanical testing of samples from bovine forelimb extensor and flexor tendons[90,137,138] and human patellar tendons.[139] These observations have also been reported using single-fibril tensile experiments.[140,141] Comparison of bovine forelimb flexor to extensor tendon fibrils,[140] and rat Achilles to tail tendon fibrils[141] have shown that the more crosslinked flexor and Achilles tendon fibrils are no stronger than the less crosslinked extensor and tail tendon fibrils.

It is interesting that tissues with greater enzymatic crosslinking, higher thermal stability, and smaller collagen fibrils in several studies have proven to be less strong relative to those with less enzymatic crosslinking, lower thermal stability, and larger diameter fibrils. As Figure 5.3C illustrates, while there may be a relationship between UTS with T_d, there appears to be no relationship between UTS with $t_{1/2}$ for these particular tissues. Thus, thermal stability may be a determinant of strength for some collagenous tissues, rather than crosslinking density. It is possible that the relationship between thermal stability and strength is tied to relative differences in the size of fibrils. Collagen fibrils have been described as inhomogeneous structures composed of a stiff shell and a softer core when examined with atomic force microscopy.[142] There is evidence suggesting that the shell of fibrils is more thermally stable than the core.[143] If fibrils are structured that way, it is possible that smaller diameter fibrils would have a greater shell/core ratio; if so, this may play a role in explaining why smaller diameter fibrils have greater thermal

stability. For example, it has been shown that the diameter of collagen fibrils from flexor tendons are approximately half the size of fibrils from extensor tendons.[90] As Table 5.3 indicated, flexor tendons – relative to extensor tendons – were also weaker, had a higher density of enzymatic crosslinks, and had more thermally stable collagen.[90,140] Another instance of a tissue fitting these trends is the human sartorius tendon, which has smaller collagen fibrils relative to fibrils from other collagenous tissues.[132] As Table 5.3 illustrates, sartorius tendons are also weaker and have collagen with higher thermal stability and a higher density of crosslinking relative to other the collagenous tissues. Although no studies were identified that have explored whether collagen fibril diameter changes with annular region within the annulus, the fact that the posterior annulus is weaker, more heavily crosslinked, and has collagen with higher thermal stability relative to the anterior annulus may suggest that the posterior annulus is accompanied with smaller-diameter collagen fibrils.

Another factor that may contribute to the differences in mechanical properties observed between the anterior and posterior annulus are differences in the types of crosslinks present. Studies have shown that collagen fibril elongation depends on both crosslinking density and crosslinking type. [136,140,141,144] Atomistic modeling has described collagen fibril elongation as occurring over three phases.[136] While the initial phase is characterized by deformation due to straightening of the triple helix of collagen molecules, the second phase is characterized by a plateau region with a reduced elastic modulus governed primarily by intermolecular sliding. The final phase, which is accompanied by a high elastic modulus, occurs once the limit to intermolecular sliding has been reached, where extension proceeds via direct stretching of alpha-chains and intermolecular crosslinks.[136] These findings are supported by studies that performed stress-strain experiments on single collagen fibrils from functionally-distinct collagenous tissues.[140,141,144] For example, post-rupture imaging of collagen fibrils from extensor tendons – which primarily contain divalent crosslinks – indicate that they experience significant intermolecular sliding.[140] In contrast, collagen fibrils from flexor tendons – which primarily contain trivalent crosslinks – appear to better resist intermolecular sliding.[140] A higher capacity for intermolecular sliding implies less emphasis placed on extension via

stretching of alpha-chains and intermolecular crosslinks, which in turn could allow for collagen fibrils to more evenly distribute load between fibrils. [136] Because tissues are composed of collagen fibrils with a distribution of different lengths, shorter fibrils will be straightened before longer fibrils are straightened in response to an applied tensile load. Accordingly, shorter fibrils will generate larger stresses relative to longer fibrils for any given strain. Because intermolecular sliding is characterized by a reduced elastic modulus relative to the other phases of collagen fibril elongation,[136] tissues that demonstrate a higher capacity for intermolecular sliding (such as extensor fibrils relative to flexor fibrils, see Figure 5.4) could recruit a larger amount of fibrils under a similar stress, and thus more evenly distribute the load between fibrils. This, in turn, could lead to an increase in strength, as observed when comparing flexor tendons to extensor tendons.[90] These implications may explain why the anterior annulus is significantly stronger than the posterior annulus: its collagen fibrils may better permit molecular sliding to occur as a result of the difference in the types of crosslinks present, much to the same extent as the differences observed between fibrils from extensor and flexor tendons.[144]

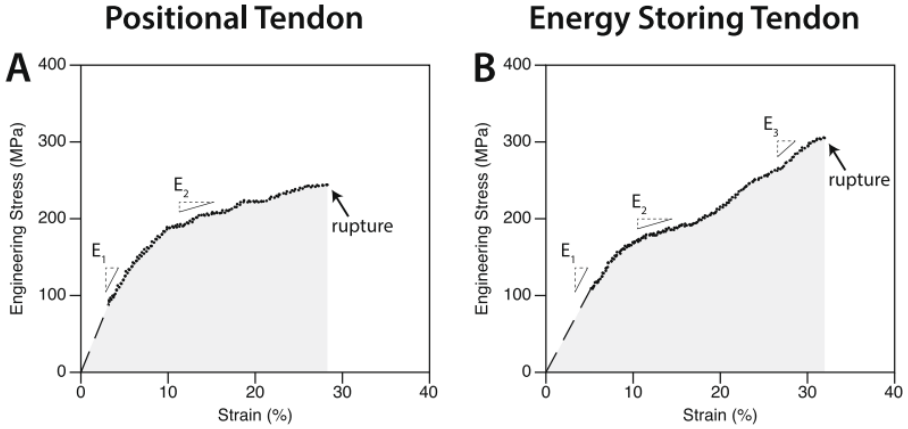

Figure 5.4: The engineering stress-strain diagrams for single fibrils from extensor tendons (A) and flexor tendons (B). Fibrils from extensor tendons experience significant intermolecular sliding relative to flexor fibrils, as characterized by a region with a reduced elastic modulus (indicated by E_2). Modified, with permission, from Quigley.[140]

5.4 Relationships Between Collagen Fibril Structure and Potential for Loading-Induced Fibril Damage

Given that significant differences in the structure of collagen fibrils between anterior and posterior regions were revealed through HIT analysis and DSC, it is likely that these differences in structure are accompanied by differences in how these regions accumulate damage. For example, through atomic-force microscopy and scanning electron microscopy, it has been shown that less crosslinked fibrils of low stress tendons undergo significant fibril plasticity at failure (Figure 5.5A and Figure 5.5C), while the more highly crosslinked fibrils of high stress tendons show minimal signs of disruption at failure (Figure 5.5B and Figure 5.5D).[90,133,140] Similar findings in fibril plasticity in response to tensile overload have also been reported when comparing rat-tail tendon fibrils to human patellar tendon fibrils, where fibrils from rat-tail tendons (composed primarily of divalent crosslinks) showed significant disruption at failure, while fibrils from human patellar tendons (composed primarily of trivalent crosslinks) showed minimal signs of disruption.[144] These findings illustrate how differences in the molecular structure of collagen (as seen in Table 5.3 for flexor and extensor tendons) are accompanied by differences in how these tissues accumulate damage. Given the similarities between the extensor tendon and the anterior annulus in terms of thermal stability and crosslinking, collagen fibrils from the anterior annulus when overloaded may be accompanied by longitudinal fibril disruption. Similarly, fibrils in the posterior annulus may undergo minimal disruption at failure as observed with fibrils from the flexor tendon. The accumulation of damage observed in extensor fibrils – termed discrete plasticity damage[145] – is associated with a decrease in lateral packing density of collagen fibrils, as reflected through a decrease in T_{onset} and an increase in $FWHM$ relative to undamaged tissue.[119] It is therefore possible that ruptured anterior samples measured with DSC would show similar changes in T_{onset} and $FWHM$ as observed in ruptured extensor fibrils.

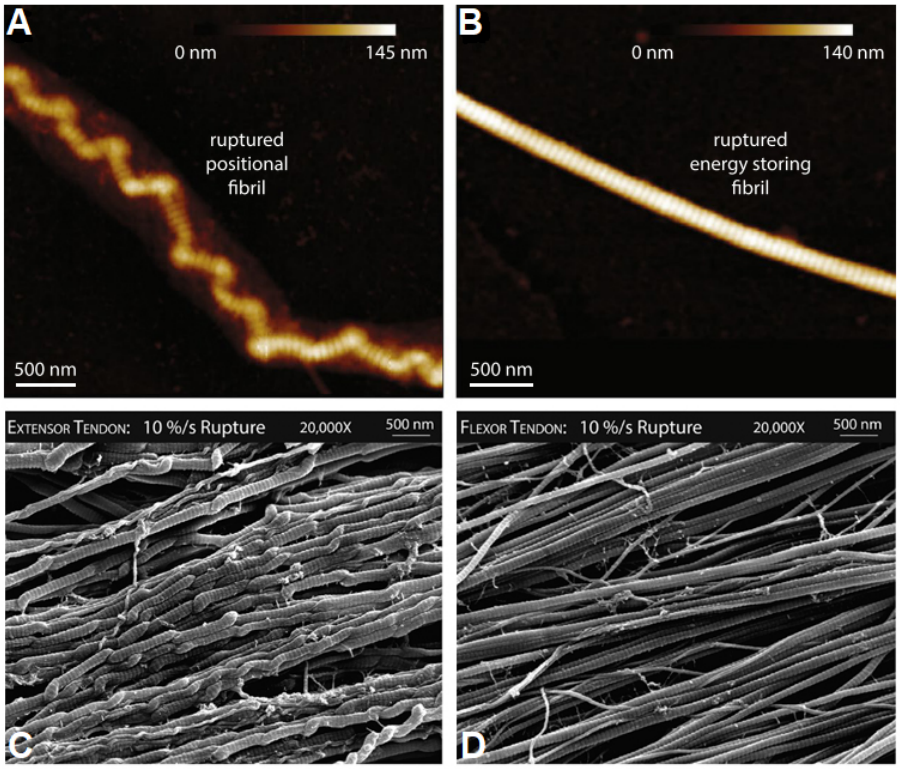

Figure 5.5: The difference in disruption between collagen fibrils from functionally distinct tendons as captured through atomic force microscopy (top) and scanning electron microscopy (bottom). A: A single collagen fibril from an extensor tendon following rupture, showing significant distortion throughout its length. B: A single collagen fibril from a flexor tendon following rupture, showing no signs of disruption. C: Collagen fibrils from an extensor tendon showing discrete plasticity damage following rupture. D: Collagen fibrils from a flexor tendon showing minimal disruption following rupture. A & B: Modified per the terms outlined by the Creative Commons Attribution 4.0 International Licenses (see Appendix).[140] C & D: Modified, with permission, from Chambers.[133]

While differences in the tensile properties of the annulus were directly assessed through the experiments performed, these regions may also differ in how they accumulate other types of damage, such as through prolonged loading or cyclic loading. For example, several studies have reported that collagen fibrils in flexor tendons, although weaker, showed significantly greater resistance to fatigue loading compared to fibrils from extensor tendons, which rapidly accumulated damage.[90,137] Improved fatigue resistance could be associated with a higher density of total crosslinks.[79] If so, its possible that the posterior annulus, despite being weaker, may have a molecular structure that is optimized

for fatigue resistance, rather than strength. Prolonged loading has also shown to cause extensive damage to collagen fibrils from bovine tail tendons through SEM.[146] Given that bovine tail tendons have comparable thermal stability to the extensor tendon and the anterior annulus (Table 5.3), its possible that more highly-crosslinked tissue, such as the posterior annulus, would accumulate less damage from static loading when compared to the less-crosslinked tissue, such as the anterior annulus.

5.5 Contributions to the Mechanics of Annular Disruption

The images taken with light microscopy, while primarily serving to allow for measurements of the radial depth of the annulus in samples prepared for mechanical testing, also revealed several interesting findings related to the interlamellar cohesion of the annulus, the role of cross bridges, and how intervertebral discs fail under tension.

Light microscopy revealed that all the samples pulled to rupture during mechanical testing primarily failed due to annular rupture near mid-disc height (Table 4.8). Three types of interlamellar damage were observed across samples, classified by their proximity to the ruptured ends of lamellae (see Figure 4.10 and Figure 4.11). Lamellae are interconnected through heterogeneously distributed cross-bridges that span in the radial direction.[26,28,103,147] While several different studies have shown that cross-bridges form a complex and interconnected network throughout the annulus, their precise structural role remains unclear. It is likely that cross-bridges serve to limit interlamellar movement,[103] and may play an important role in restricting the movement of nuclear material following a circumferential tear. The images in the current work illustrate that significant interlamellar damage can result from tensile loading, resulting in the loss of cohesion between adjacent layers. Yet, while extensive interlamellar damage was observed, it appears that cross-bridges may have played a role in resisting further disruption: in some samples, interlamellar damage appeared to terminate at a cross-bridge (Figure 5.6). These observations reinforce the idea that cross-bridges can serve as a means to limit interlamellar damage: had cross-bridges not been present, it appears that interlamellar damage would have extended further towards the endplate, further increasing the loss of

cohesion between lamellae. Given that the posterior annulus is placed in tension when the spine undergoes flexion, damaging flexion loads can lead to an accumulation of interlamellar damage; and indeed, the posterior annulus is reported as being particularly susceptible to concentric tears.[58] It is possible that cross-bridges may serve an important role in limiting the extent of concentric tearing within the posterior annulus.

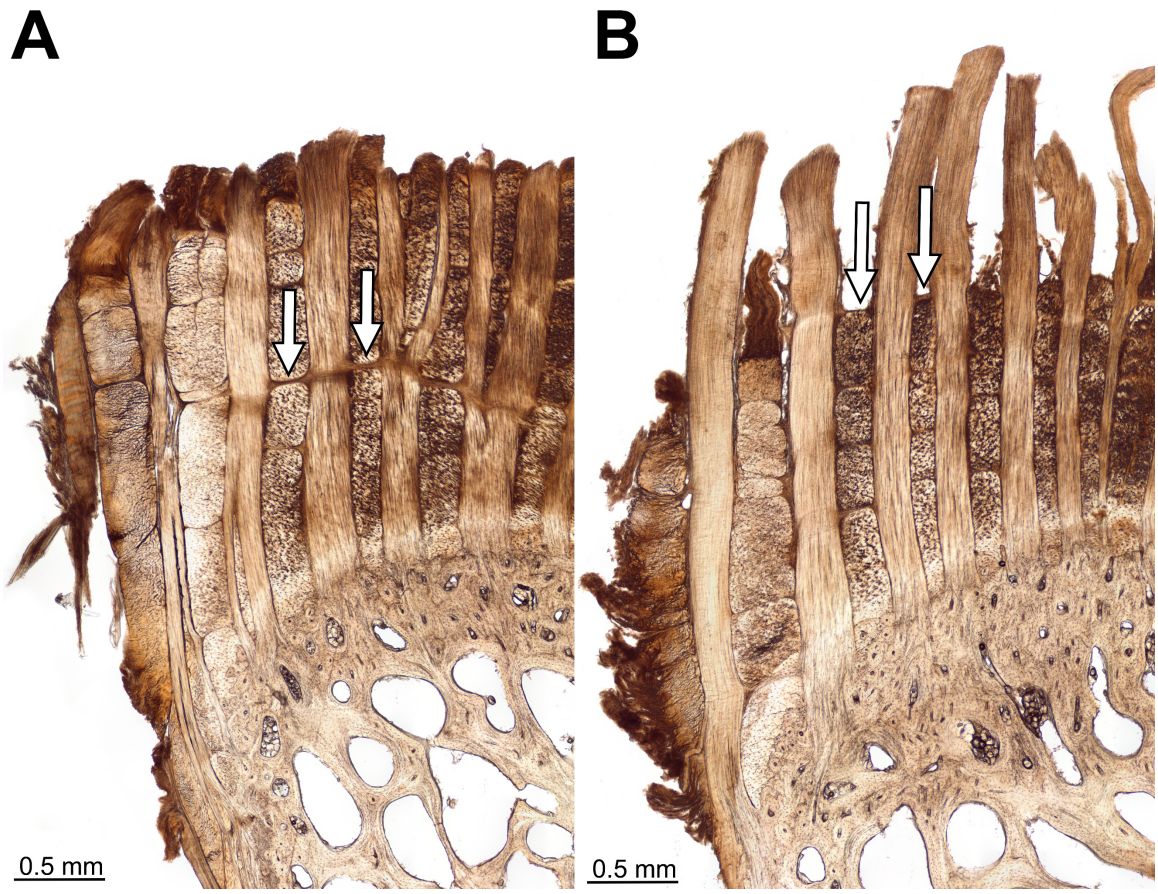

Figure 5.6: An example of cross-bridges that appear to limit interlamellar damage. A: A slice taken from an undamaged region, with arrows identifying cross-bridges spanning radially between lamellae. B: A slice taken from a damaged region, with arrows pointing to cross-bridges that correspond to locations where interlamellar damage terminates. Images are unstained cryosections of the same L6-7 disc taken using transmission light microscopy.

The images obtained from light microscopy also have implications for how disc herniations occur. It is well known that disc herniations favor the posterior annulus: approximately 80% are reported to occur in the paracentral region.[60] Moreover,

approximately 50% of protruded material following a disc herniation is reported to contain fragmented pieces of endplate material.[63] Given the complex loading environment of the intervertebral disc, the exact biomechanical factors involved in disc herniation are still not fully understood. *In vitro* biomechanical studies have shown that the endplate-vertebra junction at mid-anulus is particularly vulnerable to failure in response to hydrostatically-induced disruption.[148] Furthermore, the influence of torsion on disc herniation when combined with flexion has illustrated that the endplate-vertebra junction is likely sensitive to shear stress due to the increase in axial stress for annular fibres oriented in the direction of rotation.[32] The low prevalence of endplate damage amongst posterior samples in the current work (~17%, see Table 4.8) was significantly lower than the prevalence of endplate material observed in protruded material following a disc herniation (~50%).[63] This finding may highlight the vulnerability of the endplate-vertebra interface to shear stress, rather than tensile stress, reinforcing the notion that torsion is likely a key biomechanical factor in producing the endplate damage that ultimately results in disc herniation.

Lastly, while the ultimate tensile strength of collagen fibres from the anterior and posterior regions have been discussed prior, these measurements do not capture how much tension the structure of the annulus wall can support (accounting for the differences in the thicknesses of the annulus). Calculations of the tension strength of the annulus wall account for this by considering (i) how strong the material is, and (ii) how much material is present. The experiments performed revealed that the tension strength of the anterior annulus wall is over three times as strong as the posterior wall. While the posterior annulus is clearly the smaller and more vulnerable region relative to the anterior annulus (see Figure 1.5), it is surprising just how large the disparity in strength is: these findings help in understanding why the posterior annulus is particularly susceptible to injuries such as disc herniation.[60]

Chapter 6: Conclusion

The results of the experiments performed in the current work show that significant variations exist in collagen structure between the anterior and posterior annular regions of lumbar intervertebral discs, and that these variations are accompanied by differences in tensile mechanics. Collagen molecules from the posterior annulus have greater thermal stability and a higher density of intermolecular crosslinking relative to the anterior annulus throughout the lumbar spine, from L5-6 to L1-2. Variations in collagen were also observed with radial depth: the inner annulus has greater heterogeneity in collagen thermal stability relative to the outer annulus, but only for the anterior region. Despite being more heavily crosslinked, the posterior annulus has significantly lower ultimate tensile strength than the anterior annulus. The question of whether the differing structure of the posterior annulus is functionally advantageous in some way remains to be seen; while collagen molecules from the posterior region are more thermally-stable and contain a significantly higher density of crosslinking relative to the anterior region, these structural differences did not manifest in terms of strength. It is possible that the posterior annulus is optimized for a role other than strength, such as fatigue resistance.

In terms of significance, these findings pertain most importantly to the field of tissue repair and regeneration. Therapies designed to reverse damage depend on a fundamental understanding of native tissue structure. Tissue engineered scaffolds may benefit from incorporating how the annulus varies at the molecular level. Obtaining a better understanding of how these molecular-level structural differences serve the posterior annulus would have important implications for tissue-engineered scaffolds. If the posterior annulus is, for example, optimized for fatigue loading, designing biomaterials that match this functional role may lead to improved scaffold performance.

Future Works

While the results presented in the current work revealed many novel findings on how the native structure of collagen in lumbar intervertebral discs varies regionally, there remains

several unanswered questions that further investigations should seek to clarify. First, chemical crosslink analysis, such as high-performance liquid chromatography (HPLC), should be used to determine the different types of crosslinks present in lumbar intervertebral discs. While there is evidence suggesting that pyridinoline crosslinks exist, other crosslinks may also be present; moreover, their proportions may significantly differ between anterior and posterior regions, which could contribute to the observed differences in thermal stability observed between these regions. Second, the native structure of collagen fibrils should be assessed using SEM to determine if ultrastructural variations between the anterior and posterior regions exist. If differences in fibril diameter are observed, this could help in explaining the observed differences in thermal stability and strength between these regions. The structure of collagen may also vary in other ways: for example, collagen fibrils in flexor tendons, but not extensor tendons, were bundled laterally by a filamentous webbing, likely composed of type VI collagen.[90] Given that the presence of type VI collagen has been confirmed for human lumbar intervertebral discs,[149] it would be interesting to see if a similar webbing is present in the annulus and if so, if it favors a particular region.

Beyond further characterizing the native structure of collagen in lumbar intervertebral discs, future experiments should also seek to better understand whether the anterior and posterior regions accumulate damage in different ways. Performing DSC on samples that have been pulled to rupture would allow for determination of how the molecular structure of collagen responds to tensile damage, and whether this response varies between regions. Moreover, performing SEM on samples that have been ruptured would determine whether discrete plasticity damage is present, and if so, whether it favors one region more than the other. The response of anterior and posterior samples to other types of damage would be important to consider as well. Given that back injuries are often associated with repetitive or static flexion of the lumbar spine, future mechanical testing that utilizes cyclic loading or static loading would be relevant physiologically. Because there is evidence suggesting that significant differences in crosslinking are accompanied by differing abilities in withstanding fatigue damage,[90] cyclic loading tests may reveal that the posterior annulus is optimized for fatigue resistance rather than strength.

References

1. Bogduk N, Baker RM. *Clinical and Radiological Anatomy of the Lumbar Spine (5th Edition)*. Sydney: Churchill Livingstone; 2012.

2. White AA, Panjabi MM. *Clinical Biomechanics of the Spine (2nd Edition)*. Philidelphia: Lippincott; 1990.

3. Moore K, Dalley A, Agur A. *Clinically Oriented Anatomy (7th Edition)*. Baltimore: Lippincott Williams and Wilkins; 2014.

4. Cole MH, Grimshaw PN. Low Back Pain and Lifting: A Review Of Epidemiology and Aetiology. *Work*. 2003;21(2):173-184.

5. Rodrigues S. A Structural Exploration of Annulus-Endplate Integration in the Ovine Intervertebral Disc (Doctoral Dissertation). The University of Auckland. 2015.

6. Lundon K, Bolton K. Structure and Function of the Lumbar Intervertebral Disc in Health, Aging and Pathologic Conditions. *J Orthop Sport Phys Ther*. 2001;31(6):291-306.

7. Iatridis JC, MacLean JJ, O'Brien M, Stokes IAF. Measurements of Proteoglycan and Water Content Distribution in Human Lumbar Intervertebral Discs. *Spine (Phila Pa 1976)*. 2012;32(14):1493-1497.

8. Adams MA, Roughley PJ. What is Intervertebral Disc Degeneration, and What Causes It? *Spine (Phila Pa 1976)*. 2006;31(18):2151-2161.

9. Inoue H. Three-Dimensional Architecture of Lumbar Intervertebral Discs. *Spine (Phila Pa 1976)*. 1981;6(2):139-146.

10. Inoue H, Takeda T. Three-Dimensional Observation of Collagen Framework of Lumbar Intervertebral Discs. *Acta Orthop Scand*. 1975;6470(46):949-956.

11. Eyre DR, Muir H. Biochemical Aspects of Development and Ageing of Human Lumbar Intervertebral Discs. *Rheumatol Rehabil*. 1977;16(1):22-29.

12. Wade KR, Robertson PA, Broom ND. On the Extent and Nature of Nucleus-Annulus Integration. *Spine (Phila Pa 1976)*. 2012;37(21):1826-1833.

13. Wade KR, Robertson PA, Broom ND. On How Nucleus-Endplate Integration is Achieved at the Fibrillar Level in the Ovine Lumbar Disc. *J Anat*. 2012;221(1):39-46.

14. Wade KR, Robertson PA, Broom ND. A Fresh Look at the Nucleus-Endplate Region: New Evidence for Significant Structural Integration. *Eur Spine J*. 2011;20(8):1225-1232.

15. Veres SP. Studies on the Internal Failure Mechanics of Lumbar Intervertebral Discs (Doctoral Dissertation). The University of Auckland. 2009.

16. Eyre DR, Muir H. Quantitative Analysis of Types I and II Collagens in Human Intervertebral Discs at Various Ages. *Biochim Biophys Acta*. 1977;492(1):29-42.

17. Eyre DR, Muir H. Types I and II Collagens in Intervertebral Disc. *Biochem J*. 1976;157(1):267-270.

18. Cassidy JJ, Hiltner A, Baer E. Hierarchical Structure of the Intervertebral Disc. *Connect Tissue Res*. 1989;23(1):75-88.

19. Marchand F, Ahmed AM. Investigation of the Laminate Structure of Lumbar Disc Anulus Fibrosus. *Spine (Phila Pa 1976)*. 1990;15(5):402-410.

20. Holzapfel GA, Schulze-Bauer CAJ, Feigl G, Regitnig P. Single Lamellar Mechanics of the Human Lumbar Anulus Fibrosus. *Biomechan Model Mechanobiol*. 2005;3(3):125-140.

21. Tsuji H, Hirano N, Ohshima H, Ishihara H, Terahata N, Motoe T. Structural Variation of the Anterior and Posterior Anulus Fibrosus in the Development of Human Lumbar Intervertebral Disc - A Risk Factor for Intervertebral Disc Rupture. *Spine (Phila Pa 1976)*. 1993;18(2):204-210.

22. Hashizume H. Three-Dimensional Architecture and Development of Lumbar Intervertebral Discs. *Acta Med Okayama*. 1980;34(5):301-314.

23. Roberts S, Menage J, Urban JPG. Biochemical and Structural Properties of the Cartilage End-Plate and its Relation to the Intervertebral Disc. *Spine (Phila Pa 1976)*. 1988;14(2):166-174.

24. Smith LJ, Elliott DM. Formation of Lamellar Cross Bridges in the Annulus Fibrosus of the Intervertebral Disc is a Consequence of Vascular Regression. *Matrix Biol*. 2011;30(4):267-274.

25. Brown S, Rodrigues S, Sharp C, et al. Staying Connected: Structural Integration at the Intervertebral Disc – Vertebra Interface of Human Lumbar Spines. *Eur Spine J*. 2016;26(1):248-258.

26. Pezowicz CA, Robertson PA, Broom ND. The Structural Basis of Interlamellar Cohesion in the Intervertebral Disc Wall. *J Anat*. 2006;208(3):317-330.

27. Han SK, Chen C, Labus KM, Puttlitz CM, Chen Y, Hsieh AH. Optical Coherence Tomagraphic Elastography Reveals Mesoscale Shear Strain Inhomogeneities in the Annulus Fibrosus. *Spine (Phila Pa 1976)*. 2017;41(13):1-16.

28. Schollum ML, Robertson PA, Broom ND. ISSLS Prize Winner: Microstructure and Mechanical Disruption of the Lumbar Disc Annulus. Part I: A Microscopic Investigation of the Translamellar Bridging Network. *Spine (Phila Pa 1976)*. 2008;33(25):2702-2710.

29. Paietta RC, Burger EL, Ferguson VL. Mineralization and Collagen Orientation Throughout Aging at the Vertebral Endplate in the Human Lumbar Spine. *J Struct Biol*. 2013;184(2):310-320.

30. Coventry MB, Ghormley RK, Kernohan JW. The Intervertebral Disc: Its Microscopic Anatomy and Pathology. Part I: Anatomy, Development, and Physiology. *J Bone Jt Surg*. 1945;27(1):105-112.

31. Francois RJ, Dhem A. Microradiographic Study of the Normal Human Vertebral Body. *Acta Anat*. 1974;89(2):251-265.

32. Veres SP, Robertson PA, Broom ND. The Influence of Torsion on Disc Herniation When Combined With Flexion. *Eur Spine J*. 2010;19(9):1468-1478.

33. Francois RJ. Ligament Insertions Into the Human Lumbar Vertebral Body. *Acta Anat*. 1975;91(3):467-480.

34. Nosikova YS, Santerre JP, Grynpas M, Gibson G, Kandel RA. Characterization of the Annulus Fibrosus-Vertebral Body Interface: Identification of New Structural Features. *J Anat*. 2012;221(6):577-589.

35. Schollmeier G, Lewandrowski K. Observations on Fiber-Forming Collagens in the Anulus Fibrosus. *Spine (Phila Pa 1976)*. 2000;25(21):2736-2741.

36. Dar G, Marsharawi Y, Peleg S, et al. The Epiphyseal Ring. *Spine (Phila Pa 1976)*. 2011;36(11):850-856.

37. Nachemson A. The Load on Lumbar Discs in Different Positions of the Body. *Clin Orthop Relat Res*. 1966;45:107-122.

38. Shirazi-Adl SA, Shrivastava SC, Ahmed AM. Stress Analysis of the Lumbar Disc-Body Unit in Compression: A Three-Dimensional Nonlinear Finite Element Study. *Spine (Phila Pa 1976)*. 1984;9(2):120-134.

39. Schmidt H, Galbusera F, Rohlmann A, Shirazi-adl A. What Have We Learned From Finite Element Model Studies of Lumbar Intervertebral Discs in the Past Four Decades ? *J Biomech*. 2013;46(14):2342-2355.

40. Shapiro IM, Risbud M V. *The Intervertebral Disc - Molecular and Structural Studies of the Disc in Health and Disease*. Springer; 2014.

41. Urban JPG, McMullin JF. Swelling Pressure of the Lumbar Intervertebral Discs: Influence of Age, Spinal Level, Composition, and Degeneration. *Spine (Phila Pa 1976)*. 1988;13(2):179-187.

42. Mcmillan DW, Garbutt G, Adams MA. Effect of Sustained Loading on the Water Content of Intervertebral Discs: Implications for Disc Metabolism. *Ann Rheum Dis*. 1996;55(12):880-887.

43. Urban JPG, Maroudas A. Swelling of the Intervertebral Disc In Vitro. *Connect Tissue Res*. 1981;9(1):1-10.

44. Adams MA, McMillan DW, Green TP, Dolan P. Sustained Loading Generates Stress Concentrations in Lumbar Intervertebral Discs. *Spine (Phila Pa 1976)*. 1996;21(4):434-438.

45. Malko JA, Hutton WC, Fajman WA. An In Vivo MRI Study of the Changes in Volume (and Fluid Content) of the Lumbar Intervertebral Disc After Overnight Bed Rest and During an 8-Hour Walking Protocol. *J Spinal Disord Tech*. 2002;15(2):157-163.

46. Wilke H, Neef P, Caimi M, Hoogland T, Claes LE. New In Vivo Measurements of Pressures in the Intervertebral Disc in Daily Life. *Spine (Phila Pa 1976)*. 1999;24(8):755-762.

47. Lu M, Hutton WC, Gharpuray VM. Do Bending, Twisting, and Diurnal Fluid Changes in the Disc Affect the Propensity to Prolapse? A Viscoelastic Finite Element Model. *Spine (Phila Pa 1976)*. 1996;21(22):2570-2579.

48. Adams MA, McNally DS. Internal Intervertebral Disc Mechanics as Revealed by Stress Profilometry. *Spine (Phila Pa 1976)*. 1992;17(1):66-73.

49. McMillan DW, McNally DS, Garbutt G, Adams MA. Stress Distributions Inside Intervertebral Discs: The Validity of Experimental 'Stress Profilometry'. *Proc Instn Mech Engrs*. 1996;210(2):81-87.

50. Pearcy MJ, Tibrewal SB. Lumbar Intervertebral Disc and Ligament Deformations Measured In Vivo. *Clin Orthop Relat Res*. 1984;191:281-286.

51. Alexander LA, Hancock E, Agouris I, Smith FW, Macsween A. The Response of the Nucleus Pulposus of the Lumbar Intervertebral Discs to Functionally Loaded Positions. *Spine (Phila Pa 1976)*. 2007;32(14):1508-1512.

52. Seroussi RE, Krag MH, Muller DL, Pope MH. Internal Deformations of Intact and Denucleated Human Lumbar Discs Subjected to Compression, Flexion, and Extension Loads. *J Orthop Res*. 1989;7(1):122-131.

53. Krismer M, Haid C, Rabl W. The Contribution of Anulus Fibers to Torque Resistance. *Spine (Phila Pa 1976)*. 1996;21(22):2551-2557.

54. Drake JDM, Aultman CD, Mcgill SM, Callaghan JP. The Influence of Static Axial Torque in Combined Loading on Intervertebral Joint Failure Mechanics Using a Porcine Model. *Clin Biomech*. 2005;20(10):1038-1045.

55. Schwarzer AC, Aprill CN, Derby R, Fortin J, Kine G, Bogduk N. The Prevalence and Clinical Features of Internal Disc Disruption in Patients With Chronic Low Back Pain. *Spine (Phila Pa 1976)*. 1995;20(17):1878-1883.

56. Fardon DF, Milette PC. Nomenclature and Classification of Lumbar Disc Pathology. Recommendations of the Combined Task Forces of the North American Spine Society, American Society of Spine Radiology, and American Society of Neuroradiology. *Spine (Phila Pa 1976)*. 2001;26(5):93-113.

57. Aprill C, Bogduk N. High-Intensity Zone: A Diagnostic Sign of Painful Lumbar Disc on MRI. *Br J Radiol*. 1992;65(773):361-369.

58. Vernon-Roberts B, Moore RJ, Fraser RD. The Natural History of Age-Related Disc Degeneration The Pathology and Sequelae of Tears. *Spine (Phila Pa 1976)*. 2007;32(25):2797-2804.

59. Moneta GB, Videman T, Kaivanto K, et al. Reported Pain During Lumbar Discography as a Function of Anular Ruptures and Disc Degeneration. *Spine (Phila Pa 1976)*. 1994;19(17):1968-1974.

60. Garcia-Cosamalon J, Valle MED, Calavia MG, et al. Intervertebral Disc, Sensory Nerves, and Neurotrophins: Who is Who in Discogenic Pain? *J Anat*. 2010;217(1):1-15.

61. Bogduk N, Tynan W, Wilson AS. The Nerve Supply to the Human Lumbar Intervertebral Discs. *J Anat*. 1981;132(1):39-56.

62. Raj PP. Intervertebral Disc: Anatomy-Physiology-Pathophysiology-Treatment. *Pain Pract*. 2008;8(1):18-44.

63. Moore RJ, Vernon-Roberts B, Fraser RD, Schembri M. The Origin and Fate of Herniated Lumbar Intervertebral Disc Tissue. *Spine (Phila Pa 1976)*. 1996;21(18):2149-2155.

64. Rajasekaran S, Bajaj N, Tubaki V, Kanna RM, Shetty AP. ISSLS Prize Winner: The Anatomy of Failure in Lumbar Disc Herniation. *Spine (Phila Pa 1976)*. 2013;38(17):1491-1500.

65. Ebeling U, Reulen HJ. Are There Typical Localisations of Lumbar Disc Herniations ? A Prospective Study. *Acta Neurochir*. 1992;117(3-4):143-148.

66. Adams MA, Hutton WC. Prolapsed Intervertebral Disc - A Hyperflexion Study. *Spine (Phila Pa 1976)*. 1982;7(3):184-191.

67. Kelsey JL, Githens PB, White AA, et al. An Epidemiologic Study of Lifting and Twisting on the Job and Risk for Acute Prolapsed Lumbar Intervertebral Disc. *J Orthop Res*. 1984;2(1):61-66.

68. Bogduk N. On the Definitions and Physiology of Back Pain, Referred Pain, and Radicular Pain. *Pain*. 2009;147(1):17-19.

69. Antoniou J, Aebi M, Alini M. The Human Lumbar Intervertebral Disc: Evidence for Changes in the Biosynthesis and Denaturation of the Extracellular Matrix With Growth, Maturation, Ageing, and Degeneration. *J Clin Invest*. 1996;98(4):996-1003.

70. Stefanakis M, Luo J, Pollintine P, Dolan P, Adams MA. ISSLS Prize Winner: Mechanical Influences in Progressive Intervertebral Disc Degeneration. *Spine (Phila Pa 1976)*. 2014;39(17):1365-1372.

71. Pfirrmann CWA, Metzdorf A, Zanetti M, Hodler J, Boos N. Magnetic Resonance Classification of Lumbar Intervertebral Disc Degeneration. *Spine (Phila Pa 1976)*. 2001;26(17):1873-1878.

72. Thompson JP, Pearce RH, Schechter MT, Adams ME, Tsang IKY, Bishop PB. Preliminary Evaluation of a Scheme for Grading the Gross Morphology of the Human Intervertebral Disc. *Spine (Phila Pa 1976)*. 1990;15(5):411-415.

73. Adams MA, Dolan P, Hutton WC. The Stages of Disc Degeneration As Revealed By Discograms. *J Bone Jt Surg*. 1986;68(1):36-41.

74. Videman T, Battié MC, Gibbons LE, Gill K. A New Quantitative Measure of Disc Degeneration. *Spine J*. 2017;17(5):746–753.

75. Rutges JPHJ, Duit RA, Kummer JA, et al. A Validated New Histological Class for Intervertebral Disc Degeneration. *Osteoarthr Cartil*. 2013;21(12):2039-2047.

76. Schmidt H, Kettler A, Heuer F, Simon U, Claes L, Wilke H-J. Intradiscal Pressure, Shear Strain, and Fiber Strain in the Intervertebral Disc Under Combined Loading. *Spine (Phila Pa 1976)*. 2007;32(7):748-755.

77. Villa T, Wilke H-J, Galbusera F, Berger-Roscher N, Bassani T, Casaroli G. Numerical Prediction of the Mechanical Failure of the Intervertebral Disc under Complex Loading Conditions. *Materials (Basel)*. 2017;10(1):1-14.

78. Haut RG. The Effect of a Lathyritic Diet on the Sensitivity of Tendon to Strain Rate. *J Biomech Eng*. 1985;107(2):166-174.

79. Herod TW, Veres SP. Development of Overuse Tendinopathy: A New Descriptive Model for the Initiation of Tendon Damage During Cyclic Loading. *J Orthop Res*. 2018;36(1):1-10.

80. Willett TL, Labow RS, Lee JM. Mechanical Overload Decreases the Thermal Stability of Collagen in an In Vitro Tensile Overload Tendon Model. *J Orthop Res*. 2008;26:1605-1610.

81. Newell N, Little JP, Christou A, Adams MA, Adam CJ, Masouros SD. Biomechanics of the Human Intervertebral Disc: A Review of Testing Techniques and Results. *J Mech Behav Biomed Mater*. 2017;69:420-434.

82. Shan Z, Li S, Liu J, Mamuti M, Wang C, Zhao F. Correlation Between Biomechanical Properties of the Annulus Fibrosus and Magnetic Resonance Imaging (MRI) Findings. *Eur Spine J*. 2015;24(9):1909-1916.

83. Acaroglu ER, Iatridis JC, Setton LA, Foster RJ, Mow VC, Weidenbaum M. Degeneration and Aging Affect the Tensile Behavior of Human Lumbar Anulus Fibrosus. *Spine (Phila Pa 1976)*. 1995;20(24):2690-2701.

84. Ebara S, Iatridis J, Setton L, Foster R, Mow V, Weidenbaum M. Tensile Properties of Nondegenerate Human Lumbar Anulus Fibrosus. *Spine (Phila Pa 1976)*. 1996;21(4):452-461.

85. Skaggs D, Weidenbaum M, Iatridis J, Ratcliffe A, Mow V. Regional Variation in Tensile Properties and Biochemical Composition of the Human Lumbar Anulus Fibrosus. *Spine (Phila Pa 1976)*. 1994;19(12):1310-1319.

86. Skrzypiec D, Tarala M, Pollintine P, Dolan P, Adams MA. When Are Intervertebral Discs Stronger Than Their Adjacent Vertebrae? *Spine (Phila Pa 1976)*. 2007;32(22):2455-2461.

87. Green TP, Adams MA, Dolan P. Tensile Properties of the Annulus Fibrosus II. Ultimate Tensile Strength and Fatigue Life. *Eur Spine J*. 1993;2(4):209-214.

88. Zak M, Pezowicz C. Spinal Sections and Regional Variations in the Mechanical Properties of the Annulus Fibrosus Subjected to Tensile Loading. *Acta Bioeng Biomech*. 2013;15(1):51-59.

89. Wells SM, Adamson SL, Langille BL, Lee JM. Thermomechanical Analysis of Collagen Crosslinking in the Developing Ovine Thoracic Aorta. *Biorheology*. 1998;35(6):399-414.

90. Herod TW, Chambers NC, Veres SP. Collagen Fibrils in Functionally Distinct Tendons Have Differing Structural Responses to Tendon Rupture and Fatigue Loading. *Acta Biomater*. 2016;42:296-307.

91. Nachemson AL, Schultz AB, Berkson MH. Mechanical Properties of Human Lumbar Spine Motion Segments - Influences of Age, Sex, Disc Level, and Degeneration. *Spine (Phila Pa 1976)*. 1979;4(1):1-8.

92. Maroudas A, Stockwell RA, Nachemson A, Urban J. Factors Involved in the Nutrition of the Human Lumbar Intervertebral Disc: Cellularity and Diffusion of Glucose In Vitro. *J Anat*. 1975;120(1):113-130.

93. Heeswijk VM V, Thambyah A, Robertson PA, Broom ND. Does An Annular Puncture Influence the Herniation Path? *Spine (Phila Pa 1976)*. 2018;43(7):467-476.

94. Berger-Roscher N, Casaroli G, Rasche V, Villa T, Galbusera F, Wilke H. Influence of Complex Loading Conditions on Intervertebral Disc Failure. *Spine (Phila Pa 1976)*. 2017;42(2):78-85.

95. Bae HW, Patel V V, Sardar ZM, et al. Transient Local Bone Remodeling Effects of rhBMP-2 in an Ovine Interbody Spine Fusion Model. *J Bone Jt Surg*. 2016;98(24):2061-2070.

96. Wilke HJ, Kettler A, Wenger KH, Claes LE. Anatomy of the Sheep Spine and Its Comparison to the Human Spine. *Anat Rec*. 1997;247(4):542-555.

97. Easley NE, Wang M, McGrady LM, Toth JM. Biomechanical and Radiographic Evaluation of an Ovine Model for the Human Lumbar Spine. *Proc Inst Mech Eng Part H J Eng Med*. 2008;222(6):915-922.

98. Smit TH. The Use of a Quadruped as an In Vivo Model for the Study of the Spine - Biomechanical Considerations. *Eur Spine J*. 2002;11(2):137-144.

99. Wolff J. Das Gesetz der Transformation der Knochen. Translated as: The Law of Bone Remodelling. *Springer Verlag*. 1892;1:1-152.

100. Adams MA, Lama P, Zehra U, Dolan P. Why Do Some Intervertebral Discs Degenerate, When Others (in the Same Spine) Do Not? *Clin Anat*. 2015;28(2):195-204.

101. Monaco LA, Dewitte-Orr SJ, Gregory DE. A Comparison Between Porcine, Ovine, and Bovine Intervertebral Disc Anatomy and Single Lamella Annulus Fibrosus Tensile Properties. *J Morphol*. 2016;277(2):244-251.

102. Reid JE, Meakin JR, Robins SP, Skakle JMS, Hukins DWL. Sheep Lumbar Intervertebral Discs as Models for Human Discs. *Clin Biomech*. 2002;17(4):312-314.

103. Schollum ML, Robertson PA, Broom ND. A Microstructural Investigation of Intervertebral Disc Lamellar Connectivity: Detailed Analysis of the Translamellar Bridges. *J Anat*. 2009;214(6):805-816.

104. Beckstein JC, Sen S, Schaer TP, Vresilovic EJ, Elliott DM. Comparison of Animal Discs Used in Disc Research to Human Lumbar Disc: Axial Compression Mechanics and Glycosaminoglycan Content. *Spine (Phila Pa 1976)*. 2008;33(6):166-173.

105. Showalter BL, Beckstein JC, Martin JT, et al. Comparison of Animal Discs Used in Disc Research to Human Lumbar Disc: Torsion Mechanics and Collagen Content. *Spine (Phila Pa 1976)*. 2013;37(15):1-17.

106. Bick EM, Copel JW. Longtidunal Growth of the Human Vertebra. *J Bone Jt Surg*. 1950;32(4):803-814.

107. Alini M, Eisenstein SM, Ito K, et al. Are Animal Models Useful for Studying Human Disc Disorders/Degeneration? *Eur Spine J*. 2008;17(1):2-19.

108. Aldous IF, Veres SP, Jahangir A, Lee JM. Differences in Collagen Cross-Linking Between the Four Valves of the Bovine Heart: A Possible Role in Adaptation to Mechanical Fatigue. *Am J Physiol Hear Circ Physiol*. 2009;296(6):1898–1906.

109. Lee JM, Pereira CA, Abdulla D, Naimark WA, Crawford I. A Multi-Sample Denaturation Temperature Tester for Collagenous Biomaterials. *Med Eng Phys*. 1995;17(2):115-121.

110. Veres SP, Harrison JM, Lee JM. Cross-Link Stabilization Does Not Affect the Response of Collagen Molecules, Fibrils, or Tendons to Tensile Overload. *J Orthop Res*. 2013;31(12):1907-1913.

111. Willett TL. *Molecular-Level Changes in Collagen Due to In Vitro Tensile Overload in a Tendon Model (Doctoral Dissertation). Dalhousie University.*; 2007.

112. Miles CA, Ghelashvili M. Polymer-in-a-Box Mechanism for the Thermal Stabilization of Collagen Molecules in Fibers. *Biophys J*. 1999;76(6):3243-3252.

113. Fratzl P. *Collagen Structure and Mechanics*. New York: Springer; 2008.

114. Tan CI, Kent GN, Randall AG, Edmondston SJ, Singer KP. Collagen and Elastin Crosslinks in Human Intervertebral Discs and Ligamentum Flavum: Age, Gender, and Spinal Level Influences. *J Musculoskelet Res*. 2002;6(2):73-88.

115. Bailey AJ, Paul RG, Knott L. Mechanisms of Maturation and Ageing of Collagen. *Mech Ageing Dev*. 1998;106(1-2):1-56.

116. Gautieri A, Redaelli A, Buehler MJ, Vesentini S. Age- and Diabetes-Related Nonenzymatic Crosslinks in Collagen Fibrils: Candidate Amino Acids Involved in Advanced Glycation End-Products. *Matrix Biol*. 2014;34:89-95.

117. Tan CI, Kent GN, Randall AG, Edmondston SJ, Singer KP. Age-Related Changes in Collagen, Pyridinoline, and Deoxypyridinoline in Normal Human Thoracic Intervertebral Discs. *J Gerontol Biol Sci*. 2003;58(5):387-393.

118. Pokharna HK, Phillips FM. Collagen Crosslinks in Human Lumbar Intervertebral Disc Aging. *Spine (Phila Pa 1976)*. 1998;23(15):1645-1648.

119. Veres SP, Harrison JM, Lee JM. Mechanically Overloading Collagen Fibrils Uncoils Collagen Molecules, Placing Them in a Stable, Denatured State. *Matrix Biol*. 2014;33:54-59.

120. Nachemson A. Lumbar Intradiscal Pressure: Experimental Studies on Post-Mortem Material. *Acta Orthop Scand*. 1960;31(43):1-104.

121. Hutton WC, Adams MA. Can the Lumbar Spine Be Crushed in Heavy Lifting? *Spine (Phila Pa 1976)*. 1982;7(6):586-590.

122. Tang R, Gungor C, Sesek RF, Bo K, Gallagher S, Davis GA. Morphometry of the Lower Lumbar Intervertebral Discs and Endplates: Comparative Analyses of New MRI Data With Previous Findings. *Eur Spine J*. 2016;25(12):4116-4131.

123. Pooni JS, Hukins DWL, Harris PF, Hilton RC, Davies KE. Comparison of the Structure of Human Intervertebral Discs in the Cervical, Thoracic and Lumbar Regions of the Spine. *Surg Radiol Anat*. 1986;8(3):175-182.

124. Sims TJ, Avery NC, Bailey AJ. Quantitative Determination of Collagen Crosslinks. *Methods Mol Biol*. 2000;139(3):11-26.

125. Bruehlmann SB, Rattner JB, Matyas JR, Duncan NA. Regional Variations in the Cellular Matrix of the Annulus Fibrosus of the Intervertebral Disc. *J Anat*. 2002;201(2):159-171.

126. Setton LA, Chen J. Cell Mechanics and Mechanobiology in the Intervertebral Disc. *Spine (Phila Pa 1976)*. 2004;29(23):2710-2723.

127. Urban JPG, Smith S, Fairbank JCT. Nutrition of the Intervertebral Disc. *Spine (Phila Pa 1976)*. 2004;29(23):2700-2709.

128. Urban JPG, Holm S, Maroudas A, Nachemson A. Nutrition of the Intervertebral Disk - An In Vitro Study of Solute Transport. *Clin Orthop Relat Res*. 1977;129:101-114.

129. Roughley PJ. Biology of Intervertebral Disc Aging and Degeneration - Involvement of the Extracellular Matrix. *Spine (Phila Pa 1976)*. 2004;29(23):2691-2699.

130. Aldous IG, Lee JM, Wells SM. Differential Changes in the Molecular Stability of Collagen from the Pulmonary and Aortic Valves During the Fetal-to-Neonatal Transition. *Ann Biomed Eng*. 2010;38(9):3000-3009.

131. Willett TL, Labow RS, Aldous IG, Avery NC, Lee JM. Changes in Collagen With Aging Maintain Molecular Stability After Overload: Evidence From an In Vitro Tendon Model. *J Biomech Eng*. 2010;132(3):1-8.

132. Sparavalo S. Age-Related Changes in Structure and Biomechanics of Human Sartorius Tendon (Master's Thesis). Dalhousie University. 2017.

133. Chambers NC, Herod TW, Veres SP. Ultrastructure of Tendon Rupture Depends on Strain Rate and Tendon Type. *J Orthop Res*. 2018;36(11):1-9.

134. Willett TL, Labow RS, Avery NC, Lee JM. Increased Proteolysis of Collagen in an In Vitro Tensile Overload Tendon Model. *Ann Biomed Eng*. 2007;35(11):1961-1972.

135. Hansen P, Haraldsson BT, Kjaer M, Magnusson P. Glutaraldehyde Cross-Linking of Tendon - Mechanical Effects at the Level of the Tendon Fascicle and Fibril. *Connect Tissue Res*. 2009;50(4):211-222.

136. Depalle B, Qin Z, Shefelbine SJ, Buehler MJ. Influence of Cross-Link Structure, Density and Mechanical Properties in the Mesoscale Deformation Mechanisms of Collagen Fibrils. *J Mech Behav Biomed Mater*. 2015;52:1-13.

137. Shepherd JH, Legerlotz K, Demirci T, Klemt C, Riley GP, Screen HRC. Functionally Distinct Tendon Fascicles Exhibit Different Creep and Stress Relaxation Behaviour. *Proc Inst Mech Eng Part H J Eng Med*. 2014;228(1):49-59.

138. Birch HL, Clegg PD, Screen HRC, Udeze CP, Thorpe CT. Specialization of Tendon Mechanical Properties Results From Interfascicular Differences. *J R Soc Interface*. 2012;9(76):3108-3117.

139. Hansen P, Haraldsson BT, Aagaard P, et al. Lower Strength of the Human Posterior Patellar Tendon Seems Unrelated to Mature Collagen Cross-Linking and Fibril Morphology. *J Appl Physiol*. 2010;108(3):47-52.

140. Quigley AS, Banceli S, Deska-gauthier D, Légaré F, Kreplak L, Veres SP. In Tendons, Differing Physiological Requirements Lead to Functionally Distinct Nanostructures. *Nat Sci Reports*. 2018;8(1):1-14.

141. Svensson RB, Smith ST, Moyer PJ, Magnusson SP. Effects of Maturation and Advanced Glycation on Tensile Mechanics of Collagen Fibrils From Rat Tail and Achilles Tendons. *Acta Biomater*. 2018;70:270-280.

142. Thompson JB, Kindt JH, Morse DE, et al. Evidence that Collagen Fibrils in Tendons Are Inhomogeneously Structured in a Tubelike Manner. *Biophys J*. 2009;84(4):2593-2598.

143. Kronick P, Maleeff B, Carroll R. The Locations of Collagens With Different Thermal Stabilities in Fibrils of Bovine Reticular Dermis. *Connect Tissue Res*. 1988;18(2):123-134.

144. Svensson RB, Mulder H, Kovanen V, Magnusson SP. Fracture Mechanics of Collagen Fibrils: Influence of Natural Cross-Links. *Biophys J*. 2013;104(11):2476-2484.

145. Veres SP, Lee JM. Designed to Fail : A Novel Mode of Collagen Fibril Disruption and Its Relevance to Tissue Toughness. *Biophys J*. 2012;102(12):2876-2884.

146. Hijazi KMA. Effect of Creep Loading on the Nanostructure of Tendons (Master's Thesis). Saint Mary's University. 2017.

147. Han SK, Chen C, Wierwille J, Chen Y, Hsieh AH. Three Dimensional Mesoscale Analysis of Translamellar Cross-Bridge Morphologies in the Annulus Fibrosus using Optical Coherence Tomography. *J Orthop Res*. 2015;33(3):304-311.

148. Veres SP, Robertson PA, Broom ND. The Morphology of Acute Disc Herniation: A Clinically Relevant Model Defining the Role of Flexion. *Spine (Phila Pa 1976)*. 2009;34(21):2288-2296.

149. Nerlich AG, Schleicher ED, Boos N. 1997 Volvo Award Winner in Basic Science Studies. Immunohistologic Markers for Age-Related Changes of Human Lumbar Intervertebral Discs. *Spine (Phila Pa 1976)*. 1997;22(24):2781-2795.

Appendix: Licenses for Copyrighted Material

Rights and permissions

Gmail **Tyler Herod <tylerherod92@gmail.com>**

Follow Up - Permission To Use Figures in Thesis

2 messages

Tyler Herod <ty469725@dal.ca> Thu, Mar 14, 2019 at 2:15 PM
To: samantha.a.rodrigues@gmail.com

Hi Sam,

[redacted]

[redacted]

In terms of adapted material, I've used (and for some, made modifications) to the following figures from your thesis:

-Figure 2.1
-Figure 2.2
-Figure 2.3
-Figure A.5

Attached are the modified versions of your figures that I'd like to use in my thesis. [redacted]

[redacted]

Tyler Herod, B. Eng.

Masters of Applied Science Candidate
Department of Biomedical Engineering
Dalhousie University
Halifax, NS, Canada

6 attachments

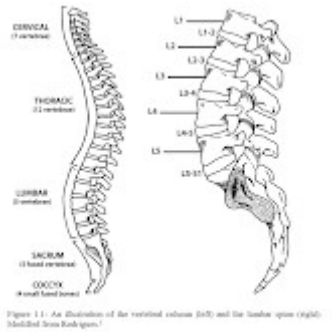

Figure 1.1.png
164K

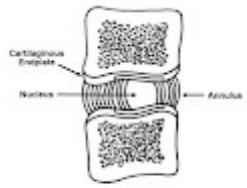

Figure 1.3.png
69K

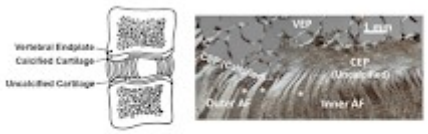

Figure 1.8.png
134K

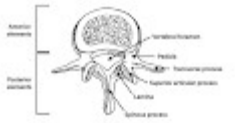

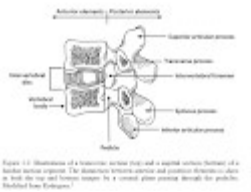

Figure 1.2.png
167K

Figure 1.6.png
522K

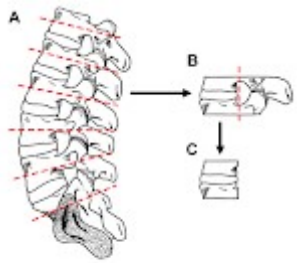

Figure 3.1.png
128K

Samantha Rodrigues <samantha.a.rodrigues@gmail.com> Mon, Mar 18, 2019 at 3:28 AM
To: Tyler Herod <ty469725@dal.ca>

Hi Tyler,

[redacted]

You have my permission to use the images in your thesis.

[redacted]

Cheers,
Sam
[Quoted text hidden]

Gmail **Tyler Herod <tylerherod92@gmail.com>**

Permission To Use Figures in Thesis

2 messages

Tyler Herod <ty469725@dal.ca> Tue, Mar 26, 2019 at 12:54 PM
To: Samuel Veres <Sam.Veres@smu.ca>

Hi Sam,

[redacted]

In terms of adapted material, I've used (and made modifications) to the following figure from your thesis:

-Figure 1.6

Attached are the modified versions of this figure that I'd like to use in my thesis

Best,

Tyler

2 attachments

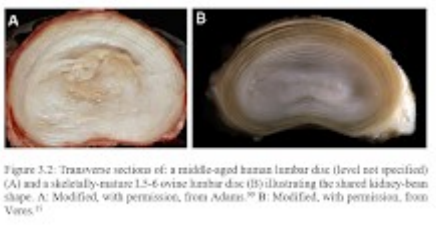

Figure 3.2: Transverse sections of: a middle-aged human lumbar disc (level not specified) (A) and a skeletally-mature 1.5-6 ovine lumbar disc (B) illustrating the shared kidney-bean shape. A: Modified, with permission, from Adams.[9] B: Modified, with permission, from Veres.[1]

Figure 3.2.png
284K

Figure 1.5: A transverse section of an 1.5-6 disc from a skeletally mature ewe (24+ months old) showing the different circumferential regions. The radial depths for the central anterior and central posterior regions are indicated, which measure the distance from the periphery of the disc to the innermost lamella. Modified, with permission, from Veres.[1]

Figure 1.5.png
370K

Sam Veres <Sam.Veres@smu.ca> Tue, Mar 26, 2019 at 3:14 PM
To: Tyler Herod <ty469725@dal.ca>

Hi Tyler,

You have my permission to re-use the materials mentioned below in your thesis, modified however you would like.

Best,
Sam

Samuel P. Veres, PhD, P.Eng.

Applied Science Graduate Program Coordinator
Saint Mary's University

Associate Professor
Division of Engineering
Saint Mary's University

Adjunct Professor
School of Biomedical Engineering
Dalhousie University

Office: McNally Main, MM304-B
Mobile: +1 (902) 719-1178 (preferred)
Voice: +1 (902) 420-5697

Mailing Address:

Dr. Samuel Veres
Division of Engineering,
Saint Mary's University
923 Robie Street,
Halifax, Nova Scotia
Canada
B3H 3C3

> [Quoted text hidden]
> [Quoted text hidden]
> <Figure 3.2.png><Figure 1.5.png>

Gmail **Tyler Herod <tylerherod92@gmail.com>**

Inquiry About Using Modified Figures For Thesis

Journalpermissions <journalpermissions@springernature.com> Tue, Mar 19, 2019 at 1:23 PM
To: Tyler Herod <ty469725@dal.ca>

Dear Tyler,

Thank you for providing.

Please accept this email as confirmation of permission for the following modified figures

· Figure 5 from " Brown S, Rodrigues S, Sharp C, Wade K, Broom N, McCall IW, Roberts S. Staying connected: structural integration at the intervertebral disc–vertebra interface of human lumbar spines. European Spine Journal. 2017 Jan 1;26(1):248-58. DOI 10.1007/s00586-016-4560-y "

· Figure 6 from " Brown S, Rodrigues S, Sharp C, Wade K, Broom N, McCall IW, Roberts S. Staying connected: structural integration at the intervertebral disc–vertebra interface of human lumbar spines. European Spine Journal. 2017 Jan 1;26(1):248-58. DOI 10.1007/s00586-016-4560-y "

· Figure 1 from " Green TP, Adams MA, Dolan P. Tensile properties of the annulus fibrosus. European Spine Journal. 1993 Dec 1;2(4):209-14. https://doi.org/10.1007/BF00299448”

Best wishes,

[Quoted text hidden]

6 attachments

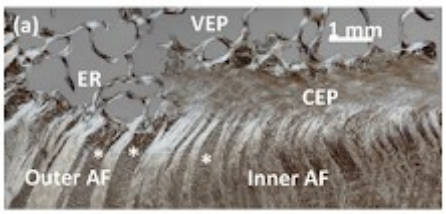

Brown, Figure 5 - Original.png
247K

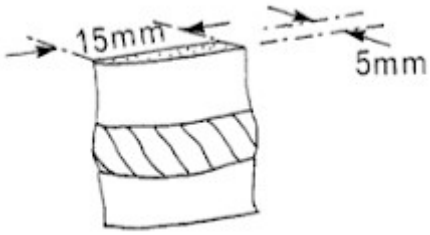

Green, Figure 1 - Modified.png
12K

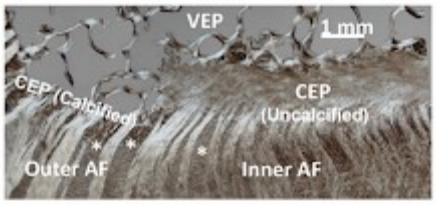

Brown, Figure 5 - Modified.png
259K

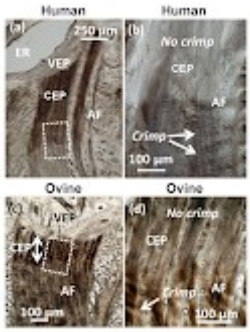

Brown, Figure 6 - Modified.png
766K

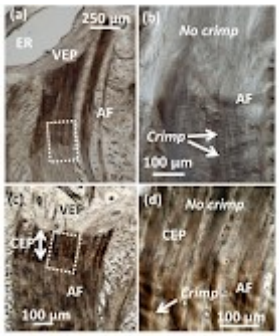

Brown, Figure 6 - Original.png
840K

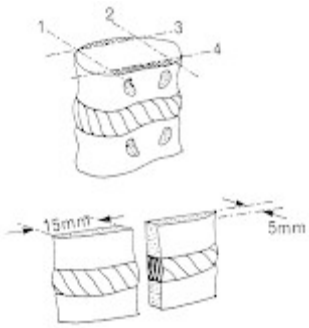

Green, Figure 1 - Original.png
73K

Gmail

Tyler Herod <tylerherod92@gmail.com>

Author requesting permission to use and modify own material in thesis

Rights DE <RIGHTS-and-LICENCES@wiley-vch.de> Mon, Mar 18, 2019 at 11:18 AM
To: Wiley Global Permissions <permissions@wiley.com>
Cc: "ty469725@dal.ca" <ty469725@dal.ca>

Dear colleagues,

Please find below a request for one of your journals.

Best regards

Bettina

Von: Tyler Herod <ty469725@dal.ca>
Gesendet: Montag, 18. März 2019 3:15
An: Rights DE <RIGHTS-and-LICENCES@wiley-vch.de>
Betreff: Re: Inquiry About Using Modified Figure For Thesis

Hi Bettina, thanks for the quick response.

I'm looking to use Figure 3 from "Chambers NC, Herod TW, Veres SP. Ultrastructure of tendon rupture depends on strain rate and tendon type. Journal of Orthopaedic Research®. 2018 Nov;36(11):2842-50. https://doi.org/10.1002/jor.24067"

Best,

Tyler Herod

On Mon, Mar 18, 2019 at 11:09 AM Rights DE <RIGHTS-and-LICENCES@wiley-vch.de> wrote:

> Dear Tyler Herod,

Please let me know which figure from which article you would like to sue and we'll be happy to grant the requested permission.

Kind regards

Bettina Loycke
Senior Rights Manager
Rights & Licenses

Wiley-VCH Verlag GmbH & Co. KGaA
Boschstraße 12
69469 Weinheim
Germany

www.wiley-vch.de

T +(49) 6201 606-280
F +(49) 6201 606-332
rightsDE@wiley.com

WILEY

From: Tyler Herod <ty469725@dal.ca>
Sent: Friday, March 15, 2019 20:16
To: Advanced Science
Subject: Inquiry About Using Modified Figure For Thesis

Hello,

[redacted]

I've identified a journal article containing one figure that I would like to use for my thesis (in both paper and electronic format). [redacted]

> Could you please instruct me on how to proceed with making this inquiry?
>
> [redacted]
>
> --
>
> **Tyler Herod, B. Eng.**
>
> Masters of Applied Science Candidate
>
> Department of Biomedical Engineering
>
> Dalhousie University
>
> Halifax, NS, Canada

--

Tyler Herod, B. Eng.

Masters of Applied Science Candidate

Department of Biomedical Engineering

Dalhousie University

Halifax, NS, Canada

Gmail

Tyler Herod <tylerherod92@gmail.com>

Urgent/ WG: Author requesting permission to use and modify own material in thesis

Wiley Global Permissions <permissions@wiley.com> Tue, Mar 26, 2019 at 4:25 PM
To: "ty469725@dal.ca" <ty469725@dal.ca>

Dear Mr. Herod:

Thank you for your email.

Permission is hereby granted for the use requested subject to the usual acknowledgements (author, title of material, title of journal, ourselves as publisher). You should also duplicate the copyright notice that appears in the Wiley publication; this can be found on the copyright page in the journal.

Any third party material is expressly excluded from this permission. If any of the material you wish to use appears within our work with credit to another source, authorization from that source must be obtained.

This permission does not include the right to grant others permission to photocopy or otherwise reproduce this material except for accessible versions made by non-profit organizations serving the blind, visually impaired and other persons with print disabilities (VIPs).

Sincerely,

Sheik Safdar

Sales Specialist – Permissions

Global Sales Partnerships

Wiley

ssafdar@wiley.com

T +1 201-748-6512

111 River Street

Hoboken, NJ 07030-5774

U.S.

permissions@wiley.com

WILEY

[Quoted text hidden]

JOURNAL OF
Orthopaedic
Research®

A Journal for Musculoskeletal Investigation
Official Publication of the Orthopaedic Research Society

The *JOURNAL OF ORTHOPAEDIC RESEARCH*® (Print ISSN 0736-0266; Online ISSN 1554-527X) is published monthly on behalf of the Orthopaedic Research Society by Wiley Subscription Services, Inc., a Wiley Company, 111 River Street, Hoboken, NJ 07030-5774 USA. Periodicals postage paid at Hoboken, NJ and additional offices. **Postmaster:** Send all address changes to *The JOURNAL OF ORTHOPAEDIC RESEARCH*®, John Wiley & Sons Inc., C/O The Sheridan Press, PO Box 465, Hanover, PA 17331 USA.
Information for Subscribers: Journal of Orthopaedic Research® is published in 12 issues per year. Institutional subscription prices for 2018 are: Print and Online: US$1308 (US), US$1682 (Rest of World), €1088 (Europe), £862 (UK). Prices are exclusive of tax. Asia-Pacific GST, Canadian GST/HST, and European VAT will be applied at the appropriate rates. For more information on current tax rates, please go to www.wileyonlinelibrary.com/tax–vat. The price includes online access to the current and all online back files to January 1st 2014, where available. For other pricing options, including access information and terms and conditions, please visit wileyonlinelibrary.com/access. **Delivery Terms and Legal Title:** Where the subscription price includes print issues and delivery is to the recipient's address, delivery terms are Delivered at Place (DAP); the recipient is responsible for paying any import duty or taxes. Title to all issues transfers Free of Board (FOB) our shipping point, freight prepaid. We will endeavour to fulfil claims for missing or damaged copies within six months of publication, within our reasonable discretion and subject to availability. View this journal online at wileyonlinelibrary.com/journal/10.1002/(ISSN)1554-527X. For **submission instructions**, subscription and all other information, visit: wileyonlinelibrary.com/journal/10.1002/(ISSN)1554-527X; **production questions** may be directed to jorprod@wiley.com; **other correspondence** may be directed to *JOURNAL OF ORTHOPAEDIC RESEARCH*®, Publisher, STMS, c/o, John Wiley & Sons, Inc., 111 River St., Hoboken, NJ 07030. The *JOURNAL OF ORTHOPAEDIC RESEARCH*® accepts articles for **Open Access publication.** Please visit http://olabout.wiley.com/WileyCDA/Section/id-828081.html for further information about OnlineOpen. **Back Issues:** Single issues from current and recent volumes are available at the current single issue price from cs-journals@wiley.com. **Commercial Reprints:** Email: corporatesaleseurope@wiley.com; corporatesalesusa@wiley.com; or corporatesalesaustralia@wiley.com. **Author Reprints (50–500 copies):** Order online at http://www.sheridanreprints.com/orderForm.html. E-mail: erica.garrett@sheridan.com

Advertising Sales: Inquiries concerning advertising should be forwarded to Joe Tomaszewski, Advertising Sales Manager, Sciences, Corporate Sales, Americas, Wiley-Blackwell (Email: jtomaszews@wiley.com).
Publication of an advertisement or other discussions of products in The *JOURNAL OF ORTHOPAEDIC RESEARCH*® should not be construed as an endorsement of the products or the manufacturers' claims. Readers are encouraged to contact the manufacturers with any questions about the features or limitations of the products mentioned.

Journal Customer Services: For ordering information, claims and any enquiry concerning your journal subscription please go to www.wileycustomerhelp.com/ask or contact your nearest office. **Americas:** Email: cs-journals@wiley.com; Tel: +1 781 388 8598 or 1 800 835 6770 (Toll free in the USA & Canada). **Europe, Middle East and Africa:** Email: cs-journals@wiley.com; Tel: +44 (0) 1865 778315. **Asia Pacific:** Email: cs-journals@wiley.com; Tel: +65 6511 8000. **Japan:** For Japanese speaking support, Email: cs-japan@wiley.com. **Visit our *Online Customer Help*** available in 7 languages at www.wileycustomerhelp.com/ask.
Disclaimer: The Publisher, the Orthopaedic Research Society, and Editors cannot be held responsible for errors or any consequences arising from the use of information contained in this journal; the views and opinions expressed do not necessarily reflect those of the Publisher, the Orthopaedic Research Society, and Editors, neither does the publication of advertisements constitute any endorsement by the Publisher, the Orthopaedic Research Society, and Editors of the products advertised.

Wiley's Corporate Citizenship initiative seeks to address the environmental, social, economic, and ethical challenges faced in our business and which are important to our diverse stakeholder groups. Since launching the initiative, we have focused on sharing our content with those in need, enhancing community philanthropy, reducing our carbon impact, creating global guidelines and best practices for paper use, establishing a vendor code of ethics, and engaging our colleagues and other stakeholders in our efforts. Follow our progress at www.wiley.com/go/citizenship **Research4Life:** Wiley is a founding member of the UN-backed HINARI, AGORA, and OARE initiatives. They are now collectively known as Research4Life, making online scientific content available free or at nominal cost to researchers in developing countries. Please visit Wiley's Content Access – Corporate Citizenship site: http://www.wiley.com/WileyCDA/Section/id-390082.html. **Indexed by:** *Biological Abstracts®, BIOSIS Previews®, Biotechnology & Bioengineering Abstracts, Cambridge Scientifi c Abstracts, Chemical Abstracts Service/ SciFinder, CSA Biological Sciences Database, Current Contents®/Life Sciences, EMBASE/Excerpta Medica, EMNursing, Index Medicus/ MEDLINE/PubMed, Journal Citation Reports/Science Edition, Science Citation Index ExpandedTM, Science Citation Index®, Web of Science®.*
Printed in the USA by The Sheridan Group.
This paper meets the requirements of DIN ISO 9706 (Requirements for Permanence), Section 5.2 to 5.5.

SPRINGER NATURE LICENSE TERMS AND CONDITIONS

Mar 13, 2019

This Agreement between Dalhousie University -- Tyler Herod ("You") and Springer Nature ("Springer Nature") consists of your license details and the terms and conditions provided by Springer Nature and Copyright Clearance Center.

License Number	4547241500876
License date	Mar 13, 2019
Licensed Content Publisher	Springer Nature
Licensed Content Publication	European Spine Journal
Licensed Content Title	A fresh look at the nucleus-endplate region: new evidence for significant structural integration
Licensed Content Author	Kelly R. Wade, Peter A. Robertson, Neil D. Broom
Licensed Content Date	Jan 1, 2011
Licensed Content Volume	20
Licensed Content Issue	8
Type of Use	Thesis/Dissertation
Requestor type	academic/university or research institute
Format	print and electronic
Portion	figures/tables/illustrations
Number of figures/tables /illustrations	1
Will you be translating?	no
Circulation/distribution	<501
Author of this Springer Nature content	no
Title	Regional Variations in the Molecular Structure and Mechanics of the Lumbar Intervertebral Disc Annulus
Institution name	Dalhousie University
Expected presentation date	Apr 2019
Portions	Figure 6
Requestor Location	Dalhousie University Room 5200 Biomedical Engineering Department 5981 University Ave Halifax, NS B3H 4R2 Canada Attn: Tyler Herod
Billing Type	Invoice
Billing Address	Dalhousie University Room 5200 Biomedical Engineering Department 5981 University Ave Halifax, NS B3H 4R2

Canada
Attn: Tyler Herod

Total 0.00 CAD

Terms and Conditions

Springer Nature Terms and Conditions for RightsLink Permissions

Springer Nature Customer Service Centre GmbH (the Licensor) hereby grants you a non-exclusive, world-wide licence to reproduce the material and for the purpose and requirements specified in the attached copy of your order form, and for no other use, subject to the conditions below:

1. The Licensor warrants that it has, to the best of its knowledge, the rights to license reuse of this material. However, you should ensure that the material you are requesting is original to the Licensor and does not carry the copyright of another entity (as credited in the published version).

   If the credit line on any part of the material you have requested indicates that it was reprinted or adapted with permission from another source, then you should also seek permission from that source to reuse the material.

2. Where **print only** permission has been granted for a fee, separate permission must be obtained for any additional electronic re-use.

3. Permission granted **free of charge** for material in print is also usually granted for any electronic version of that work, provided that the material is incidental to your work as a whole and that the electronic version is essentially equivalent to, or substitutes for, the print version.

4. A licence for 'post on a website' is valid for 12 months from the licence date. This licence does not cover use of full text articles on websites.

5. Where **'reuse in a dissertation/thesis'** has been selected the following terms apply: Print rights of the final author's accepted manuscript (for clarity, NOT the published version) for up to 100 copies, electronic rights for use only on a personal website or institutional repository as defined by the Sherpa guideline (www.sherpa.ac.uk/romeo/).

6. Permission granted for books and journals is granted for the lifetime of the first edition and does not apply to second and subsequent editions (except where the first edition permission was granted free of charge or for signatories to the STM Permissions Guidelines http://www.stm-assoc.org/copyright-legal-affairs/permissions/permissions-guidelines/), and does not apply for editions in other languages unless additional translation rights have been granted separately in the licence.

7. Rights for additional components such as custom editions and derivatives require additional permission and may be subject to an additional fee. Please apply to Journalpermissions@springernature.com/bookpermissions@springernature.com for these rights.

8. The Licensor's permission must be acknowledged next to the licensed material in print. In electronic form, this acknowledgement must be visible at the same time as the figures/tables/illustrations or abstract, and must be hyperlinked to the journal/book's homepage. Our required acknowledgement format is in the Appendix below.

9. Use of the material for incidental promotional use, minor editing privileges (this does not include cropping, adapting, omitting material or any other changes that affect the meaning, intention or moral rights of the author) and copies for the disabled are permitted under this licence.

10. Minor adaptations of single figures (changes of format, colour and style) do not require the Licensor's approval. However, the adaptation should be credited as shown in Appendix below.

Appendix — Acknowledgements:

For Journal Content:
Reprinted by permission from [**the Licensor**]: [**Journal Publisher** (e.g. Nature/Springer/Palgrave)] [**JOURNAL NAME**] [**REFERENCE CITATION** (Article name, Author(s) Name), [**COPYRIGHT**] (year of publication)

For **Advance Online Publication papers:**
Reprinted by permission from [**the Licensor**]: [**Journal Publisher** (e.g. Nature/Springer/Palgrave)] [**JOURNAL NAME**] [**REFERENCE CITATION** (Article name, Author(s) Name), [**COPYRIGHT**] (year of publication), advance online publication, day month year (doi: 10.1038/sj.[JOURNAL ACRONYM].)

For Adaptations/Translations:
Adapted/Translated by permission from [**the Licensor**]: [**Journal Publisher** (e.g. Nature/Springer/Palgrave)] [**JOURNAL NAME**] [**REFERENCE CITATION** (Article name, Author(s) Name), [**COPYRIGHT**] (year of publication)

Note: For any republication from the British Journal of Cancer, the following credit line style applies:

Reprinted/adapted/translated by permission from [**the Licensor**]: on behalf of Cancer Research UK: : [**Journal Publisher** (e.g. Nature/Springer/Palgrave)] [**JOURNAL NAME**] [**REFERENCE CITATION** (Article name, Author(s) Name), [**COPYRIGHT]** (year of publication)

For **Advance Online Publication** papers:
Reprinted by permission from The [**the Licensor**]: on behalf of Cancer Research UK: [**Journal Publisher** (e.g. Nature/Springer/Palgrave)] [**JOURNAL NAME**] [**REFERENCE CITATION** (Article name, Author(s) Name), [**COPYRIGHT**] (year of publication), advance online publication, day month year (doi: 10.1038/sj.[JOURNAL ACRONYM])

For Book content:
Reprinted/adapted by permission from [**the Licensor**]: [**Book Publisher** (e.g. Palgrave Macmillan, Springer etc) [**Book Title**] by [**Book author**(s)] [**COPYRIGHT**] (year of publication)

Other Conditions:

Version 1.1

WOLTERS KLUWER HEALTH, INC. LICENSE TERMS AND CONDITIONS

Mar 15, 2019

This Agreement between Dalhousie University -- Tyler Herod ("You") and Wolters Kluwer Health, Inc. ("Wolters Kluwer Health, Inc.") consists of your license details and the terms and conditions provided by Wolters Kluwer Health, Inc. and Copyright Clearance Center.

License Number	4550341445929
License date	Mar 15, 2019
Licensed Content Publisher	Wolters Kluwer Health, Inc.
Licensed Content Publication	Spine
Licensed Content Title	ISSLS Prize Winner: Microstructure and Mechanical Disruption of the Lumbar Disc Annulus: Part I: A Microscopic Investigation of the Translamellar Bridging Network
Licensed Content Author	Meredith Schollum, Peter Robertson, and Neil Broom
Licensed Content Date	Dec 1, 2008
Licensed Content Volume	33
Licensed Content Issue	25
Type of Use	Dissertation/Thesis
Requestor type	Individual
STM publisher name	
Portion	Figures/table/illustration
Number of figures/tables /illustrations	1
Figures/tables/illustrations used	Figure 2
Author of this Wolters Kluwer article	No
Title of your thesis / dissertation	Regional Variations in the Molecular Structure and Mechanics of the Lumbar Intervertebral Disc Annulus
Expected completion date	Apr 2019
Estimated size(pages)	105
Requestor Location	Dalhousie University Room 5200 Biomedical Engineering Department 5981 University Ave Halifax, NS B3H 4R2 Canada Attn: Tyler Herod
Billing Type	Invoice
Billing Address	Dalhousie University Room 5200 Biomedical Engineering Department 5981 University Ave Halifax, NS B3H 4R2 Canada

Attn: Tyler Herod

Total 0.00 CAD

Terms and Conditions

Wolters Kluwer Health Inc. Terms and Conditions

1. **Duration of License:** Permission is granted for a one time use only. Rights herein do not apply to future reproductions, editions, revisions, or other derivative works. This permission shall be effective as of the date of execution by the parties for the maximum period of 12 months and should be renewed after the term expires.
    i. When content is to be republished in a book or journal the validity of this agreement should be the life of the book edition or journal issue.
    ii. When content is licensed for use on a website, internet, intranet, or any publicly accessible site (not including a journal or book), you agree to remove the material from such site after 12 months, or request to renew your permission license
2. **Credit Line:** A credit line must be prominently placed and include: For book content: the author(s), title of book, edition, copyright holder, year of publication; For journal content: the author(s), titles of article, title of journal, volume number, issue number, inclusive pages and website URL to the journal page; If a journal is published by a learned society the credit line must include the details of that society.
3. **Warranties:** The requestor warrants that the material shall not be used in any manner which may be considered derogatory to the title, content, authors of the material, or to Wolters Kluwer Health, Inc.
4. **Indemnity:** You hereby indemnify and hold harmless Wolters Kluwer Health, Inc. and its respective officers, directors, employees and agents, from and against any and all claims, costs, proceeding or demands arising out of your unauthorized use of the Licensed Material
5. **Geographical Scope:** Permission granted is non-exclusive and is valid throughout the world in the English language and the languages specified in the license.
6. **Copy of Content:** Wolters Kluwer Health, Inc. cannot supply the requestor with the original artwork, high-resolution images, electronic files or a clean copy of content.
7. **Validity:** Permission is valid if the borrowed material is original to a Wolters Kluwer Health, Inc. imprint (J.B Lippincott, Lippincott-Raven Publishers, Williams & Wilkins, Lea & Febiger, Harwal, Rapid Science, Little Brown & Company, Harper & Row Medical, American Journal of Nursing Co, and Urban & Schwarzenberg - English Language, Raven Press, Paul Hoeber, Springhouse, Ovid), and the Anatomical Chart Company
8. **Third Party Material:** This permission does not apply to content that is credited to publications other than Wolters Kluwer Health, Inc. or its Societies. For images credited to non-Wolters Kluwer Health, Inc. books or journals, you must obtain permission from the source referenced in the figure or table legend or credit line before making any use of the image(s), table(s) or other content.
9. **Adaptations:** Adaptations are protected by copyright. For images that have been adapted, permission must be sought from the rightsholder of the original material and the rightsholder of the adapted material.
10. **Modifications:** Wolters Kluwer Health, Inc. material is not permitted to be modified or adapted without written approval from Wolters Kluwer Health, Inc. with the exception of text size or color. The adaptation should be credited as follows: Adapted with permission from Wolters Kluwer Health, Inc.: [the author(s), title of book, edition, copyright holder, year of publication] or [the author(s), titles of article, title of journal, volume number, issue number, inclusive pages and website URL to the journal page].
11. **Full Text Articles:** Republication of full articles in English is prohibited.
12. **Branding and Marketing:** No drug name, trade name, drug logo, or trade logo can be included on the same page as material borrowed from *Diseases of the Colon & Rectum, Plastic Reconstructive Surgery, Obstetrics & Gynecology (The Green Journal), Critical Care Medicine, Pediatric Critical Care Medicine, the American Heart Association publications and the American Academy of Neurology publications.*
13. **Open Access:** Unless you are publishing content under the same Creative Commons license, the following statement must be added when reprinting material in Open Access journals: "The Creative Commons license does not apply to this content. Use of the material in any format is prohibited without written permission from the publisher, Wolters Kluwer Health, Inc. Please contact permissions@lww.com for further information."
14. **Translations:** The following disclaimer must appear on all translated copies: Wolters Kluwer Health, Inc. and its Societies take no responsibility for the accuracy of the

translation from the published English original and are not liable for any errors which may occur.

15. **Published Ahead of Print (PAP):** Articles in the PAP stage of publication can be cited using the online publication date and the unique DOI number.
    i. Disclaimer: Articles appearing in the PAP section have been peer-reviewed and accepted for publication in the relevant journal and posted online before print publication. Articles appearing as PAP may contain statements, opinions, and information that have errors in facts, figures, or interpretation. Any final changes in manuscripts will be made at the time of print publication and will be reflected in the final electronic version of the issue. Accordingly, Wolters Kluwer Health, Inc., the editors, authors and their respective employees are not responsible or liable for the use of any such inaccurate or misleading data, opinion or information contained in the articles in this section.
16. **Termination of Contract:** Wolters Kluwer Health, Inc. must be notified within 90 days of the original license date if you opt not to use the requested material.
17. **Waived Permission Fee:** Permission fees that have been waived are not subject to future waivers, including similar requests or renewing a license.
18. **Contingent on payment:** You may exercise these rights licensed immediately upon issuance of the license, however until full payment is received either by the publisher or our authorized vendor, this license is not valid. If full payment is not received on a timely basis, then any license preliminarily granted shall be deemed automatically revoked and shall be void as if never granted. Further, in the event that you breach any of these terms and conditions or any of Wolters Kluwer Health, Inc.'s other billing and payment terms and conditions, the license is automatically revoked and shall be void as if never granted. Use of materials as described in a revoked license, as well as any use of the materials beyond the scope of an unrevoked license, may constitute copyright infringement and publisher reserves the right to take any and all action to protect its copyright in the materials.
19. **STM Signatories Only:** Any permission granted for a particular edition will apply to subsequent editions and for editions in other languages, provided such editions are for the work as a whole in situ and do not involve the separate exploitation of the permitted illustrations or excerpts. Please view: STM Permissions Guidelines
20. **Warranties and Obligations:** LICENSOR further represents and warrants that, to the best of its knowledge and belief, LICENSEE's contemplated use of the Content as represented to LICENSOR does not infringe any valid rights to any third party.
21. **Breach:** If LICENSEE fails to comply with any provisions of this agreement, LICENSOR may serve written notice of breach of LICENSEE and, unless such breach is fully cured within fifteen (15) days from the receipt of notice by LICENSEE, LICENSOR may thereupon, at its option, serve notice of cancellation on LICENSEE, whereupon this Agreement shall immediately terminate.
22. **Assignment:** License conveyed hereunder by the LICENSOR shall not be assigned or granted in any manner conveyed to any third party by the LICENSEE without the consent in writing to the LICENSOR.
23. **Governing Law:** The laws of The State of New York shall govern interpretation of this Agreement and all rights and liabilities arising hereunder.
24. **Unlawful:** If any provision of this Agreement shall be found unlawful or otherwise legally unenforceable, all other conditions and provisions of this Agreement shall remain in full force and effect.

For Copyright Clearance Center / RightsLink Only:

1. **Service Description for Content Services:** Subject to these terms of use, any terms set forth on the particular order, and payment of the applicable fee, you may make the following uses of the ordered materials:
    i. **Content Rental:** You may access and view a single electronic copy of the materials ordered for the time period designated at the time the order is placed. Access to the materials will be provided through a dedicated content viewer or other portal, and access will be discontinued upon expiration of the designated time period. An order for Content Rental does not include any rights to print, download, save, create additional copies, to distribute or to reuse in any way the full text or parts of the materials.
    ii. **Content Purchase:** You may access and download a single electronic copy of the materials ordered. Copies will be provided by email or by such other means as publisher may make available from time to time. An order for Content Purchase does

not include any rights to create additional copies or to distribute copies of the materials

Other Terms and Conditions:
v1.18

Questions? customercare@copyright.com or +1-855-239-3415 (toll free in the US) or +1-978-646-2777.

SPRINGER NATURE LICENSE TERMS AND CONDITIONS

Mar 15, 2019

This Agreement between Dalhousie University -- Tyler Herod ("You") and Springer Nature ("Springer Nature") consists of your license details and the terms and conditions provided by Springer Nature and Copyright Clearance Center.

License Number	4550350323918
License date	Mar 15, 2019
Licensed Content Publisher	Springer Nature
Licensed Content Publication	European Spine Journal
Licensed Content Title	The influence of torsion on disc herniation when combined with flexion
Licensed Content Author	Samuel P. Veres, Peter A. Robertson, Neil D. Broom
Licensed Content Date	Jan 1, 2010
Licensed Content Volume	19
Licensed Content Issue	9
Type of Use	Thesis/Dissertation
Requestor type	academic/university or research institute
Format	print and electronic
Portion	figures/tables/illustrations
Number of figures/tables /illustrations	1
Will you be translating?	no
Circulation/distribution	<501
Author of this Springer Nature content	no
Title	Regional Variations in the Molecular Structure and Mechanics of the Lumbar Intervertebral Disc Annulus
Institution name	Dalhousie University
Expected presentation date	Apr 2019
Portions	Figure 7
Requestor Location	Dalhousie University Room 5200 Biomedical Engineering Department 5981 University Ave Halifax, NS B3H 4R2 Canada Attn: Tyler Herod
Billing Type	Invoice
Billing Address	Dalhousie University Room 5200 Biomedical Engineering Department 5981 University Ave Halifax, NS B3H 4R2

Canada
Attn: Tyler Herod

Total 0.00 CAD

Terms and Conditions

Springer Nature Terms and Conditions for RightsLink Permissions

Springer Nature Customer Service Centre GmbH (the Licensor) hereby grants you a non-exclusive, world-wide licence to reproduce the material and for the purpose and requirements specified in the attached copy of your order form, and for no other use, subject to the conditions below:

1. The Licensor warrants that it has, to the best of its knowledge, the rights to license reuse of this material. However, you should ensure that the material you are requesting is original to the Licensor and does not carry the copyright of another entity (as credited in the published version).

   If the credit line on any part of the material you have requested indicates that it was reprinted or adapted with permission from another source, then you should also seek permission from that source to reuse the material.

2. Where **print only** permission has been granted for a fee, separate permission must be obtained for any additional electronic re-use.

3. Permission granted **free of charge** for material in print is also usually granted for any electronic version of that work, provided that the material is incidental to your work as a whole and that the electronic version is essentially equivalent to, or substitutes for, the print version.

4. A licence for 'post on a website' is valid for 12 months from the licence date. This licence does not cover use of full text articles on websites.

5. Where **'reuse in a dissertation/thesis'** has been selected the following terms apply: Print rights of the final author's accepted manuscript (for clarity, NOT the published version) for up to 100 copies, electronic rights for use only on a personal website or institutional repository as defined by the Sherpa guideline (www.sherpa.ac.uk/romeo/).

6. Permission granted for books and journals is granted for the lifetime of the first edition and does not apply to second and subsequent editions (except where the first edition permission was granted free of charge or for signatories to the STM Permissions Guidelines http://www.stm-assoc.org/copyright-legal-affairs/permissions/permissions-guidelines/), and does not apply for editions in other languages unless additional translation rights have been granted separately in the licence.

7. Rights for additional components such as custom editions and derivatives require additional permission and may be subject to an additional fee. Please apply to Journalpermissions@springernature.com/bookpermissions@springernature.com for these rights.

8. The Licensor's permission must be acknowledged next to the licensed material in print. In electronic form, this acknowledgement must be visible at the same time as the figures/tables/illustrations or abstract, and must be hyperlinked to the journal/book's homepage. Our required acknowledgement format is in the Appendix below.

9. Use of the material for incidental promotional use, minor editing privileges (this does not include cropping, adapting, omitting material or any other changes that affect the meaning, intention or moral rights of the author) and copies for the disabled are permitted under this licence.

10. Minor adaptations of single figures (changes of format, colour and style) do not require the Licensor's approval. However, the adaptation should be credited as shown in Appendix below.

Appendix — Acknowledgements:

For Journal Content:
Reprinted by permission from [**the Licensor**]: [**Journal Publisher** (e.g. Nature/Springer/Palgrave)] [**JOURNAL NAME**] [**REFERENCE CITATION** (Article name, Author(s) Name), [**COPYRIGHT**] (year of publication)

For **Advance Online Publication papers:**
Reprinted by permission from [**the Licensor**]: [**Journal Publisher** (e.g. Nature/Springer/Palgrave)] [**JOURNAL NAME**] [**REFERENCE CITATION** (Article name, Author(s) Name), [**COPYRIGHT**] (year of publication), advance online publication, day month year (doi: 10.1038/sj.[JOURNAL ACRONYM].)

For Adaptations/Translations:
Adapted/Translated by permission from [**the Licensor**]: [**Journal Publisher** (e.g. Nature/Springer/Palgrave)] [**JOURNAL NAME**] [**REFERENCE CITATION** (Article name, Author(s) Name), [**COPYRIGHT**] (year of publication)

Note: For any republication from the British Journal of Cancer, the following credit line style applies:

Reprinted/adapted/translated by permission from [**the Licensor**]: on behalf of Cancer Research UK: : [**Journal Publisher** (e.g. Nature/Springer/Palgrave)] [**JOURNAL NAME**] [**REFERENCE CITATION** (Article name, Author(s) Name), [**COPYRIGHT]** (year of publication)

For **Advance Online Publication** papers:
Reprinted by permission from The [**the Licensor**]: on behalf of Cancer Research UK: [**Journal Publisher** (e.g. Nature/Springer/Palgrave)] [**JOURNAL NAME**] [**REFERENCE CITATION** (Article name, Author(s) Name), [**COPYRIGHT**] (year of publication), advance online publication, day month year (doi: 10.1038/sj.[JOURNAL ACRONYM])

For Book content:
Reprinted/adapted by permission from [**the Licensor**]: [**Book Publisher** (e.g. Palgrave Macmillan, Springer etc) [**Book Title**] by [**Book author**(s)] [**COPYRIGHT**] (year of publication)

Other Conditions:

Version 1.1

WOLTERS KLUWER HEALTH, INC. LICENSE TERMS AND CONDITIONS

Mar 13, 2019

This Agreement between Dalhousie University -- Tyler Herod ("You") and Wolters Kluwer Health, Inc. ("Wolters Kluwer Health, Inc.") consists of your license details and the terms and conditions provided by Wolters Kluwer Health, Inc. and Copyright Clearance Center.

License Number	4547140957129
License date	Mar 13, 2019
Licensed Content Publisher	Wolters Kluwer Health, Inc.
Licensed Content Publication	Spine
Licensed Content Title	Intradiscal Pressure, Shear Strain, and Fiber Strain in the Intervertebral Disc Under Combined Loading
Licensed Content Author	Hendrik Schmidt, Annette Kettler, Frank Heuer, et al
Licensed Content Date	Apr 1, 2007
Licensed Content Volume	32
Licensed Content Issue	7
Type of Use	Dissertation/Thesis
Requestor type	Individual
STM publisher name	
Portion	Figures/table/illustration
Number of figures/tables /illustrations	2
Figures/tables/illustrations used	Figure 4 and Figure 7
Author of this Wolters Kluwer article	No
Title of your thesis / dissertation	Regional Variations in the Molecular Structure and Mechanics of the Lumbar Intervertebral Disc Annulus
Expected completion date	Apr 2019
Estimated size(pages)	105
Requestor Location	Dalhousie University Room 5200 Biomedical Engineering Department 5981 University Ave Halifax, NS B3H 4R2 Canada Attn: Tyler Herod
Billing Type	Invoice
Billing Address	Dalhousie University Room 5200 Biomedical Engineering Department 5981 University Ave Halifax, NS B3H 4R2 Canada Attn: Dalhousie University

Total 0.00 CAD

Terms and Conditions

Wolters Kluwer Health Inc. Terms and Conditions

1. **Duration of License:** Permission is granted for a one time use only. Rights herein do not apply to future reproductions, editions, revisions, or other derivative works. This permission shall be effective as of the date of execution by the parties for the maximum period of 12 months and should be renewed after the term expires.
    i. When content is to be republished in a book or journal the validity of this agreement should be the life of the book edition or journal issue.
    ii. When content is licensed for use on a website, internet, intranet, or any publicly accessible site (not including a journal or book), you agree to remove the material from such site after 12 months, or request to renew your permission license
2. **Credit Line:** A credit line must be prominently placed and include: For book content: the author(s), title of book, edition, copyright holder, year of publication; For journal content: the author(s), titles of article, title of journal, volume number, issue number, inclusive pages and website URL to the journal page; If a journal is published by a learned society the credit line must include the details of that society.
3. **Warranties:** The requestor warrants that the material shall not be used in any manner which may be considered derogatory to the title, content, authors of the material, or to Wolters Kluwer Health, Inc.
4. **Indemnity:** You hereby indemnify and hold harmless Wolters Kluwer Health, Inc. and its respective officers, directors, employees and agents, from and against any and all claims, costs, proceeding or demands arising out of your unauthorized use of the Licensed Material
5. **Geographical Scope:** Permission granted is non-exclusive and is valid throughout the world in the English language and the languages specified in the license.
6. **Copy of Content:** Wolters Kluwer Health, Inc. cannot supply the requestor with the original artwork, high-resolution images, electronic files or a clean copy of content.
7. **Validity:** Permission is valid if the borrowed material is original to a Wolters Kluwer Health, Inc. imprint (J.B Lippincott, Lippincott-Raven Publishers, Williams & Wilkins, Lea & Febiger, Harwal, Rapid Science, Little Brown & Company, Harper & Row Medical, American Journal of Nursing Co, and Urban & Schwarzenberg - English Language, Raven Press, Paul Hoeber, Springhouse, Ovid), and the Anatomical Chart Company
8. **Third Party Material:** This permission does not apply to content that is credited to publications other than Wolters Kluwer Health, Inc. or its Societies. For images credited to non-Wolters Kluwer Health, Inc. books or journals, you must obtain permission from the source referenced in the figure or table legend or credit line before making any use of the image(s), table(s) or other content.
9. **Adaptations:** Adaptations are protected by copyright. For images that have been adapted, permission must be sought from the rightsholder of the original material and the rightsholder of the adapted material.
10. **Modifications:** Wolters Kluwer Health, Inc. material is not permitted to be modified or adapted without written approval from Wolters Kluwer Health, Inc. with the exception of text size or color. The adaptation should be credited as follows: Adapted with permission from Wolters Kluwer Health, Inc.: [the author(s), title of book, edition, copyright holder, year of publication] or [the author(s), titles of article, title of journal, volume number, issue number, inclusive pages and website URL to the journal page].
11. **Full Text Articles:** Republication of full articles in English is prohibited.
12. **Branding and Marketing:** No drug name, trade name, drug logo, or trade logo can be included on the same page as material borrowed from *Diseases of the Colon & Rectum, Plastic Reconstructive Surgery, Obstetrics & Gynecology (The Green Journal), Critical Care Medicine, Pediatric Critical Care Medicine, the American Heart Association publications and the American Academy of Neurology publications.*
13. **Open Access:** Unless you are publishing content under the same Creative Commons license, the following statement must be added when reprinting material in Open Access journals: "The Creative Commons license does not apply to this content. Use of the material in any format is prohibited without written permission from the publisher, Wolters Kluwer Health, Inc. Please contact permissions@lww.com for further information."
14. **Translations:** The following disclaimer must appear on all translated copies: Wolters Kluwer Health, Inc. and its Societies take no responsibility for the accuracy of the translation from the published English original and are not liable for any errors which may occur.

15. **Published Ahead of Print (PAP):** Articles in the PAP stage of publication can be cited using the online publication date and the unique DOI number.
    i. Disclaimer: Articles appearing in the PAP section have been peer-reviewed and accepted for publication in the relevant journal and posted online before print publication. Articles appearing as PAP may contain statements, opinions, and information that have errors in facts, figures, or interpretation. Any final changes in manuscripts will be made at the time of print publication and will be reflected in the final electronic version of the issue. Accordingly, Wolters Kluwer Health, Inc., the editors, authors and their respective employees are not responsible or liable for the use of any such inaccurate or misleading data, opinion or information contained in the articles in this section.
16. **Termination of Contract:** Wolters Kluwer Health, Inc. must be notified within 90 days of the original license date if you opt not to use the requested material.
17. **Waived Permission Fee:** Permission fees that have been waived are not subject to future waivers, including similar requests or renewing a license.
18. **Contingent on payment:** You may exercise these rights licensed immediately upon issuance of the license, however until full payment is received either by the publisher or our authorized vendor, this license is not valid. If full payment is not received on a timely basis, then any license preliminarily granted shall be deemed automatically revoked and shall be void as if never granted. Further, in the event that you breach any of these terms and conditions or any of Wolters Kluwer Health, Inc.'s other billing and payment terms and conditions, the license is automatically revoked and shall be void as if never granted. Use of materials as described in a revoked license, as well as any use of the materials beyond the scope of an unrevoked license, may constitute copyright infringement and publisher reserves the right to take any and all action to protect its copyright in the materials.
19. **STM Signatories Only:** Any permission granted for a particular edition will apply to subsequent editions and for editions in other languages, provided such editions are for the work as a whole in situ and do not involve the separate exploitation of the permitted illustrations or excerpts. Please view: STM Permissions Guidelines
20. **Warranties and Obligations:** LICENSOR further represents and warrants that, to the best of its knowledge and belief, LICENSEE's contemplated use of the Content as represented to LICENSOR does not infringe any valid rights to any third party.
21. **Breach:** If LICENSEE fails to comply with any provisions of this agreement, LICENSOR may serve written notice of breach of LICENSEE and, unless such breach is fully cured within fifteen (15) days from the receipt of notice by LICENSEE, LICENSOR may thereupon, at its option, serve notice of cancellation on LICENSEE, whereupon this Agreement shall immediately terminate.
22. **Assignment:** License conveyed hereunder by the LICENSOR shall not be assigned or granted in any manner conveyed to any third party by the LICENSEE without the consent in writing to the LICENSOR.
23. **Governing Law:** The laws of The State of New York shall govern interpretation of this Agreement and all rights and liabilities arising hereunder.
24. **Unlawful:** If any provision of this Agreement shall be found unlawful or otherwise legally unenforceable, all other conditions and provisions of this Agreement shall remain in full force and effect.

For Copyright Clearance Center / RightsLink Only:

1. **Service Description for Content Services:** Subject to these terms of use, any terms set forth on the particular order, and payment of the applicable fee, you may make the following uses of the ordered materials:
    i. **Content Rental:** You may access and view a single electronic copy of the materials ordered for the time period designated at the time the order is placed. Access to the materials will be provided through a dedicated content viewer or other portal, and access will be discontinued upon expiration of the designated time period. An order for Content Rental does not include any rights to print, download, save, create additional copies, to distribute or to reuse in any way the full text or parts of the materials.
    ii. **Content Purchase:** You may access and download a single electronic copy of the materials ordered. Copies will be provided by email or by such other means as publisher may make available from time to time. An order for Content Purchase does not include any rights to create additional copies or to distribute copies of the materials

Other Terms and Conditions:
v1.18

Questions? customercare@copyright.com or +1-855-239-3415 (toll free in the US) or +1-978-646-2777.

JOHN WILEY AND SONS LICENSE TERMS AND CONDITIONS

Mar 15, 2019

This Agreement between Dalhousie University -- Tyler Herod ("You") and John Wiley and Sons ("John Wiley and Sons") consists of your license details and the terms and conditions provided by John Wiley and Sons and Copyright Clearance Center.

License Number	4550350663529
License date	Mar 15, 2019
Licensed Content Publisher	John Wiley and Sons
Licensed Content Publication	Clinical Anatomy
Licensed Content Title	Why do some intervertebral discs degenerate, when others (in the same spine) do not?
Licensed Content Author	Michael A. Adams, Polly Lama, Uruj Zehra, et al
Licensed Content Date	Apr 19, 2014
Licensed Content Volume	28
Licensed Content Issue	2
Licensed Content Pages	10
Type of use	Dissertation/Thesis
Requestor type	University/Academic
Format	Print and electronic
Portion	Figure/table
Number of figures/tables	1
Original Wiley figure/table number(s)	Figure 4
Will you be translating?	No
Title of your thesis / dissertation	Regional Variations in the Molecular Structure and Mechanics of the Lumbar Intervertebral Disc Annulus
Expected completion date	Apr 2019
Expected size (number of pages)	105
Requestor Location	Dalhousie University Room 5200 Biomedical Engineering Department 5981 University Ave Halifax, NS B3H 4R2 Canada Attn: Tyler Herod
Publisher Tax ID	EU826007151
Total	0.00 CAD
Terms and Conditions	

TERMS AND CONDITIONS

This copyrighted material is owned by or exclusively licensed to John Wiley & Sons, Inc. or

one of its group companies (each a"Wiley Company") or handled on behalf of a society with which a Wiley Company has exclusive publishing rights in relation to a particular work (collectively "WILEY"). By clicking "accept" in connection with completing this licensing transaction, you agree that the following terms and conditions apply to this transaction (along with the billing and payment terms and conditions established by the Copyright Clearance Center Inc., ("CCC's Billing and Payment terms and conditions"), at the time that you opened your RightsLink account (these are available at any time at http://myaccount.copyright.com).

Terms and Conditions

- The materials you have requested permission to reproduce or reuse (the "Wiley Materials") are protected by copyright.

- You are hereby granted a personal, non-exclusive, non-sub licensable (on a stand-alone basis), non-transferable, worldwide, limited license to reproduce the Wiley Materials for the purpose specified in the licensing process. This license, **and any CONTENT (PDF or image file) purchased as part of your order,** is for a one-time use only and limited to any maximum distribution number specified in the license. The first instance of republication or reuse granted by this license must be completed within two years of the date of the grant of this license (although copies prepared before the end date may be distributed thereafter). The Wiley Materials shall not be used in any other manner or for any other purpose, beyond what is granted in the license. Permission is granted subject to an appropriate acknowledgement given to the author, title of the material/book/journal and the publisher. You shall also duplicate the copyright notice that appears in the Wiley publication in your use of the Wiley Material. Permission is also granted on the understanding that nowhere in the text is a previously published source acknowledged for all or part of this Wiley Material. Any third party content is expressly excluded from this permission.

- With respect to the Wiley Materials, all rights are reserved. Except as expressly granted by the terms of the license, no part of the Wiley Materials may be copied, modified, adapted (except for minor reformatting required by the new Publication), translated, reproduced, transferred or distributed, in any form or by any means, and no derivative works may be made based on the Wiley Materials without the prior permission of the respective copyright owner.**For STM Signatory Publishers clearing permission under the terms of the STM Permissions Guidelines only, the terms of the license are extended to include subsequent editions and for editions in other languages, provided such editions are for the work as a whole in situ and does not involve the separate exploitation of the permitted figures or extracts,** You may not alter, remove or suppress in any manner any copyright, trademark or other notices displayed by the Wiley Materials. You may not license, rent, sell, loan, lease, pledge, offer as security, transfer or assign the Wiley Materials on a stand-alone basis, or any of the rights granted to you hereunder to any other person.

- The Wiley Materials and all of the intellectual property rights therein shall at all times remain the exclusive property of John Wiley & Sons Inc, the Wiley Companies, or their respective licensors, and your interest therein is only that of having possession of and the right to reproduce the Wiley Materials pursuant to Section 2 herein during the continuance of this Agreement. You agree that you own no right, title or interest in or to the Wiley Materials or any of the intellectual property rights therein. You shall have

no rights hereunder other than the license as provided for above in Section 2. No right, license or interest to any trademark, trade name, service mark or other branding ("Marks") of WILEY or its licensors is granted hereunder, and you agree that you shall not assert any such right, license or interest with respect thereto

- NEITHER WILEY NOR ITS LICENSORS MAKES ANY WARRANTY OR REPRESENTATION OF ANY KIND TO YOU OR ANY THIRD PARTY, EXPRESS, IMPLIED OR STATUTORY, WITH RESPECT TO THE MATERIALS OR THE ACCURACY OF ANY INFORMATION CONTAINED IN THE MATERIALS, INCLUDING, WITHOUT LIMITATION, ANY IMPLIED WARRANTY OF MERCHANTABILITY, ACCURACY, SATISFACTORY QUALITY, FITNESS FOR A PARTICULAR PURPOSE, USABILITY, INTEGRATION OR NON-INFRINGEMENT AND ALL SUCH WARRANTIES ARE HEREBY EXCLUDED BY WILEY AND ITS LICENSORS AND WAIVED BY YOU.

- WILEY shall have the right to terminate this Agreement immediately upon breach of this Agreement by you.

- You shall indemnify, defend and hold harmless WILEY, its Licensors and their respective directors, officers, agents and employees, from and against any actual or threatened claims, demands, causes of action or proceedings arising from any breach of this Agreement by you.

- IN NO EVENT SHALL WILEY OR ITS LICENSORS BE LIABLE TO YOU OR ANY OTHER PARTY OR ANY OTHER PERSON OR ENTITY FOR ANY SPECIAL, CONSEQUENTIAL, INCIDENTAL, INDIRECT, EXEMPLARY OR PUNITIVE DAMAGES, HOWEVER CAUSED, ARISING OUT OF OR IN CONNECTION WITH THE DOWNLOADING, PROVISIONING, VIEWING OR USE OF THE MATERIALS REGARDLESS OF THE FORM OF ACTION, WHETHER FOR BREACH OF CONTRACT, BREACH OF WARRANTY, TORT, NEGLIGENCE, INFRINGEMENT OR OTHERWISE (INCLUDING, WITHOUT LIMITATION, DAMAGES BASED ON LOSS OF PROFITS, DATA, FILES, USE, BUSINESS OPPORTUNITY OR CLAIMS OF THIRD PARTIES), AND WHETHER OR NOT THE PARTY HAS BEEN ADVISED OF THE POSSIBILITY OF SUCH DAMAGES. THIS LIMITATION SHALL APPLY NOTWITHSTANDING ANY FAILURE OF ESSENTIAL PURPOSE OF ANY LIMITED REMEDY PROVIDED HEREIN.

- Should any provision of this Agreement be held by a court of competent jurisdiction to be illegal, invalid, or unenforceable, that provision shall be deemed amended to achieve as nearly as possible the same economic effect as the original provision, and the legality, validity and enforceability of the remaining provisions of this Agreement shall not be affected or impaired thereby.

- The failure of either party to enforce any term or condition of this Agreement shall not constitute a waiver of either party's right to enforce each and every term and condition of this Agreement. No breach under this agreement shall be deemed waived or excused by either party unless such waiver or consent is in writing signed by the party granting such waiver or consent. The waiver by or consent of a party to a breach of

any provision of this Agreement shall not operate or be construed as a waiver of or consent to any other or subsequent breach by such other party.

- This Agreement may not be assigned (including by operation of law or otherwise) by you without WILEY's prior written consent.
- Any fee required for this permission shall be non-refundable after thirty (30) days from receipt by the CCC.
- These terms and conditions together with CCC's Billing and Payment terms and conditions (which are incorporated herein) form the entire agreement between you and WILEY concerning this licensing transaction and (in the absence of fraud) supersedes all prior agreements and representations of the parties, oral or written. This Agreement may not be amended except in writing signed by both parties. This Agreement shall be binding upon and inure to the benefit of the parties' successors, legal representatives, and authorized assigns.
- In the event of any conflict between your obligations established by these terms and conditions and those established by CCC's Billing and Payment terms and conditions, these terms and conditions shall prevail.
- WILEY expressly reserves all rights not specifically granted in the combination of (i) the license details provided by you and accepted in the course of this licensing transaction, (ii) these terms and conditions and (iii) CCC's Billing and Payment terms and conditions.
- This Agreement will be void if the Type of Use, Format, Circulation, or Requestor Type was misrepresented during the licensing process.
- This Agreement shall be governed by and construed in accordance with the laws of the State of New York, USA, without regards to such state's conflict of law rules. Any legal action, suit or proceeding arising out of or relating to these Terms and Conditions or the breach thereof shall be instituted in a court of competent jurisdiction in New York County in the State of New York in the United States of America and each party hereby consents and submits to the personal jurisdiction of such court, waives any objection to venue in such court and consents to service of process by registered or certified mail, return receipt requested, at the last known address of such party.

WILEY OPEN ACCESS TERMS AND CONDITIONS

Wiley Publishes Open Access Articles in fully Open Access Journals and in Subscription journals offering Online Open. Although most of the fully Open Access journals publish open access articles under the terms of the Creative Commons Attribution (CC BY) License only, the subscription journals and a few of the Open Access Journals offer a choice of Creative Commons Licenses. The license type is clearly identified on the article.

The Creative Commons Attribution License

The Creative Commons Attribution License (CC-BY) allows users to copy, distribute and transmit an article, adapt the article and make commercial use of the article. The CC-BY license permits commercial and non-

Creative Commons Attribution Non-Commercial License

The Creative Commons Attribution Non-Commercial (CC-BY-NC)License permits use,

distribution and reproduction in any medium, provided the original work is properly cited and is not used for commercial purposes.(see below)

Creative Commons Attribution-Non-Commercial-NoDerivs License
The Creative Commons Attribution Non-Commercial-NoDerivs License (CC-BY-NC-ND) permits use, distribution and reproduction in any medium, provided the original work is properly cited, is not used for commercial purposes and no modifications or adaptations are made. (see below)
Use by commercial "for-profit" organizations
Use of Wiley Open Access articles for commercial, promotional, or marketing purposes requires further explicit permission from Wiley and will be subject to a fee.
Further details can be found on Wiley Online Library http://olabout.wiley.com/WileyCDA/Section/id-410895.html

Other Terms and Conditions:

v1.10 Last updated September 2015

Questions? customercare@copyright.com or +1-855-239-3415 (toll free in the US) or +1-978-646-2777.

WOLTERS KLUWER HEALTH, INC. LICENSE TERMS AND CONDITIONS

Mar 13, 2019

This Agreement between Dalhousie University -- Tyler Herod ("You") and Wolters Kluwer Health, Inc. ("Wolters Kluwer Health, Inc.") consists of your license details and the terms and conditions provided by Wolters Kluwer Health, Inc. and Copyright Clearance Center.

License Number	4547130867047
License date	Mar 13, 2019
Licensed Content Publisher	Wolters Kluwer Health, Inc.
Licensed Content Publication	Spine
Licensed Content Title	Tensile Properties of Nondegenerate Human Lumbar Anulus Fibrosus
Licensed Content Author	Sohei Ebara, James Iatridis, Lori Setton, et al
Licensed Content Date	Feb 15, 1996
Licensed Content Volume	21
Licensed Content Issue	4
Type of Use	Dissertation/Thesis
Requestor type	Individual
STM publisher name	
Portion	Figures/table/illustration
Number of figures/tables /illustrations	1
Figures/tables/illustrations used	Figure 1
Author of this Wolters Kluwer article	No
Title of your thesis / dissertation	Regional Variations in the Molecular Structure and Mechanics of the Lumbar Intervertebral Disc Annulus
Expected completion date	Apr 2019
Estimated size(pages)	105
Requestor Location	Dalhousie University Room 5200 Biomedical Engineering Department 5981 University Ave Halifax, NS B3H 4R2 Canada Attn: Tyler Herod
Billing Type	Invoice
Billing Address	Dalhousie University Room 5200 Biomedical Engineering Department 5981 University Ave Halifax, NS B3H 4R2 Canada Attn: Dalhousie University
Total	0.00 CAD

Terms and Conditions

Wolters Kluwer Health Inc. Terms and Conditions

1. **Duration of License:** Permission is granted for a one time use only. Rights herein do not apply to future reproductions, editions, revisions, or other derivative works. This permission shall be effective as of the date of execution by the parties for the maximum period of 12 months and should be renewed after the term expires.
    i. When content is to be republished in a book or journal the validity of this agreement should be the life of the book edition or journal issue.
    ii. When content is licensed for use on a website, internet, intranet, or any publicly accessible site (not including a journal or book), you agree to remove the material from such site after 12 months, or request to renew your permission license
2. **Credit Line:** A credit line must be prominently placed and include: For book content: the author(s), title of book, edition, copyright holder, year of publication; For journal content: the author(s), titles of article, title of journal, volume number, issue number, inclusive pages and website URL to the journal page; If a journal is published by a learned society the credit line must include the details of that society.
3. **Warranties:** The requestor warrants that the material shall not be used in any manner which may be considered derogatory to the title, content, authors of the material, or to Wolters Kluwer Health, Inc.
4. **Indemnity:** You hereby indemnify and hold harmless Wolters Kluwer Health, Inc. and its respective officers, directors, employees and agents, from and against any and all claims, costs, proceeding or demands arising out of your unauthorized use of the Licensed Material
5. **Geographical Scope:** Permission granted is non-exclusive and is valid throughout the world in the English language and the languages specified in the license.
6. **Copy of Content:** Wolters Kluwer Health, Inc. cannot supply the requestor with the original artwork, high-resolution images, electronic files or a clean copy of content.
7. **Validity:** Permission is valid if the borrowed material is original to a Wolters Kluwer Health, Inc. imprint (J.B Lippincott, Lippincott-Raven Publishers, Williams & Wilkins, Lea & Febiger, Harwal, Rapid Science, Little Brown & Company, Harper & Row Medical, American Journal of Nursing Co, and Urban & Schwarzenberg - English Language, Raven Press, Paul Hoeber, Springhouse, Ovid), and the Anatomical Chart Company
8. **Third Party Material:** This permission does not apply to content that is credited to publications other than Wolters Kluwer Health, Inc. or its Societies. For images credited to non-Wolters Kluwer Health, Inc. books or journals, you must obtain permission from the source referenced in the figure or table legend or credit line before making any use of the image(s), table(s) or other content.
9. **Adaptations:** Adaptations are protected by copyright. For images that have been adapted, permission must be sought from the rightsholder of the original material and the rightsholder of the adapted material.
10. **Modifications:** Wolters Kluwer Health, Inc. material is not permitted to be modified or adapted without written approval from Wolters Kluwer Health, Inc. with the exception of text size or color. The adaptation should be credited as follows: Adapted with permission from Wolters Kluwer Health, Inc.: [the author(s), title of book, edition, copyright holder, year of publication] or [the author(s), titles of article, title of journal, volume number, issue number, inclusive pages and website URL to the journal page].
11. **Full Text Articles:** Republication of full articles in English is prohibited.
12. **Branding and Marketing:** No drug name, trade name, drug logo, or trade logo can be included on the same page as material borrowed from *Diseases of the Colon & Rectum, Plastic Reconstructive Surgery, Obstetrics & Gynecology (The Green Journal), Critical Care Medicine, Pediatric Critical Care Medicine, the American Heart Association publications and the American Academy of Neurology publications.*
13. **Open Access:** Unless you are publishing content under the same Creative Commons license, the following statement must be added when reprinting material in Open Access journals: "The Creative Commons license does not apply to this content. Use of the material in any format is prohibited without written permission from the publisher, Wolters Kluwer Health, Inc. Please contact permissions@lww.com for further information."
14. **Translations:** The following disclaimer must appear on all translated copies: Wolters Kluwer Health, Inc. and its Societies take no responsibility for the accuracy of the translation from the published English original and are not liable for any errors which may occur.
15. **Published Ahead of Print (PAP):** Articles in the PAP stage of publication can be cited using the online publication date and the unique DOI number.

i. Disclaimer: Articles appearing in the PAP section have been peer-reviewed and accepted for publication in the relevant journal and posted online before print publication. Articles appearing as PAP may contain statements, opinions, and information that have errors in facts, figures, or interpretation. Any final changes in manuscripts will be made at the time of print publication and will be reflected in the final electronic version of the issue. Accordingly, Wolters Kluwer Health, Inc., the editors, authors and their respective employees are not responsible or liable for the use of any such inaccurate or misleading data, opinion or information contained in the articles in this section.

16. **Termination of Contract:** Wolters Kluwer Health, Inc. must be notified within 90 days of the original license date if you opt not to use the requested material.
17. **Waived Permission Fee:** Permission fees that have been waived are not subject to future waivers, including similar requests or renewing a license.
18. **Contingent on payment:** You may exercise these rights licensed immediately upon issuance of the license, however until full payment is received either by the publisher or our authorized vendor, this license is not valid. If full payment is not received on a timely basis, then any license preliminarily granted shall be deemed automatically revoked and shall be void as if never granted. Further, in the event that you breach any of these terms and conditions or any of Wolters Kluwer Health, Inc.'s other billing and payment terms and conditions, the license is automatically revoked and shall be void as if never granted. Use of materials as described in a revoked license, as well as any use of the materials beyond the scope of an unrevoked license, may constitute copyright infringement and publisher reserves the right to take any and all action to protect its copyright in the materials.
19. **STM Signatories Only:** Any permission granted for a particular edition will apply to subsequent editions and for editions in other languages, provided such editions are for the work as a whole in situ and do not involve the separate exploitation of the permitted illustrations or excerpts. Please view: STM Permissions Guidelines
20. **Warranties and Obligations:** LICENSOR further represents and warrants that, to the best of its knowledge and belief, LICENSEE's contemplated use of the Content as represented to LICENSOR does not infringe any valid rights to any third party.
21. **Breach:** If LICENSEE fails to comply with any provisions of this agreement, LICENSOR may serve written notice of breach of LICENSEE and, unless such breach is fully cured within fifteen (15) days from the receipt of notice by LICENSEE, LICENSOR may thereupon, at its option, serve notice of cancellation on LICENSEE, whereupon this Agreement shall immediately terminate.
22. **Assignment:** License conveyed hereunder by the LICENSOR shall not be assigned or granted in any manner conveyed to any third party by the LICENSEE without the consent in writing to the LICENSOR.
23. **Governing Law:** The laws of The State of New York shall govern interpretation of this Agreement and all rights and liabilities arising hereunder.
24. **Unlawful:** If any provision of this Agreement shall be found unlawful or otherwise legally unenforceable, all other conditions and provisions of this Agreement shall remain in full force and effect.

For Copyright Clearance Center / RightsLink Only:

1. **Service Description for Content Services:** Subject to these terms of use, any terms set forth on the particular order, and payment of the applicable fee, you may make the following uses of the ordered materials:
    i. **Content Rental:** You may access and view a single electronic copy of the materials ordered for the time period designated at the time the order is placed. Access to the materials will be provided through a dedicated content viewer or other portal, and access will be discontinued upon expiration of the designated time period. An order for Content Rental does not include any rights to print, download, save, create additional copies, to distribute or to reuse in any way the full text or parts of the materials.
    ii. **Content Purchase:** You may access and download a single electronic copy of the materials ordered. Copies will be provided by email or by such other means as publisher may make available from time to time. An order for Content Purchase does not include any rights to create additional copies or to distribute copies of the materials

Other Terms and Conditions:

v1.18

Questions? customercare@copyright.com or +1-855-239-3415 (toll free in the US) or +1-978-646-2777.

WOLTERS KLUWER HEALTH, INC. LICENSE TERMS AND CONDITIONS

Mar 13, 2019

This Agreement between Dalhousie University -- Tyler Herod ("You") and Wolters Kluwer Health, Inc. ("Wolters Kluwer Health, Inc.") consists of your license details and the terms and conditions provided by Wolters Kluwer Health, Inc. and Copyright Clearance Center.

License Number	4547131456555
License date	Mar 13, 2019
Licensed Content Publisher	Wolters Kluwer Health, Inc.
Licensed Content Publication	Spine
Licensed Content Title	Regional Variation in Tensile Properties and Biochemical Composition of the Human Lumbar Anulus Fibrosus
Licensed Content Author	D. Skaggs, M. Weidenbaum, J. latridis, et al
Licensed Content Date	Jun 1, 1994
Licensed Content Volume	19
Licensed Content Issue	12
Type of Use	Dissertation/Thesis
Requestor type	Individual
STM publisher name	
Portion	Figures/table/illustration
Number of figures/tables /illustrations	1
Figures/tables/illustrations used	Figure 4
Author of this Wolters Kluwer article	No
Title of your thesis / dissertation	Regional Variations in the Molecular Structure and Mechanics of the Lumbar Intervertebral Disc Annulus
Expected completion date	Apr 2019
Estimated size(pages)	105
Requestor Location	Dalhousie University Room 5200 Biomedical Engineering Department 5981 University Ave Halifax, NS B3H 4R2 Canada Attn: Tyler Herod
Billing Type	Invoice
Billing Address	Dalhousie University Room 5200 Biomedical Engineering Department 5981 University Ave Halifax, NS B3H 4R2 Canada Attn: Dalhousie University

Total 0.00 CAD

Terms and Conditions

Wolters Kluwer Health Inc. Terms and Conditions

1. **Duration of License:** Permission is granted for a one time use only. Rights herein do not apply to future reproductions, editions, revisions, or other derivative works. This permission shall be effective as of the date of execution by the parties for the maximum period of 12 months and should be renewed after the term expires.
    i. When content is to be republished in a book or journal the validity of this agreement should be the life of the book edition or journal issue.
    ii. When content is licensed for use on a website, internet, intranet, or any publicly accessible site (not including a journal or book), you agree to remove the material from such site after 12 months, or request to renew your permission license
2. **Credit Line:** A credit line must be prominently placed and include: For book content: the author(s), title of book, edition, copyright holder, year of publication; For journal content: the author(s), titles of article, title of journal, volume number, issue number, inclusive pages and website URL to the journal page; If a journal is published by a learned society the credit line must include the details of that society.
3. **Warranties:** The requestor warrants that the material shall not be used in any manner which may be considered derogatory to the title, content, authors of the material, or to Wolters Kluwer Health, Inc.
4. **Indemnity:** You hereby indemnify and hold harmless Wolters Kluwer Health, Inc. and its respective officers, directors, employees and agents, from and against any and all claims, costs, proceeding or demands arising out of your unauthorized use of the Licensed Material
5. **Geographical Scope:** Permission granted is non-exclusive and is valid throughout the world in the English language and the languages specified in the license.
6. **Copy of Content:** Wolters Kluwer Health, Inc. cannot supply the requestor with the original artwork, high-resolution images, electronic files or a clean copy of content.
7. **Validity:** Permission is valid if the borrowed material is original to a Wolters Kluwer Health, Inc. imprint (J.B Lippincott, Lippincott-Raven Publishers, Williams & Wilkins, Lea & Febiger, Harwal, Rapid Science, Little Brown & Company, Harper & Row Medical, American Journal of Nursing Co, and Urban & Schwarzenberg - English Language, Raven Press, Paul Hoeber, Springhouse, Ovid), and the Anatomical Chart Company
8. **Third Party Material:** This permission does not apply to content that is credited to publications other than Wolters Kluwer Health, Inc. or its Societies. For images credited to non-Wolters Kluwer Health, Inc. books or journals, you must obtain permission from the source referenced in the figure or table legend or credit line before making any use of the image(s), table(s) or other content.
9. **Adaptations:** Adaptations are protected by copyright. For images that have been adapted, permission must be sought from the rightsholder of the original material and the rightsholder of the adapted material.
10. **Modifications:** Wolters Kluwer Health, Inc. material is not permitted to be modified or adapted without written approval from Wolters Kluwer Health, Inc. with the exception of text size or color. The adaptation should be credited as follows: Adapted with permission from Wolters Kluwer Health, Inc.: [the author(s), title of book, edition, copyright holder, year of publication] or [the author(s), titles of article, title of journal, volume number, issue number, inclusive pages and website URL to the journal page].
11. **Full Text Articles:** Republication of full articles in English is prohibited.
12. **Branding and Marketing:** No drug name, trade name, drug logo, or trade logo can be included on the same page as material borrowed from *Diseases of the Colon & Rectum, Plastic Reconstructive Surgery, Obstetrics & Gynecology (The Green Journal), Critical Care Medicine, Pediatric Critical Care Medicine, the American Heart Association publications and the American Academy of Neurology publications.*
13. **Open Access:** Unless you are publishing content under the same Creative Commons license, the following statement must be added when reprinting material in Open Access journals: "The Creative Commons license does not apply to this content. Use of the material in any format is prohibited without written permission from the publisher, Wolters Kluwer Health, Inc. Please contact permissions@lww.com for further information."
14. **Translations:** The following disclaimer must appear on all translated copies: Wolters Kluwer Health, Inc. and its Societies take no responsibility for the accuracy of the translation from the published English original and are not liable for any errors which may occur.

15. **Published Ahead of Print (PAP):** Articles in the PAP stage of publication can be cited using the online publication date and the unique DOI number.
    i. Disclaimer: Articles appearing in the PAP section have been peer-reviewed and accepted for publication in the relevant journal and posted online before print publication. Articles appearing as PAP may contain statements, opinions, and information that have errors in facts, figures, or interpretation. Any final changes in manuscripts will be made at the time of print publication and will be reflected in the final electronic version of the issue. Accordingly, Wolters Kluwer Health, Inc., the editors, authors and their respective employees are not responsible or liable for the use of any such inaccurate or misleading data, opinion or information contained in the articles in this section.
16. **Termination of Contract:** Wolters Kluwer Health, Inc. must be notified within 90 days of the original license date if you opt not to use the requested material.
17. **Waived Permission Fee:** Permission fees that have been waived are not subject to future waivers, including similar requests or renewing a license.
18. **Contingent on payment:** You may exercise these rights licensed immediately upon issuance of the license, however until full payment is received either by the publisher or our authorized vendor, this license is not valid. If full payment is not received on a timely basis, then any license preliminarily granted shall be deemed automatically revoked and shall be void as if never granted. Further, in the event that you breach any of these terms and conditions or any of Wolters Kluwer Health, Inc.'s other billing and payment terms and conditions, the license is automatically revoked and shall be void as if never granted. Use of materials as described in a revoked license, as well as any use of the materials beyond the scope of an unrevoked license, may constitute copyright infringement and publisher reserves the right to take any and all action to protect its copyright in the materials.
19. **STM Signatories Only:** Any permission granted for a particular edition will apply to subsequent editions and for editions in other languages, provided such editions are for the work as a whole in situ and do not involve the separate exploitation of the permitted illustrations or excerpts. Please view: STM Permissions Guidelines
20. **Warranties and Obligations:** LICENSOR further represents and warrants that, to the best of its knowledge and belief, LICENSEE's contemplated use of the Content as represented to LICENSOR does not infringe any valid rights to any third party.
21. **Breach:** If LICENSEE fails to comply with any provisions of this agreement, LICENSOR may serve written notice of breach of LICENSEE and, unless such breach is fully cured within fifteen (15) days from the receipt of notice by LICENSEE, LICENSOR may thereupon, at its option, serve notice of cancellation on LICENSEE, whereupon this Agreement shall immediately terminate.
22. **Assignment:** License conveyed hereunder by the LICENSOR shall not be assigned or granted in any manner conveyed to any third party by the LICENSEE without the consent in writing to the LICENSOR.
23. **Governing Law:** The laws of The State of New York shall govern interpretation of this Agreement and all rights and liabilities arising hereunder.
24. **Unlawful:** If any provision of this Agreement shall be found unlawful or otherwise legally unenforceable, all other conditions and provisions of this Agreement shall remain in full force and effect.

For Copyright Clearance Center / RightsLink Only:

1. **Service Description for Content Services:** Subject to these terms of use, any terms set forth on the particular order, and payment of the applicable fee, you may make the following uses of the ordered materials:
    i. **Content Rental:** You may access and view a single electronic copy of the materials ordered for the time period designated at the time the order is placed. Access to the materials will be provided through a dedicated content viewer or other portal, and access will be discontinued upon expiration of the designated time period. An order for Content Rental does not include any rights to print, download, save, create additional copies, to distribute or to reuse in any way the full text or parts of the materials.
    ii. **Content Purchase:** You may access and download a single electronic copy of the materials ordered. Copies will be provided by email or by such other means as publisher may make available from time to time. An order for Content Purchase does not include any rights to create additional copies or to distribute copies of the materials

Other Terms and Conditions:
v1.18

Questions? customercare@copyright.com or +1-855-239-3415 (toll free in the US) or +1-978-646-2777.